(12) INTERNATIONAL APPLICATION PUBLISHED UNDER THE PATENT COOPERATION TREATY (PCT)

(51) International Patent Classification⁷: A61N

(21) International Application Number: PCT/US02/39427

(22) International Filing Date: 4 December 2002 (04.12.2002)

(25) Filing Language: English

(26) Publication Language: English

(30) Priority Data:
60/336,587   4 December 2001 (04.12.2001)   US

(71) Applicant: UNIVERSITY OF SOUTHERN CALIFORNIA [US/US]; 3716 South Hope St., Suite 313, Los Angeles, CA 90007 (US).

(72) Inventors: GUNDERSEN, Martin, A.; 6828 No. La Presa, San Gabriel, CA 91775 (US). MARCU, Laura; 97 E. Highland Ave., Unit E, Sierra Madre, CA 91024 (US).

CRAFT, Cheryl, M.; 1191 Brookmere Road, Pasadena, CA 91105 (US). VERNIER, P., Thomas; 7808 Goddard, Los Angeles, CA 90045 (US). LIN, Aimin; 1720 Mission St., #8, South Pasadena, CA 91030 (US). ZHU, Xiemei; 25 N. 4th St., #D, Alhambra, CA 91801 (US).

(74) Agent: ALTMAN, Daniel, E.; Knobbe, Martens, Olson & Bear, LLP, 2040 Main Street, Fourteenth Floor, Irvine, CA 92614 (US).

(81) Designated States *(national)*: AE, AG, AL, AM, AT, AU, AZ, BA, BB, BG, BR, BY, BZ, CA, CH, CN, CO, CR, CU, CZ (utility model), CZ, DE (utility model), DE, DK (utility model), DK, DM, DZ, EC, EE (utility model), EE, ES, FI (utility model), FI, GB, GD, GE, GH, GM, HR, HU, ID, IL, IN, IS, JP, KE, KG, KP, KR, KZ, LC, LK, LR, LS, LT, LU, LV, MA, MD, MG, MK, MN, MW, MX, MZ, NO, NZ, OM, PH, PL, PT, RO, RU, SC, SD, SE, SG, SK (utility model), SK, SL, TJ, TM, TN, TR, TT, TZ, UA, UG, UZ, VC, VN, YU, ZA, ZM, ZW.

[Continued on next page]

(54) Title: METHOD FOR INTRACELLULAR MODIFICATIONS WITHIN LIVING CELLS USING PULSED ELECTRIC FIELDS


A

B
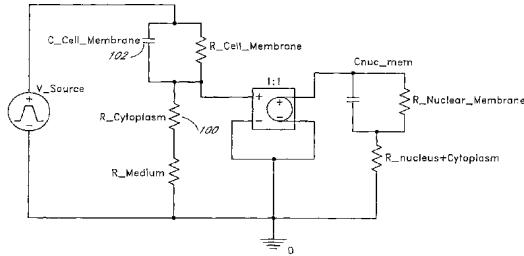
(57) Abstract: The present invention is related to methods in which an electric field pulse is applied to cells and tissue. Several embodiments of the present invention relate to the application of electric field pulses to cells to regulate the physiology and biophysical properties of various cell types, including terminally differentiated and rapidly dividing cells. Methods of regulating transcription of a gene in a cell, marking a cell for diagnostic or therapeutic procedures, determining cellular tolerance to electroperturbation, selectively electroperturbing a population of cells, reducing proliferation of rapidly dividing cells in a patient, and facilitating entry of a diagnostic or therapeutic agent into a cell's intracellular structures are also provided.
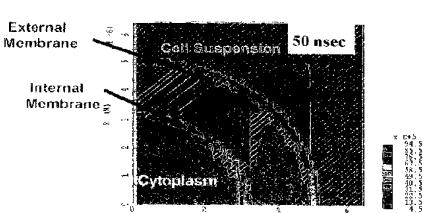
(84) Designated States *(regional)*: ARIPO patent (GH, GM, KE, LS, MW, MZ, SD, SL, SZ, TZ, UG, ZM, ZW), Eurasian patent (AM, AZ, BY, KG, KZ, MD, RU, TJ, TM), European patent (AT, BE, BG, CH, CY, CZ, DE, DK, EE, ES, FI, FR, GB, GR, IE, IT, LU, MC, NL, PT, SE, SI, SK, TR), OAPI patent (BF, BJ, CF, CG, CI, CM, GA, GN, GQ, GW, ML, MR, NE, SN, TD, TG).

Published:

— *without international search report and to be republished upon receipt of that report*

For two-letter codes and other abbreviations, refer to the "Guidance Notes on Codes and Abbreviations" appearing at the beginning of each regular issue of the PCT Gazette.

METHOD FOR INTRACELLULAR MODIFICATIONS WITHIN LIVING CELLS USING PULSED ELECTRIC FIELDS

5   Field of the Invention

The present invention is related generally to the application of electric field pulses to cells to regulate the physiology and biophysical properties of various cell types, including terminally differentiated and rapidly dividing cells, and tissues. Methods of regulating gene transcription, marking cells and selectively reducing cellular proliferation are also provided.

10   Background of the Invention

Electroporation refers to the phenomena of rearranging the structure of the membrane or membranes of cells to introduce or modify porosity across the membrane film, thereby creating a mechanism for transport between the extra-cellular and intracellular fluids, caused by application of an electric field. (Zimmerman U, Electromanipulation of

15   Cells, CRC Press, Boca Raton FL, 1996, herein incorporated by reference).

Pulsed electric fields have long been under investigation for causing many different biological effects. Yet, in spite of decades of research, there is an incomplete understanding of the interaction of electromagnetic fields within biological cells and tissues. Investigations of pulsed electric fields and microwave radiation aimed at achieving

20   cell effects such as electroporation have historically utilized relatively long pulse lengths, such as pulses greater than 1 μsecond, and microwave radiation approaching the thermal-heating regime. Studies of the interactions of RF and microwave electromagnetic fields on biological systems have been limited by the use of these long pulse lengths, or continuous wave radiation, which reduces the coupling of high electric fields into the interior of the

25   cell.

Aqueous pores, typically about 1 nm in diameter, have creation rates typically on the order of microseconds, and possibly shorter with rapidly pulsed fields. Depending on the process for pore formation, resealing of a pore may take much longer (Weaver JC, Chizmadzhev YA, Theory of Electroporation: A Review, *Bioelectrochemistry and*

30   *Bioenergetics*, v41, 1996, pp. 135-160; Bier M, Hammer SM, Canaday DJ, Lee RC, Kinetics of Sealing for Transient Electropores in Isolated Mammalian Skeletal Muscle Cells, *Bioelectromagnetics*, v20, 1999, pp. 194-201, herein incorporated by reference).

Typical field strengths required for electroporation vary between hundreds of volts/cm to kilovolts/cm, depending on the duration of the field. The external field increases the transmembrane potential from about 80 mV to a much larger value, facilitating porosity. It has been consistently shown that once the transmembrane potential reaches or exceeds about the one volt threshold, pores form, resulting in membrane permeabilization, molecular uptake, or lysis from osmosis. There is limited understanding of the membrane dynamics during pore formation. Although modeling captures some linear and even nonlinear aspects of electroporation, the model itself must use variables empirically derived from gathered data, and are qualitative, because of the present limited understanding of membrane physics (Schoenbach KH, Perterkin FE, Alden RW, Beebe SJ, The Effect of Pulsed Electric Fields on Biological Cells: Experiments and Applications, *IEEE Transactions on Plasma Science*, v25, 1997, pp. 284-292, herein incorporated by reference).

Summary of the Invention

It is one object of the current invention to provide a method in which one or more electric field pulses are applied to a cell to regulate cellular physiology and biophysical properties. In one embodiment, gene transcription is regulated. In another embodiment, an electric field pulse is applied to a eukaryotic cell at a voltage and duration sufficient to cause electroperturbation. In one embodiment, the electric field pulse has a pulse duration of less than about 100 nanoseconds. In one embodiment, the electric field is greater than 10 kV/cm. In one embodiment, at least one electric field pulse has a pulse duration of less than about 10 nanoseconds. In another embodiment, the pulse duration is less than about 1 nanosecond. In a further embodiment, one or more genes are selected for transcription. These selected genes include genes that show transcriptional changes after about one hour post electroperturbation. These "one hour" genes include, but are not limited to, ASNS, CHOP (GADD153), CLIC4, CD45, CD53, p36, CD58, AICL FOS, FOSB, DUSP1, JUN, TOB2, GADD34, CLK1, HSPA1B, JUND, EGR1, CACNA1E, CD69 and ETR01. In another embodiment, these selected genes include genes that show transcriptional changes after about six hours post electroperturbation. These "six hour" genes include, but are not limited to, ITPKA, AHNAK, EMP3, ADORA2B, POU2AF1, AIM1, ATP1G1, ASNS, ETS2, CD45, VIM, TGIF, LAT, CLIC4, SLC7A5, ZFP36L2, RUNX1, SLC3A2, IFRD1, and PrP.

It is another object of several embodiments of the present invention to provide a method to determine the induction of cellular gene transcription in response to electropertubation. In one embodiment, at least one electric field pulse is applied to one or more cells. In one embodiment, each electric field pulse has a pulse duration of less than

5   about 100 nanoseconds. In another embodiment, at least one electric field pulse has a pulse duration of less than about 10 nanoseconds. In yet another embodiment, the pulse duration is less than about 1 nanosecond. After the electric field pulse is applied, at least one cell that is electroperturbed is identified and isolated. Cellular gene transcription in the electroperturbed cell is then determined. In a preferred embodiment, the electroperturbed

10   cell is identified based upon cellular morphology or cellular biochemistry. In one embodiment, fluorescent staining is used as a tool to identify changes in cellular morphology or cellular biochemistry.

It is another object of several embodiments of the current invention to provide a method of sensitizing a eukaryotic cell to a therapeutic agent. In one embodiment, at least

15   one electric field pulse is applied to a cell to produce a sensitized cell. Each electric field pulse has a pulse duration of less than about 100 nanoseconds. In one embodiment, at least one electric field pulse has a pulse duration of less than about 10 nanoseconds. In another embodiment, the pulse duration is less than about 1 nanosecond. One or more therapeutic agents is applied to the sensitized cell and the effect of the therapeutic agent is enhanced in

20   the sensitized cells. Therapeutic agents include, but are not limited to, nucleic acids, polypeptides, viruses, enzymes, vitamins, minerals, antibodies, vaccines and pharmaceutical agents. In one embodiment, the pharmaceutical agent is a chemotherapeutic compound. One skilled in the art will understand that one or more therapeutic agents can be applied to the cell and that these agents can be applied before,

25   after or during sensitization of the cell. In one embodiment, the pulse duration is less than about 1 nanosecond and the electric field is greater than about 10 kV/cm.

It is another object of the present invention to provide a method of sensitizing a eukaryotic cell to a therapeutic method. In one embodiment, at least one electric field pulse to a cell, wherein each electric field pulse has a pulse duration of less than about 100

30   nanoseconds, to produce a sensitized cell. In one embodiment, at least one electric field pulse has a pulse duration of less than about 10 nanoseconds. In another embodiment, the pulse duration is less than about 1 nanosecond. One or more therapeutic methods are then

applied to the cell. The effect of the therapeutic method is enhanced in the sensitized cells. Therapeutic methods include, but are not limited to, photodynamic therapy, radiation therapy and vaccine therapy. One skilled in the art will understand that one or more therapeutic methods can be applied to the cell and that these methods can be applied before,

5   after or during sensitization of the cell. In one embodiment, the pulse duration is less than about 1 nanosecond and the electric field is greater than about 10 kV/cm.

It is another object of several embodiments of the current invention to provide a method in which one or more electric field pulses are applied to a cell to mark or target the cell for diagnostic or therapeutic procedures. In one embodiment, at least one electric field

10   pulse is applied to one or more cells. At least one electric field pulse has a pulse sufficient to induce a cellular response in said cell, wherein the cellular response marks the cell for diagnostic or therapeutic procedures. In one embodiment, the duration of each pulse is less than about 100 nanoseconds. In a further embodiment, at least one electric field pulse has a pulse duration of less than about 10 nanoseconds. In another embodiment, the pulse

15   duration is less than about 1 nanosecond. In one embodiment, the cell is "marked" by affecting one or more characteristics of the cell, including but not limited to, gene transcription, gene translation, protein synthesis, post-translational modifications, protein processing, cellular biosynthesis, degradative metabolism, cellular physiology, cellular biophysical properties, cellular biochemistry and cellular morphology. In one embodiment,

20   the cellular response induced by the electric field pulse includes the translocation of cellular membrane components, including proteins and phospholipids. In one embodiment, the phosphatidylserine component of the cytoplasmic membrane of the cell is inverted. In one embodiment, the diagnostic or therapeutic procedure includes lysing the cell.

In another embodiment of the present invention, a method of disrupting an

25   intracellular membrane of a eukaryotic cell is provided, including, but not limited to, the cytoplasmic membrane, nuclear membrane, mitochondrial membrane and segments of the endoplasmic reticulum. In one embodiment, at least one electric field pulse is applied to a cell at a voltage and duration sufficient to induce disruption of the membrane. In one embodiment, each electric field pulse has a pulse duration of less than about 100

30   nanoseconds. In one embodiment, at least one electric field pulse has a pulse duration of less than about 10 nanoseconds. In another embodiment, the pulse duration is less than about 1 nanosecond. In another embodiment, the electric field is greater than about 10

kV/cm. Disruption of the intracellular membrane includes, but is not limited to, translocating membrane components. These components include, but are not limited to, phospholipids, including phosphatidylserine, proteins or other components.

In yet another embodiment of the present invention, a method of marking a eukaryotic cell for phagocytosis is provided. In a further embodiment, at least one electric field pulse to the cell is applied to a cell at a voltage and duration sufficient to induce a cellular response in the cell, wherein the cellular response marks the cell for phagocytosis. The cellular response includes, but is not limited to, translocating membrane components. These components include, but are not limited to, phospholipids, including phosphatidylserine, proteins or other components. In a further embodiment, each electric field pulse has a pulse duration of less than about 100 nanoseconds. In one embodiment, at least one electric field pulse has a pulse duration of less than about 10 nanoseconds. In another embodiment, the pulse duration is less than about 1 nanosecond. In one embodiment, the electric field is greater than about 10 kV/cm.

It is yet another object to provide a method in which one or more electric pulses are applied to a cell to determine cellular tolerance to electric pulses. In one embodiment, a first electric field pulse is applied to one or more cells, and electroperturbed cell are identified, isolated and assayed for one or more indicators of cellular response. Then, a second electric field pulse is applied to the cells. In one embodiment, the second electric field is not equal to the first electric field. After this second treatment, the electroperturbed cell are again identified, isolated and assayed for one or more indicators of cellular response. The indicators of cellular response after application of the first electric field are compared with the indicators of cellular response after application of the second electric field. The indicators of cellular response include, but are not limited to, changes in gene transcription, gene translation, protein synthesis, post-translational modifications, protein processing, cellular biosynthesis, degradative metabolism, cellular physiology, cellular biophysical properties, cellular biochemistry and cellular morphology.

It is another object of several embodiments to selectively electroperturb a population of cells based upon the cell's dielectric properties. In one embodiment, the dielectric properties are exploited to selectively reduce proliferation of rapidly dividing cells in a patient. In one embodiment, dielectric properties of one or more cells in two populations of cells are determined. An electric field pulse based on these dielectric

properties is then determined, wherein the electric field pulse selectively electroperturbs the first sub-population of cells without substantially affecting the second population of cells. This electric field pulse is then applied to the cells. The first sub-population of cells includes, but is not limited to, abnormal or unhealthy cells, such as rapidly dividing cells.

5   The second population of cells includes cells that are to remain substantially unaffected by the electric pulse, such as terminally differentiated cells. In another embodiment the first sub-population of cells includes one type of rapidly dividing cell and the second population of cells includes a second type of rapidly dividing cell. In a further embodiment, the electroperturbation induces changes in a cellular response, including, but not limited to,

10   changes in gene transcription, gene translation, protein synthesis, post-translational modifications, protein processing, cellular biosynthesis, degradative metabolism, cellular physiology, cellular biophysical properties, cellular biochemistry and cellular morphology. Rapidly dividing cells, as used herein, shall be given its ordinary meaning and shall also mean cells that are metabolically active and that can divide through mitosis and duplicate

15   itself. Rapidly dividing cells include, but are not limited to tumorigenic cells and cancerous cells. Terminally differentiated cells, as used herein, shall be given its ordinary meaning and shall mean cells that are metabolically active, but cannot divide to create daughter cells. Terminally differentiated cells include, but are not limited to non-tumorigenic cells and healthy cells.

20   In another embodiment, a method of selectively regulating gene transcription in rapidly dividing cells is provided. In this embodiment, a cell suspension containing rapidly dividing cells and terminally differentiated cells is obtained and at least one electric field pulse is applied to the suspension. Each electric field pulse has a pulse duration and intensity sufficient to induce gene transcription primarily only in the rapidly dividing cells.

25   It is yet another object to provide a therapeutic method in which a patient's tissue is removed and subsequently treated with one or more electric field pulses. In one embodiment, a method of reducing proliferation of rapidly dividing cells in a patient is provided. In this embodiment, a portion of a patient's tissue that contains rapidly dividing cells and terminally differentiated cells, is removed. At least one electric field pulse is

30   applied to one or more cells in the tissue, wherein each electric field pulse has a pulse duration of less than about 100 nanoseconds. In one embodiment, at least one electric field pulse has a pulse duration of less than about 10 nanoseconds. In another embodiment, the

pulse duration is less than about 1 nanosecond. The tissue is then reintroduced to the patient. In another embodiment, one or more electric field pulses having a duration of greater than about 100 nanoseconds is used in combination with an electric field pulse having a duration of less than about 100 nanoseconds. Tissue, as defined herein, shall be given its ordinary meaning and shall also mean a collection of similar cells and the intercellular substances surrounding them. Tissue, as used herein, shall include: (1) epithelium; (2) the connective tissues, including blood, bone, and cartilage; (3) muscle tissue; and (4) nerve tissue. (Stedman's Medical Dictionary Illustrated, Twenty-Third Edition, The Williams & Wilkins Company, Baltimore.) Tissue, as used herein, shall also include, cerebrospinal fluid, lymphatic fluid and bone marrow.

It is another object of several embodiments of the current invention to provide a method in which at least two electric field pulses are applied to a cell to facilitate entry of a diagnostic or therapeutic agent into a cell's intracellular structures. In one embodiment, a relatively "long" electric field pulse is applied to cell followed by a relatively "short" electric field pulse. In one embodiment, the method includes applying at least one first electric field pulse to the cell sufficient to cause electroporation, incubating the cell with the therapeutic agent, and applying one or more second electric field pulses to one or more cells in the tissue, wherein each second electric field pulse has a pulse duration of less than about 100 nanoseconds. The therapeutic agent includes, but is not limited to, nucleic acids, polypeptides, viruses, enzymes, vitamins, minerals, antibodies, vaccines and pharmaceutical agents. In one embodiment, the pulse duration of the relatively "short" pulse is from about 1 nanosecond to about 10 nanoseconds. In another embodiment, the pulse duration of the relatively "short" pulse is less than about 1 nanosecond and the electric field is greater than about 10 kV/cm. In a further embodiment, the pulse duration of the relatively "long" pulse is greater than about 100 nanoseconds. In another embodiment, the pulse duration of the relatively "long" pulse is greater than about 1 millisecond.

It is a further object of the present invention to provide a method for identifying effective therapeutic agents. Such an agent can be effective in reducing cell proliferation. Agents that induce apoptosis can also be identified in accordance with several embodiments of the current invention. In one embodiment, at least one putative therapeutic agent is applied to a cell. The regulation of at least one cell-cycle control gene, stress-response gene

or immune response gene is then determined. If at least one of these genes is up-regulated, the putative therapeutic agent is identified as an effective therapeutic agent. In one embodiment, the cell-cycle control genes, stress-response genes or immune response genes include, but are not limited to, ASNS, CHOP (GADD153), CLIC4, CD45, CD53, p36, CD58, AICL FOS, FOSB, DUSP1, JUN, TOB2, GADD34, CLK1, HSPA1B, JUND, EGR1, CACNA1E, CD69, ETR01, ITPKA, AHNAK, EMP3, ADORA2B, POU2AF1, AIM1, ATP1G1, ASNS, ETS2, CD45, VIM, TGIF, LAT, CLIC4, SLC7A5, ZFP36L2, RUNX1, SLC3A2, IFRD1 and PrP. In one embodiment, the putative therapeutic agent includes, but is not limited to, nucleic acids, polypeptides, viruses, enzymes, vitamins, minerals, antibodies, vaccines and pharmaceutical agents.

Brief Description of the Drawings

Figure 1A shows a phenomenological lumped element circuit model of a biological cell containing a single organelle, representing the membrane of the organelle and the cytoplasmic membrane as separate capacitors, facilitating fast-rising pulses to conduct through the smaller capacitance of the nucleus (or other organelle or structure).

Figure 1B shows a 2-Dimensional electromagnetic model for cell membranes demonstrating the effect of the short pulse on interior membrane. At the early stages of a voltage pulse, the voltage (Electric field) is dropped across a resistor 101 (Cytoplasm), and at steady state condition the voltage (Electric field) is dropped across a 102 capacitor (Membrane).

Figure 2A shows Annexin V-FITC and PI flow cytometry data showing induction of apoptosis by 50 repetitive 20 nanoseconds, 40 kV/cm pulsed electrical shock as measured by Annexin V-FITC and PI staining of the shocked (50 pulses) and unshocked (0 pulse) cells at 8 hrs after the shock treatment, where the percentage of cells in the nonapoptotic (lower left), early apoptotic (lower right), and late apoptotic (upper right) quadrants is indicated.

Figure 2B shows fluorescent-tagged caspase substrate analog evidence 3 hours following pulse exposure for caspase activation after ultrashort pulsed electric field exposure.

Figure 2C shows evidence of loss of mitochondrial membrane potential, 3 hours after ultrashort pulsed electric field exposure.

Figure 2D shows flow cytometry analysis (JC-1 staining) showing increased mitochondrial membrane depolarization fraction as function of pulses with number of pulses (0, 8, 20 and 50 pulses) at 20 nanoseconds, 2 MV/m, 20 Hz.

Figure 2E shows an annexin V-FITC binding pattern on Jurkat T cells. The bottom figure a) is a control that is not fluorescing, and b) shows the results 0 to 5 minutes post-shock, with bright fluorescence.

Figure 3 is an immunoblot PVDF membrane analysis of proteins resolved on SDS-polyacrylamide electrophoresis (SDS-PAGE) that identifies the immunoreactive Poly-ADP-ribose-polymerase (PARP) cleavage in response to electric shock and triton X-100 (TX) treatments.

Figures 4A-B list up-regulated genes. Figure 4A is a table listing genes with increased transcription following 50 electric field pulses after 6 hours. Figure 4B is a table listing genes with increased transcription following electric field pulses after 1 hour.

Figure 5 is a table listing genes with decreased transcription following 50 electric field pulses after 6 hours.

Figure 6 is a table listing genes with increased transcription following 8 electric field pulses after 6 hours.

Figure 7 is a table listing genes with decreased transcription following 8 electric field pulses after 6 hours.

Figures 8A and 8B are micrographs of Jurkat T cells (A) and unshocked control cells (B) exposed to pulsed electric fields (20 nanoseconds, 20 kV/cm) showing intracellular effects of fields.

Figure 9 shows the onset of intracellular effects and penetration into the cell (upper left) as a function of pulse length and electric field.

Figure 10 shows the induction of apoptosis by 50 repetitive 20 nanosecond, 40 kV/cm pulsed electrical shock as measured by Annexin V-FITC and propidium iodide (PI staining of the shocked (50 pulses) and unshocked (0 pulse) cells at 8 hours after the shock treatment. The percentage of cells in the nonapoptotic (lower left), early apoptotic (lower right), and late apoptotic (upper right) quadrants is indicated. At right is depolarization of membrane as a function of the number of pulses.

Figure 11 is an immunoblot SDS-PAGE blot analysis of PARP cleavage in response to electric shock and triton X-100 (TX) treatments. The decrease in the quantity of native

form of PARP (113 kD) and the increase in its proteolytic cleavage products (89 kDa) are characteristic of apoptosis.

Figure 12 is a flow cytometry analysis (JC-1 staining) showing increased mitochondrial membrane depolarization as function of pulses.

Figure 13 shows capsase activation imaged with FITC-VAD-FMK.

Figure 14A shows an inductive adder pulse generator with a cuvette.

Figure 14B shows a stand alone view of the cuvette.

Figure 14C shows a typical 20 nanosecond pulse producing a field of 20 kV/cm.

Figure 15 shows the output of a pseudospark-based pulse generator. This pulse generator is designed for higher voltage needs, and is used along with other pulse generators, to provide a range of options.

Figure 16 shows a field across an internal nuclear or mitochondrial membrane, 10's of nanoseconds after pulse application.

Figure 17 illustrates simple lumped circuit elements.

Figure 18 illustrates a phenomenological lumped element circuit model of a biological cell.

Figure 19 is a 2-D simulation model showing a computational grid, where cylindrical or spherical symmetry can be modeled.

Figure 20 is a graphical comparison of 2-D and circuit (1-D) models for nuclear membrane potential induced by an ideal pulse step.

Figure 21 illustrates the Blumlein PFN configuration.

Figure 22 illustrates an asymmetric water stripline.

Figure 23 illustrates a resonant charging circuit.

Figure 24 is a photograph of a micropulse prototype circuit layout.

Figure 25 illustrates a charging circuit design for a micropulser.

Figure 26 is a micropulser RF circuit schematic.

Figure 27A and 27B show a 2-D spherical electromagnetic model for a cell demonstrating the effect of the short pulse on the interior membrane, where contour plots of the electric field are shown at 0.1 nanosecond (27A) and 50 nanoseconds (27B).

Figure 28 is a graphical representation of Jurkat T cell viability after hundreds of UPSET pulses.

Figure 29 is a graphical representation of Jurkat T cell viability after only a relatively small number of UPSET pulses.

Figure 30 shows the results of monitoring membrane potential of Jurkat T cells with JC-1.

Figure 31 shows the results of caspase activation in 50-pulse cells following FITC VAD-fmk binding, where the Jurkat T cells were electroperturbed with 20 nanosecond pulses at 20 kV/cm.

Figure 32 shows JC-1 flow cytometry scatter plots for normal, depolarized, apoptotic, 0 pulsed, and 50-pulse cells.

Figure 33 is a graphical representation of intercellular potentials over time for cell and mitochondria and their respective membranes.

Detailed Description

Recent research has demonstrated that very short, high-field, electric pulses, generated by advanced pulsed power technology, can reach the interior of biological cells without damaging the external membrane. By taking advantage of the dielectric properties of the cell and its subcellular components, nanosecond, megavolt-per-meter electric field pulses (Ultrashort Pulse Systems Electroperturbation Technology or "UPSET") can polarize internal cellular structures without developing critical voltages across the cytoplasmic membrane. These relatively intense, relatively ultrashort (relatively high power but relatively low total energy) pulses provide a mechanism for delivering variable, but precisely controllable intracellular electrical and mechanical perturbations to a variety of biological systems (single cells, cell suspensions, tissues, organs).

The term electroperturbation is used to characterize the perturbative effects of ultrashort electric pulses on internal organelles and cell membranes, and at proteomic and genomic levels. The present UPSET technology offers the possibility of applying relatively high fields that do not permanently injure the cell, but which do affect field-sensitive and stress-sensitive intracellular elements, such as nuclear and mitochondrial membranes, biochemical equilibria dependent on molecular dipoles, and stretch-sensitive components of the cytoskeleton and endoplasmic reticulum (ER).

I.   REGULATION OF GENE TRANSCRIPTION

A.   UPSET Technology

As discussed above, in several embodiments of the current invention, the novel UPSET technology provides a system for applying relatively high electric fields to cells that affect internal membrane and cytoskeletal biophysics and biochemistry, without permanently injuring the cell. UPSET technology also selectively stimulates specific populations of cells in physiologically significant ways. Some potential areas in which UPSET technology can be used are indicated in **FIG. 9**, discussed below, which shows the range of effects as a function of electric field intensity and pulse duration. Malignant cells, for example, can be more sensitive than normal cells to a sequence of ultrashort, high-field pulses, and such a differential sensitivity has important therapeutic implications.

Pulsed electric fields have been investigated for a variety of biological effects and as a tool for understanding the biophysics of cell membranes and cellular responses to fields across the frequency spectrum. Microsecond, kV/m, pulsed electric fields produce non-lethal conductive pores in the cytoplasmic membrane. This cell permeabilization technology, called electroporation, is widely used for introducing normally excluded substances into cells, including pharmaceutical compounds and nucleic acids. For example, electroporation facilitates cellular uptake and integration of genetic material and is included in protocols for genomic research, genetic engineering and gene therapy. Electroporation pulses range from a few to hundreds of kilovolts per meter in amplitude and from microseconds to milliseconds in duration. Extending the pulse period or increasing the amplitude or delivering a greater number of pulses results in a greater number of larger pores, but with the accompanying penalty of increased lethality to the cell.

As distinct from electroporative pulses, much shorter (electroperturbative) pulses with a duration less than the charging time constant of the plasma membrane (typically less than about 100 nanoseconds) produce voltages within the cell and across the intracellular membranes (dielectric shells) of the nucleus, mitochondria, and other organelles. Very short pulses, and the edges of pulses with very fast rise or fall times, "pass through" the cytoplasmic membrane and, for pulsed field magnitudes greater than about 1 megavolt per meter, produce potentials across intracellular structures large enough to cause depolarization or pore formation in the internal membranes. Electroperturbation pulses

extend the electrical regime of electroporation to high electric field amplitude and very short pulse duration.

To describe the electrical engineering aspects of electroperturbation, the biological cell may be considered to be comprised of a conductive medium surrounded by a dielectric shell, which is immersed in another conductive medium. From this starting point, Maxwell's equations and basic circuit theory lead to models of arbitrary complexity, in the simplest of which cells are represented as lumped circuit elements. These models predict that cells respond to very short pulsed fields (tens of nanoseconds or less) in such a way that instead of appearing across the external membrane "capacitor", the applied field is expressed across intracellular structures and membranes, i.e., the externally applied field is capacitively coupled into the cell.

The Analytical Platform: Experimental and Computational Systems

Experimental and computational systems, described below, are used in conjunction with several embodiments of the current invention, to provide a novel real-time and analytical platform for investigations into the effects of electric field pulses at the sub-cellular level.

Optical imaging investigations have demonstrated potential for 1) acquiring information at molecular, sub-cellular, and cellular levels, and 2) delineating and recognizing diagnostic signatures in situ, noninvasive or minimally invasive, and in near- or real-time. Therefore, development and application of non-invasive imaging and monitoring systems with high optical sensitivity and resolution enables in situ investigations of biological systems subject to external electromagnetic (including fast electric pulses), chemical, magnetic, thermal and/or mechanical stimuli. (Marcu L, Grundfest W.S., Maarek J.M, "Photobleaching of arterial fluorescent compounds: characterization of elastin, collagen, and cholesterol time-resolved spectra during prolonged ultraviolet irradiation", Photochem. Photobiol. 69:713-721, 1999; J.R. Lakowicz, "Principles of Fluorescence Spectroscopy", Plenum Press, New York (1985), all herein incorporated by reference).

Moreover, fluorescence spectroscopy/imaging provides specific signatures with respect to biochemical composition of biological systems. Time-resolved spectroscopy/imaging methods improve the specificity of fluorescence measurements and the use of time-resolved fluorescence approaches for biological systems characterization offers several distinct advantages including: 1) sensitivity to various parameters of

biological systems microenvironment (including pH, ion concentration and binding, enzymatic activity, temperature) thus allowing these variables to be analyzed; 2) discrimination between biomolecules with overlapping fluorescence emission spectra but with different fluorescence decays, thus preferable for multi-labeling experiments; and 3)

5   its ability to be contrasted against an autofluorescence background arising from the same detected microscopic volume element.

Computational science is used to develop realistic electrical models of the cell and its surroundings as the cell responds to the fields. This is used in guiding the design of pulsed field experiments and interpreting the results. This allows the experimental

10 investigation of electro-manipulation and diagnosis of cells with a computational modeling program that applies state-of-the-art tools in electromagnetic simulation from the electrical engineering community to the study of the electrical response of living cells to tailored electrical pulses. This allows for predictive modeling of the detailed three-dimensional electric field structure induced in the cell as a function of realistic applied voltage

15 characteristics and cell characteristics, and allow rapid testing and exploration of new regimes (*e.g.*, shorter pulses) that may be too expensive or time-consuming to explore experimentally. These experimental and computational systems provide a unique real-time and analytical platform for investigations at the sub-cellular level.

The use of equivalent circuits to solve partial differential equations was

20 demonstrated in the era of analog computers, but new methods of modeling biological cells are described herein. In one embodiment, circuit simulation software was used. A well-known circuit simulation program, SPICE, was used in accordance with several embodiments of the present invention. However, one skilled in the art will understand that other circuit simulation software can also be used. The use of equivalent circuits allows

25 both linear and nonlinear models to be used simultaneously for cell membrane interactions. For example, simple models for the fixed portion of the cell membrane resistance and capacitance, and more complex models to represent a population of ion channels and to represent electroporation (nonlinear transmembrane voltage dependence) are used. This approach also includes representation of both the conduction and dielectric properties of

30 intra- and extra-cellular electrolytes. Once an electrical model has been created from an experimental image, the circuit corresponding to the network is solved by SPICE in the frequency or time domain. Equipotentials, transmembrane voltages, current densities and

related distributions are then constructed from the simulation results. In the case of subcellular or cellular electroporation a nonlinear, hysteretic membrane model was used to represent poration of small membrane regions that exceed a threshold transmembrane voltage. The result was then used as a distributed input to a thermal network, and the

5 transient or steady state temperature rise was computed. This provided a basis for asserting that temperature rise distribution for "non-thermal" exposures were relatively small throughout the system. Finally, diffusion and electrophoretic molecular transport can be predicted for the same model. For ultrashort pulses that electroporate nuclear or mitochondrial membranes, models for hindered transport through pores and within the

10 cytoplasm or internal subcellular structure are used to predict movement of small and large molecules within the cell.

Intracellular Effects

Intracellular effects are caused by the application of relatively short, relatively intense electrical pulses (on the order of about 10 kV/cm or more, measured

15 macroscopically across cuvette electrodes, for times on the order of about 20 nanoseconds or less). A photograph of one study is shown in **FIG. 8**. Genomic, proteomic and subcellular biochemical studies show, from biophotonic studies and global DNA microarray analysis, that the fields thus applied either activate or inactivate specific genetic pathways located in the intracellular compartments.

20 Specific intracellular effects, including, but not limited to apoptosis, are also caused by the application of relatively short, relatively intense electrical pulses (typically about 20 nanoseconds or less). Biological experiments on human cells showed that these applied fields (1) led to and altered the subcellular and metabolic biochemical pathways; (2) either activated or inactivated a subset of genes, and (3) could be investigated using biophotonic

25 studies for imaging of morphological and functional changes at subcellular levels. Specific intracellular effects of non-ionizing sources, ranging from transcription of targeted genes to the translation of gene products and protein modifications, also occurred.

The ultrashort pulse exposures described herein were performed in physiological media, permitting direct observation of the effects of electric pulse perturbations in normal,

30 respiring, viable cultured cells. The approach described herein provides a platform for investigations at sub-cellular levels. The results provide an improved understanding of physiological responses of cells, tissues, and organs. Also, this approach facilitates

fundamental investigations of internal membrane and cytoskeletal biophysics and biochemistry and allowes selective stimulation of subsets of cell populations in physiologically significant ways.

In accordance with several embodiments of the current invention, UPSET is used as a tool for triggering apoptosis and provides a method of selectively disabling tumor or other undesirable cells. Many biochemical and genetic inducers, inhibitors, and modulators of apoptosis are known, and embodiments of the present invention provide a non-contact, non-invasive switch for directing rapidly dividing cells towards programmed cell death or altered gene expression without the intervention of pharmacological or genetic agents.

Clinical Applications

The effects of UPSET technology affects and its selectivity for certain tumors, such as glioma brain tumors, have significant clinical applications. Current treatment strategies for patients with brain cancer are ineffective. In 1999, malignant glioma, the most common primary cancer of the central nervous system (CNS), was the cause of death in approximately 13,100 people (DeAngelis, M. 2001. Brain Tumors New England Journal of Medicine 344:114-123). Despite aggressive therapy, including surgical resection, irradiation and chemotherapy, a diagnosis of a malignant glioma is uniformly fatal with survival typically measured in months. The therapeutic efficacy of stereotactic radiosurgery for treatment of patients with both primary and metastatic brain cancer is currently the focus of intense clinical investigation. In developing alternative therapies for brain cancer, several important principles apply. New therapeutic approaches should be targeted directly to the tumor to minimize local toxicity. Drug delivery or gene transfer into the CNS should take into account the blood brain barrier or bypass it.

The field of clinical neurosurgery is rapidly evolving. One of the most promising advances is in the field of "functional neurosurgery." For instance, the therapeutic application of deep brain stimulation for the treatment of Parkinson's Disease is an important example of how stimulating microelectrodes are stereotactically placed within critical structures deep within the brain such as the basal ganglia and thalamus to interrupt motor circuit pathways to influence tremor and rigidity seen in this disorder. In accordance with several embodiments of the current invention, UPSET-based microelectrodes can be stereotactically placed into regions of the brain to provide a minimally invasive, targeted strategy. In this manner, a wide range of CNS disorders may be diagnosed and/or treated.

Identification of hallmarks of apoptosis, or programmed cell death, and a rapid induction of a subset of critical transcriptional immediate early regulatory genes, by the application of intense pulsed electric fields of very short duration (*e.g.*, on the order of about tens of nanoseconds or less) are provided in several embodiments of the present

5   invention. These fields perturbed mitochondrial membranes and the compartmentalized intracellular environment of Jurkat T lymphocytes. Phosphatidylserine translocated to the external face of the lipid bilayer within minutes after exposure, followed by caspase activation and the appearance of poly (ADP-ribose) polymerase fragmentation. Pulsed fields of high instantaneous power, but low total energy, penetrated the cell, invoked

10   mechanisms associated with apoptosis, and offered a pathway for activating organelles and targeting specific genes associated with malignant cells.

The up-regulation of a small group of genes in Jurkat T cells by relatively intense electric fields applied for relatively short times is provided herein. Additional intracellular effects, including, but not limited to, electric field-induced apoptosis, or programmed cell

15   death, are also provided. The fields were tailored to match dielectric properties of the cells in such a way that they caused fields to appear and produce effects inside of the cells. The diagnostics included testing for Annexin V binding, caspase activation, mitochondria membrane permeation and a global DNA microarray analysis of gene regulation. The pulses were typically of relatively short duration, *e.g.* on the order of about tens of

20   nanoseconds or less. The electric fields perturbed intracellular elements, such as the mitochondria. Further perturbative effects influenced processes at sites within cells, i.e., those involving distinct transcription of RNA transition proteins. Such electroperturbative effects offer a pathway for fundamental investigations of internal cell biophysics and have applications in malignant cells therapy.

25   To calculate the electrical response of a cell to a fast-rising, or short electrical pulse, phenomenological data for cell dielectric properties were incorporated as parameters into a lumped electrical circuit model for a cell. **FIG. 1** shows that high frequency, or more precisely, fast-rising pulsed electrical fields introduced electric fields into the intracellular media of mammalian cells.

30   **FIG. 1A** shows a lumped circuit model of the cell. Circuit parameters for the distribution of current flow for cell membranes are estimated using values from the literature (See, for example Kotnik, T., and D. Miklavcic, Bioelectromagnetics 21:385-394

(2000), herein incorporated by reference). For these studies, an intracellular organelle was modeled as a small sphere (compared to cell radius) surrounded by a dielectric membrane, typically relative dielectric constant of 4 and a thickness of 5 nm. Other processes, such as thermal effects on induction of apoptosis, can modify the cellular physiology, or can

5   become a dominant factor in determining the consequences of electric fields on cell behavior. However, the lumped model circuit provided a clear indication of conditions (pulse width, amplitude) under which field will perturb organelles within the cell.

Electromagnetic Calculations: MAGIC Software

In several embodiments of the current invention, MAGIC software for

10   electromagnetic calculations in the presence of conductive media (available from Mission Research Corp.) was used to develop an electromagnetic model with more detail than a lumped circuit element model. MAGIC software is particularly advantageous because it uses a finite difference time domain method, has the advantage of flexibility and a well-documented code, and is suitable for defining the material properties. However, one skilled

15   in the art will understand that other types of electromagnetic calculation software can also be used in accordance with several methods of the current invention. The effects of the larger intracellular structures on the field distribution were modeled using simulations with different sizes of mitochondrion membrane to compare differences between the more sophisticated simulation and the circuit model.

20   **FIG. 1B** shows a MAGIC 2-Dimensional electromagnetic model for cell membranes demonstrating the effect of the short pulse on the interior membrane. A spherical cell is modeled in cylindrical coordinates with axial symmetry. Electric field line distribution around and through the cell at 10 nanoseconds after applying a 20 Kv/cm electric pulse to the cell is also shown in **FIG. 1B**. The Upper Plot shows contour plots of

25   electric field 1 nanosecond after applying the electric pulse for the dotted area in the left figure. Each shaded area in this figure shows locations where the electric field has the same magnitude. The nonuniformity of electric field inside the cell due to the relatively large nuclear area, and the relatively smaller electric field magnitude across the membranes at the early stages of applying the pulse, which shows that the capacitive membranes are not

30   initially charged and almost no electric field is across these membranes. The lower plot shows an electric field 50 nanoseconds after applying the pulse. A large electric field exists across these internal membranes, much smaller electric field within the cytoplasm of the

cell. This is similar to the behavior of an RC circuit. At the early stages of a voltage pulse, the voltage (Electric field) is dropped across the resistor (Cytoplasm), and at steady state condition the voltage (Electric field) is dropped across the capacitor (membrane).

FIG. 1B shows the results and a comparison of the voltage across the nucleus membrane from the two approaches for a step pulse with 1 picosecond rise time and 160 V peak voltage applied to the cell. These results show that including the geometric effects not present in the circuit model increases the electric field predictions in the interior membrane by approximately a factor of two. Both approaches support the conclusion that significant electric fields appear across intracellular membranes for pulses that are sufficiently short (on the order of about 20 nanoseconds or less).

Pulse generator characteristics were taken into account, as the pulse duration and amplitude are in ranges that typically require specialized pulse generation equipment. This is because the pulse characteristics require that the design of the pulse generator, matching of transmission line, and matching to the load (typically a cuvette with conductive solution containing cells with dielectric properties), must be engineered to match with these pulse shapes and pulse characteristics. A MOSFET-switched, inductive-adding pulse generator, using a balanced, coaxial-cable pulse-forming network and spark-gap switch for pulse shortening, was used. The pulse generators delivered electrical pulses to biological material in a variety of exposure modes, including, but not limited to, single-cell, detached-cell suspensions, and layers of cells in culture. The inductive adding pulse generator allowed application of the short pulses (typically about 5-10 kV and about 20 nanoseconds), thereby providing large amplitude electric fields at the electrical load (*e.g.*, within the cuvette).

Experimental Conditions with Jurkat Human T-Lymphoblasts and Gene Transcription

Jurkat human T-lymphoblasts were used in accordance with several embodiments of the current invention. However, one skilled in the art will understand that other cell types can also be used, including but not limited to NIH 3T3, Y79 or Weri-RB1 retinoblastoma, gliomas, COS7, hepatocytes, etc. Human cells are used in accordance with several embodiments of the current invention. However, one skilled in the art will understand that any cell type can be used, including non-human cell types. In one embodiment, UPSET is used to treat bacteria and toxins. In another embodiment, pulsed electric fields are applied to pathogens in food. In a further embodiment, UPSET is used in veterinary applications.

In yet another embodiment, UPSET is used to treat spores, including, but not limited to, Anthrax.

Jurkat human T-lymphoblasts were maintained in suspension culture for these studies (Weiss A, Wiskocil, RL, Stobo JD. J. Immunol. 133:123-128 (1984)) herein incorporated by reference). The Jurkat cells were obtained from American Type Tissue Culture, Rockville, MD. The Jurkat human T-lymphoblast cells were maintained in suspension culture in RPMI 1640 medium, supplemented with 10% fetal bovine serum (FBS), 2 mM L-glutamine, 100 U/ml penicillin and 100 µg/ml streptomycin (growth medium) at 37°C in an atmosphere containing 5% CO_2. Cells were seeded at 5 x 10^5 cells/ml in fresh medium the day before the experiment. Cells were harvested by centrifuging at 1,000 rpm for 3 min and resuspended in growth medium to a final concentration of 2 x 10^7 cells/ml. Aliquots of 100 µl of cell suspensions were transferred into standard 1-mm gap electroporation cuvettes. After shocking, the cells were transferred into 6-well tissue culture plates, diluted with RPMI medium to a final concentration of 1 x 10^6 cells/ml and incubated at 37°C. Aliquots of cell suspensions were taken at 0, 1, 2, 5, 8 and 24 hrs after shock for Trypan Blue exclusion/cell counting, Annexin V binding-Propidium iodide (PI) penetration assay, JC-1 staining and PARP cleavage assays. As a positive control for induction of apoptosis, apoptotic cells were treated with 0.0075% Triton X-100, which has been shown to induce apoptosis in a variety of cell lines (Borner MW, Schneider E, Pirnia F, Sartor O, Trepel JP, Myers CE, FEBS Lett. 353:129-132 (1994), herein incorporated by reference). Rectangular electroporation cuvettes with 1 millimeter and 4 millimeter electrode separations were used to shock dispersed cells in a defined culture media. The cuvette volumes were 75 to several hundred microliters, cell suspension, with cell concentrations up to 2 x 10^7 cells per milliliter.

FIG. 2A shows Annexin V-FITC and PI flow cytometry data showing induction of apoptosis by 50 repetitive 20 nanoseconds, 40 kV/cm pulsed electrical shock as measured by Annexin V-FITC and PI staining of the shocked (50 pulses) and unshocked (0 pulse) cells at 8 hrs after the shock treatment, where the percentage of cells in the nonapoptotic (lower left), early apoptotic (lower right), and late apoptotic (upper right) quadrants is indicated. The Annexin V-FITC apoptosis detection kit I (BD PharMingen) was used to identify apoptotic cells. For each assay 4 x 10^5 cells (400 µl of cell suspension) were transferred from 6-well plates containing the treated cells into microcentrifuge tubes,

washed once with cold PBS (200 g, 3 min) and resuspended in 300 µl of binding buffer. One hundred microliters of resuspended cells was transferred into a culture tube and 10 µl combined Annexin-V-PI solution was added. Samples were incubated in the dark for 15 min at room temperature, and 400 µl of binding buffer was added to each tube. Samples

5   were then analyzed by flow cytometry within 1 hr.

Apoptosis induction was confirmed by immunoblot analysis of Poly-ADP-ribose-polymerase (PARP) cleavage in a series of 8-, 20- and 50-shock samples at 5 and 24 hrs after shock (**FIG. 2**). Trypan blue exclusion experiments verified that the plasma membranes of the cells were lightly permeabilized by 20- and 50-shock treatments, with the

10   50-shock treatment having a relatively stronger effect. The data from these tests are summarized in **FIG. 2 (A-E)**. The cells were stained and inspected using an inverted microscope and Trypan blue. For comparison, normal cells were not stained. The stained cells reflect the uptake of dye due to a permeable outer membrane while normal live cells appear highly illuminated with clearly defined edges. Most of the cells in the 50-shock

15   samples were enlarged and lightly stained with Trypan blue at 0 hr after shock, but this morphological change and the permeabilization to Trypan blue were reversible and totally recovered at about 2 hrs after shock. **FIG. 28** shows Jurkat T cell viability after hundreds of UPSET pulses. **FIG. 29** is a graphical representation of Jurkat T cell viability after only a relatively small number of UPSET pulses.

20   **FIG. 3** shows an immunoblot analysis of immunoreactive Poly-ADP-ribose-polymerase (PARP) cleavage in response to electric shock and Triton X-100 (TX) treatments. The decrease in the quantity of native form of PARP (113 kDa) and the increase in its proteolytic cleavage products (89 kDa) are characteristic of apoptosis. Poly-ADP-ribose-polymerase (PARP), a 113-kDa DNA binding protein, is cleaved into 89- and

25   24-kDa fragments during apoptosis, which serves as an early specific marker of apoptosis. An anti-PARP polyclonal antibody (Roche Molecular Pharmaceuticals) was used to detect the cleavage of the 113-kDa PARP immunoreactive protein. Cells (5 x 10^5) were collected from the 6-well plates, 5 and 24 hrs after the shock treatments, washed with PBS, and sonicated 1 second x 10 on ice in 100 µl of PBS. Equal amounts (50 µg) of proteins from

30   whole cell homogenates were electrophoresed on 11.5% sodium dodecal sulfate-polyacrylamide gel electrophoresis (SDS-PAGE) and were electrophoretically transferred to Immobilon-P membranes (Millipore, Bedford, MA) (Craft CM, Xu J, Slepak VZ, Zhan-Poe

X, Zhu X, Brown B, and Lolley RN, Biochemistry 37:15758-15772, (1998), herein incorporated by reference). The immobilized proteins were detected with anti-PARP (1:1,000) followed with anti-rabbit secondary antibody, using an Enhanced Chemiluminescence Kit (Amersham).

5   Mitochondrial membrane potential was determined by JC-1 staining and flow cytometry analysis of the shocked and unshocked cells at 1 hr after shock (Cossarizza A, Salvioli S. *Methods Cell Biol.* 63:467-486, (2001), herein incorporated by reference). The 50-shock treatment caused mitochondrial membrane depolarization at 1 hr after shock. **FIG. 30** shows the results of monitoring membrane potential of Jurkat T cells with JC-1.

10   Translocation of the membrane phospholipid phosphatidylserine (PS) and the associated degree of membrane permeabilization were measured by flow cytometric analysis of Annexin V-FITC binding and propidium iodide (PI) uptake using commercial reagents (**FIG. 2**).

          FIG. 2B shows fluorescent-tagged caspase substrate analog evidence 3 hours
15   following pulse exposure for caspase activation after ultrashort pulsed electric field exposure. Caspase activation, a third apoptotic indicator, was demonstrated with specific binding of the fluorescent-tagged caspase inhibitor z-VAD-fmk. Morphological changes in the exposed cells, and their ability to exclude the dye Trypan Blue, were monitored with phase microscopy. The fluorescent-tagged caspase substrate analog, FITC-VAD-FMK,
20   marks cells in which caspases, the effector enzymes of apoptosis, have been activated. Jurkat T cells were exposed in growth medium to 50 pulses (3-nanosecond rise time, 20-nanosecond width, 2-megavolt/meter amplitude, 20-hertz repetition rate) and incubated at 37°C. Fluorescence micrographs recorded one and five hours after exposure also showed the appearance of increasing numbers of caspase-positive cells in the shocked population
25   with time. **FIG. 31** shows the results of caspase activation in 50-pulse cells following FITC VAD-fmk binding, where the Jurkat T cells were electroperturbed with 20 nanosecond pulses at 20 kV/cm.

          FIG. 2C shows evidence of loss of mitochondrial membrane potential, 3 hours after ultrashort pulsed electric field exposure. Fluorescence micrographs recorded three hours
30   after exposure (excitation wavelength = 436 nm, wideband emission) show a dose-dependent decrease in the punctuate, red fluorescence pattern. Similar results were observed 5 hours after shock. The potential-sensitive fluorochrome JC-1 (5,5',6,6'-

tetrachloro-1,1',3,3'-tetraethylbenzimidazolylcarbocyanine iodide) binds to and forms red-fluorescing J-aggregates in normal, polarized mitochondrial membranes in living cells. A decrease in membrane potential reduces the affinity of the dye for the membrane and promotes formation of the cytosol-dispersed, green-fluorescing JC-1 monomer. Jurkat T cells were exposed in growth medium to 8, 20, and 50 pulses (3-nanosecond rise time, 20-nanosecond width, 2-megavolt/meter amplitude, 20-hertz repetition rate) and incubated at 37 °C. A spectral shift was observed in the fluorescence of the mitochondrial membrane potential indicator JC-1. Shocked cells exhibited a shift from the red-fluorescing, J-aggregated, mitochondrial membrane-bound form of JC-1, to the green-fluorescing, monomeric form. This indicated the loss of mitochondrial membrane potential that typically accompanies apoptosis. **FIG. 32** shows JC-1 flow cytometry scatter plots for normal (A), depolarized (B), apoptotic (C), 0 pulsed (D), and 50-pulse (E) cells. **FIG. 33** is a graphical representation of intercellular potentials over time for cell and mitochondria and their respective membranes.

Affymetrix huGene FL™ array were hybridized with biotinylated *in vitro* transcription products (10 µg/chip) for 16 hrs at 45 °C using the manufacturer's hybridization buffer in a hybridization oven with constant rotation. The array then went through an automated staining/washing process using the Affymetrix fluidics station and was then scanned using the Affymetrix confocal laser scanner. The digitized image data were processed using the GeneChip software developed by Affymetrix. Hybridization on a microarraywas performed as follows. Affymetrix huGene FL™ arrays (Santa Clara, CA) containing 6800 genes were used for mRNA expression profiling. Total RNA was isolated from Jurkat T cells treated with ultra-short electric shocks as described above. The cells were incubated in RPMI growth medium at a concentration of 1 x 10^6 cells/ml at 37°C for 6 hrs before harvesting for total RNA isolation. Double-stranded cDNAs were prepared using the Life Technologies ChoiceSystem and an oligo(dT)$_{24}$-anchored T7 primer. Biotinylated RNA was synthesized using the BioArray™ HighYield™ RNA Transcript Labeling Kit (Enzo Diagnostics, Inc. New York), following the manufacturer's instructions. *In vitro* transcription products were purified using the RNeasy Mini kit (Qiagen).

cDNA preparations from post-shock cell populations were also analyzed, showing clear genetic expression variation in shocked versus control cells.

B.   **UPSET-Induced Gene Transcriptional Changes**

UPSET treatments altered the Jurkat cells' biochemical and morphological state and altered specific transcriptional pathways. Oligonucleotide array technologies
5   (AffymetrixTM) were used to monitor gene expression profiles in Jurkat cells treated with 0, 8 or 50 ultrashort, pulsed electric shocks. Established data analysis included algorithms that define up-regulated or down-regulated genes as those exhibiting more than a 2-fold difference of expression levels between shocked (8 or 50 shocks) and unshocked (0 shock) cells. Using this oligonucleotide array-based expression profiling technology, 73 genes
10 were identified whose expression increased in response to UPSET exposure after 6 hrs. These genes, included, but were not limited to ITPKA, AHNAK, EMP3, ADORA2B, POU2AF1, AIM1, ATP1G1, ASNS, ETS2, CD45, VIM, TGIF, LAT, CLIC4, SLC7A5, ZFP36L2, RUNX1, SLC3A2, IFRD1, and PrP.

The first major subset of up-regulated genes that appeared at 1 hr after UPSET
15 exposure is associated with the cellular stress response and apoptotic cell death machinery. Genes that showed enhanced expression included, but were not limited to:

i) the enzyme asparagine synthetase (ASNS);

ii) CHOP, also known as GADD153 (CHOP is induced in response to cellular stress. CHOP is involved in the process of apoptosis associated with endoplasmic
20 reticulum (ER) stress; and

iii) CLIC4 (Over-expression of CLIC4 reduces mitochondrial membrane potential, releases cytochrome c into the cytoplasm, activates caspases, and induces apoptosis).

Mitochondria are key organelles that integrate apoptotic signals in damaged cells.
25 Therefore, these data indicated that CLIC4, like Bax, Noxa, CHOP, participate in a stress-induced cell death pathway converging on mitochondria and can serve as a target to enhance cancer therapy through genetic or therapeutic interventions. Thus, although not wishing to be bound by the following theory, it is believed that UPSET triggers the cellular stress response indicated by increasing transcription of the AP-1 family of early gene
30 transcription factors after only 1 hr of exposure. **FIG. 4** and **FIG. 6** list up-regulated genes in response to electric field pulses. **FIG. 4A** list genes up-regulated after 6 hours. **FIG. 4B** lists genes up-regulated after 1 hour. It is also believed that UPSET triggers a cellular

response by down-regulating several genes. **FIG. 5** and **FIG. 7** list these down-regulated genes. These down-regulated genes, alone or in conjunction with the up-regulated genes, are believed to play a role in a cell death or anti-proliferation pathway.

Activation of a second specific set of genes after only 1 hr included, but were not limited to, genes encoding both immuno-response and immune cell activation mediators and related regulating factors. The observed up-regulated genes in this subset included, but were not limited to:

i) CD45 (Involved in maturation, activation, and migration of immune cells);

ii) CD53 (Mediates cell activation);

iii) p36 (LAT), CD58 (A co-stimulatory molecule – blocking CD58 or its ligand);

iv) CD2 (Affects activation of T cells); and

v) AICL (A new activation-induced antigen).

Other genes that were affected at one hour included FOS, FOSB, DUSP1, JUN, TOB2, GADD34, CLK1, HSPA1B, JUND, EGR1, CACNA1E, CD69, and ETR01.

Studies at 6 hours also were conducted. One skilled in the art will understand that the studies conducted at 6 hours can be performed in essentially the same manner as that described above for the 1 hour protocol. One skilled in the art will also understand that studies can also be performed at time intervals other than post 1 hour and post 6 hours after treatment.

In one embodiment of the current invention, UPSET elicited the cellular stress response through mRNA transcriptional increases of specific members of the AP-1 family of early gene transcription factors after 1 hr of exposure. These results, alone and combined with the data from the 6 hrs of exposure, showed that the endoplasmic reticulum stress-mediated cell apoptotic pathways are mechanisms for UPSET exposure.

UPSET exposure perturbs mitochondrial structures or other intracellular stress sensors. When stress signals are unable to rescue and protect the cells, the apoptotic pathway is the default. Although not wishing to be bound by the following theory, it is believed that both mitochondria and death receptor pathways contribute to the apoptosis induced by UPSET exposure. mRNA transcripts corresponding to the genes known to be involved in the induction of apoptosis, such as caspases 1, 2, 3, 6, 7, 8, 11, 12, and 14, showed no changes at the transcriptional level. Other genes, *e.g.*, *Bcl-2, Bcl-w, Bag, Bax, Bak, Bad, Bid,* and others known to be pro-apoptotic or anti-apoptotic were also

typically unchanged. This indicates that, in one embodiment of the current invention, the UPSET exposure was not a global induction of apoptosis, but rather induced programmed cell death through a selective, defined pathway.

The up-regulation of the stress-associated protein CHOP (C/EBP Homologous
5   Protein [C/EBP = CCAAT/Enhancer Binding Protein]), also known as GADD153 (Growth Arrest and DNA-Damage-inducible) provides one mechanism for electric pulse-induced apoptosis. Although not wishing to be bound by this theory, it is believed that under endoplasmic reticulum stress, the transmembrane protein p90ATF6 is cleaved to p50ATF6 and translocated to the nucleus, where it binds to the endoplasmic reticulum stress-
10   responsive element (ERSE) of the CHOP gene, which then activates CHOP transcription (Maytin, E. V., M. Ubeda, J. C. Lin, and J. F. Habener, Exp. Cell Res. 267:193-204, (2001); Gotoh, T., S. Oyadomari, K. Mori, and M. Mori, J. Biol. Chem. 277:12343-12350, (2002), all herein incorporated by reference). CHOP, in turn, induces apoptosis.

Specifically, genes that were increased demonstrate that the pulse amplitude, using
15   UPSET technology with nanosecond high field pulses to target the interior of cells, had dramatic and highly specific effects. These early response genes worked in concert to activate distinct DNA binding elements (e.g. AP-1), pushing rapidly dividing cells into a cell death pathway. This novel approach to targeting a rapidly dividing cell population, while protecting normal, nondividing or differentiated cell populations has many
20   therapeutic applications. The nanosecond time resolution of UPSET exposures, and the striking and immediate physiological effects observed, provide productive applications of this tool to transcriptomic and proteomic studies. For example, the timing of early events in the apoptotic sequence, and the cause-and-effect relationships of a number of critical actors in apoptosis (caspase activation, cytochrome c release into the cytosol, the
25   mitochondrial permeability transition, membrane phospholipid inversion, apoptosis-inducing factor) can be determined with the synchronization and uniformity of stimulus possible with UPSET treatments of single cells, cell suspensions, and tissues.

In one embodiment of the present invention, a method is provided in which tumors or other undesirable cells are disabled. Certain types of malignant cells, for example, are
30   more sensitive than normal cells to a particular sequence of relatively ultrashort, relatively high-field pulses. This differential sensitivity has significant therapeutic applications. The subset of fewer than 50 significantly up-regulated genes from the 6800 examined is much

fewer than is typical for chemotherapy treatments, which produce hundreds of varied regulated genes. Thus, UPSET treatment is a more selective form of "gene-modification therapy."

C.   Pulsed-Power Technology and Instrumentation

5   In several embodiments of the current invention, pulsed power technology and instrumentation is provided. This pulsed power technology is used to develop practical electrodes, such as catheters for medical applications. Bioengineered pulsed power technology is particularly useful to specifically design both high field/short pulses in UPSET applications. For example, to apply a relatively high electric field to the biological

10   cell, it is useful that the peak power at the load be relatively high, and that the design of pulse generator, transmission line, and coupling to the sample, whether solid tumor or individual cells. Existing electroporation devices cannot provide the relatively high field in a sufficiently short time. They typically turn on too slowly, due to limitations in circuitry, and basic switch properties.

15   In one embodiment of the present invention, MOSFET-driven, inductive-adding pulse generators using a balanced, coaxial-cable pulse-forming network and spark-gap switch were used for delivering electrical pulses to biological material for initial studies (**FIG. 8**). The initial UPSET experiments employed commercially available, rectangular electroporation cuvettes with 1- and 4-millimeter electrode separations to shock free-

20   growing cells in growth medium. The cuvettes hold one hundred and eight hundred microliters of cell suspension, respectively, with cell concentrations up to 2×10^7 cells per milliliter. The pulse generator was designed and fabricated to allow fast rising high voltage pulses to be produced with solid state switches (I. Yampolsky and M. Gundersen, "Inductive adder MOSFET-based pulse generator," Patent Pending, herein incorporated by

25   reference) and applied to the cuvettes and biological components.

MOSFET-Based Pulse Generators For High Field Applications

In one embodiment of the current invention, a MOSFET-based pulse generator was used. **FIG. 14A** shows an example of a pulse generator known as an inductive adder based on MOSFETs. This adder produces over 40 kV with a 100 nanosecond pulse width and it

30   has the advantage of having all input switches based at ground, reducing complexity of triggering, and alleviating the issue of series connections of the switches. This adder is particularly advantageous in applications where other switches are not practical.

Higher Power Pseudospark-Based Pulse Generation

In one embodiment of the current invention, a pseudospark-based pulse generator was used. This pulse generator, based on a pseudospark switch, operates in a less than about a 100 nanosecond pulse regime (**FIG. 15**), at a relatively high repetition rate, and a

5   relatively high voltage. ("Low pressure, light initiated, glow discharge switch for high power applications," G.F. Kirkman and M.A. Gundersen, Appl. Phys. Lett. 49, 494 (1986); "High power pseudospark and BLT switches," K. Frank, E. Boggasch, J. Christiansen, A. Goertler, W. Hartmann, C. Kozlik, G. Kirkman, C. G. Braun, V. Dominic, M.A. Gundersen, H. Riege and G. Mechtersheimer, IEEE Trans. Plasma Science 16 (2), 317

10   (1988), all herein incorporated by reference). This combination, with an output impedance sufficiently low to match to the biological cuvette and transmission line, is particularly advantageous because it includes the following characteristics: i) high voltage; ii) fast rising (1 to few nanoseconds); iii) high repetition rate (to about 10 kHz); and iv) optimal impedance matching (range 20 to several hundred ohms). This provides repetition rates

15   from 1 to 10,000 Hz, variable, and variable voltage.

Bioengineering of Advanced Pulsed-Power

For both laboratory and clinical applications, pulse generation for application of short pulses to the biological samples may be provided by, but not limited to, the following pulse generator types: 1) a MOSFET-based solid state pulse generator for higher voltages

20   referred to as an *inductive adder*, 2) a *minipulser*, designed for cuvette experiments, and for experiments requiring close optical observation, 3) a more general purpose device based on an advanced gas phase switch (*pseudospark*), and 4) pulse generators designed for minimal size (*Micropulser)* for both therapeutic applications (incorporation into a catheter) and biophotonic studies (fitting into a microscopy system).

25   *MOSFET-Based Inductive Adder*

The inductive adder is a pulse generator technology especially suitable for high peak power applications requiring fast rising pulses. This system is particularly advantageous because it is highly efficient in producing a fast-rising high voltage, high current pulse, providing input switches in parallel which "add" the current.

30   *Minipulser For Cuvettes*

In one embodiment of the present invention, a small, compact pulse generator for use with cuvettes was used. A compact pulse generator using a Blumlein, which is a

technique for stepping up the voltage for short pulses, was utilized to produce high current and high voltage pulses applied to a standard 1 mm electroporation cuvette. The pulse generator delivered pulses of V_P = 10 kV peak amplitude and τ_P = 5 nanoseconds duration. Bursts of pulses with pulse repetition rate of 10 kHz were achieved, allowing study with various sequences of pulses. The load can be, for example, a standard electroporation cuvette. The electrode area in such cuvettes is typically 1 cm x 2.5 cm, and the electrode gap is 1 mm. It is filled with a nutrient solution in which the cells are suspended. The water based solution has a resistivity of $\rho \sim 500$ Ω cm. The dielectric constant of the solution is close to that of water, $\varepsilon = 81$. This load behaves as a parallel combination of a resistor and a capacitor, with an RC time constant, $\tau_L = \rho \, \varepsilon \, \varepsilon_0$, of approximately 3 nanoseconds. This is comparable to the pulse length. The pulse generator is thus designed to see a load impedance of $Z_L \sim 20$ Ω. The known load characteristics and the desirability of lowest possible voltages suggest the Blumlein PFN configuration switched with a pressurized spark gap (**FIG. 9**). The Blumlein includes two identical series connected transmission lines charged to a common voltage. Each individual line has a characteristic impedance half that of the load.

The electrical length of each transmission line is half the desired output pulse length. The characteristic impedance of the water line is primarily determined by the width of the central strip conductor and the distance to the bottom ground. The interelectrode distance is chosen by the breakdown strength of water and the maximum charge voltage. The chosen width of the center electrode produces the desired $Z = 10$ Ω characteristic impedance. Alternative transmission line configurations can also be used. Two different versions of microstrip lines on high dielectric constant ceramic substrates can be used. In one embodiment of the present invention, these will use ceramic (barium titanate) microstrips that are smaller than the water lines.

In another embodiment of the present invention, a pulse generator (minipulser) that delivered pulses of V_P = 10 kV peak amplitude and τ_P = 5 nanoseconds duration with pulse repetition rate of 10 kHz was used.

Cuvette and Cells Electrical Load Characteristics

In one embodiment of the current invention, the load was a standard electroporation cuvette. The electrode area was 1 cm x 2.5 cm, and the electrode gap was 1 mm. It was filled with a nutrient solution in which the cells were suspended. The water based solution

had a resistivity of $\rho \sim 500\ \Omega$ cm. The relative dielectric constant of the solution is close to that of water, $\varepsilon = 81$. The load behaves as a parallel combination of a resistor and a capacitor, with an RC time constant, $\tau_L = \rho\ \varepsilon\ \varepsilon_0$, of approximately 3 nanoseconds. This is comparable to the pulse length. The pulse generator was designed to see A load impedance of $Z_L \sim 20\ \Omega$.

Transmission Line Design

The known load characteristics and the desirability of lowest possible voltages suggest the Blumlein PFN configuration switched with a pressurized spark gap (FIGS. 21-23). The Blumlein includes two identical series connected transmission lines charged to a common voltage. Each individual line has a characteristic impedance half that of the load.

The electrical length of each transmission line is half the desired output pulse length, $T = \frac{1}{2}\ \tau_P$. The physical length, L_{BL}, depends on the wave propagation speed in the dielectric medium storing the energy:

$$L_{BL} = \frac{c\ \tau_P}{2\sqrt{\varepsilon}} \qquad (1)$$

Using a distilled water ($\varepsilon = 81$) and glycol ($\varepsilon = 37$) mixture as dielectric in an asymmetric stripline configuration, the dielectric constant, and hence the pulse length, was adjusted between $4 < \tau_P < 6$ nanoseconds. The mechanical configuration of the water transmission line is shown in FIG. 22.

The characteristic impedance of the water line was primarily determined by the width of the central strip conductor, $w = 9.5$ mm, and the distance to the bottom ground, $d = 3.2$ mm. The interelectrode distance was chosen by the breakdown strength of water and the maximum charge voltage. The chosen width of the center electrode produced the desired $Z = 10\ \Omega$ characteristic impedance. The choice of water as dielectric led to the use of a relatively fast pulse charging system. The circuit diagram of the charger is shown in FIG. 23.

The circuit was largely immune to transients associated with the discharge of the transmission line. In this mode, the primary switching element of the resonant charger was in the off state when the transmission line is discharged. The circuit charged a 300 pF line to 10 kV in 1.1 µseconds This charging time was less than the time constant of distilled water. The maximum repetition rate of the charger was $f = 10$ kHz, limited only by the size of the primary DC storage capacitor.

Energy and Power

The energy per pulse, E_p, delivered to the load, R_L, can be determined from the pulse length, τ_p, and the pulse amplitude, V_L :

$$E_P = \frac{V_L^2}{R_L} \tau_p, \qquad (1)$$

5   and the required power, P, is:

$$P = E_p \frac{f}{\eta}. \qquad (2)$$

Here, the pulse repetition frequency is f and the efficiency is η. Thus, the charger circuit delivered approximately $E_P = 15$ mJ per pulse and provided at least $P = 300$ W of quasicontinuous power.

10   *Time Scales*

During the charging interval, the water-insulated transmission line can be represented as a capacitor in parallel with a resistor. The capacitance, C, of this combination stored the pulse energy at the peak charging voltage,

$$C = \frac{2 E_p}{V_L^2}. \qquad (3)$$

15   A properly terminated Blumlein output voltage equals the charging voltage, $V_L = V_{CH}$. The parallel equivalent resistance is calculated from the load capacitance and the time constant of the water dielectric, $\tau_W = \varepsilon_r \, \varepsilon_0 \, \rho$,

$$R = \frac{\tau_w}{C}. \qquad (4)$$

Resistivity of distilled water is $\rho > 1$ MΩ-cm and the relative dielectric constant is 20 $\varepsilon_r = 81$, hence, the time constant is about 7 µs. Water eventually acquires an ion concentration that lowers its resistivity and time constant. Keeping the charge time, $\tau_{ch} = 1.1$ µs, much less than the initial τ_w, allowed several days of operation between water replacements.

The maximum allowable charge time defines a maximum inductance, L_S, in series 25   with the transmission line. The charging waveform is approximately one quarter of the period of the resonant circuit formed by this inductance and the load capacitance. This limits the inductance of the secondary winding of the high-voltage transformer,

$$L_S \leq \frac{4\,\tau_{ch}^2}{\pi^2\,C}. \qquad (5)$$

Each charging cycle begins with the charging of the primary inductance, L_P, to the pulse energy plus losses:

$$L_P = \frac{2\,E_P}{\eta\,I_P^2}. \qquad (6)$$

The time, t_R, it takes to ramp the current to this value, I_P, depends on the DC power supply voltage, V_{DC}

$$t_R = \frac{L_P\,I_P}{V_{DC}}. \qquad (7)$$

This being the dominant time interval, it sets the absolute maximum repetition rate as well:

$$f \leq \frac{1}{t_R + \tau_{ch} + \tau_P}. \qquad (8)$$

Switch and transformer

The fast turn off requirement led to the use of solid-state devices, such as MOSFETs, for the switching devices. In one embodiment, the selected switch was the APT10035JFLL MOSFET. Its maximum allowable drain voltage is $V_D = 1$ kV, and the maximum pulse current is $I_P = 100$ A. Typical turn off time is 6 nanoseconds. Fast turn off was achieved in practice by using a fast driving circuit. The circuit in **FIG. 2** shows the driving arrangement.

During operation, the switch voltage rises to a maximum, V_D, determined by the primary resonant capacitance, C_D. The primary voltage was raised to the limit set by the switch rating, with about 10% safety margin, to reduce the turn ratio,

$$N = 1.1 \frac{V_L}{V_D}. \qquad (9)$$

In this case, the turn ratio is $N = 11$. The primary inductance calculated from Eq. (6) is $L_P = 3.4$ μH, the secondary from $L_S = L_P\,N^2$ is $L_S = 408$ μH. The secondary inductance satisfies the inequality in Eq. (5). The primary resonant capacitance, from $C_D = C\,N^2$, is $C_D = 36$ nF. This capacitance needs to be adjusted if the coupling coefficient between the primary and secondary windings of the transformer is different from the optimum value of

64%. The consequences are a small reduction in efficiency, some ringing and modified charge time. In this circuit $C_D = 33$ nF, of which about 3 nF is supplied by the drain-source capacitance of the MOSFET. At the end of the current ramp, the energy is stored in the magnetic field of the primary inductance. This field is concentrated in the transformer core. The stored energy divided by the energy density of the magnetic field, B_S, in the core indicates the minimum core volume, V_C,

$$V_C = \frac{2 \mu_0 \mu E_P}{B_S^2}. \qquad (10)$$

It is advantageous to limit the core volume to a relatively small core permeability, μ. Low permeability also helps to establish the optimum coupling coefficient for efficient resonant energy transfer. Simple separation of the primary and secondary windings, N_P and N_S turns, on different ends of the bobbin is adequate if $\mu < 100$, while external inductance in series with the secondary winding should be used to simulate the leakage inductance if the permeability is high. The minimum core cross section, A_C, is given by the flux and the saturation field B_S,

$$A_C = \frac{L_P I_P}{N_P B_S}. \qquad (11)$$

The nickel-iron powder E-core K4022E026 from Magnetics, Inc. has the proper cross section, $A_C = 2.4$ cm^2, and volume, $V_C = 23$ cm^3. Initial permeability is $\mu = 26$, and the saturation field is $B_S = 0.5$ T. A layered winding with monotonically decreasing number of turns on each successive layer results in reduced interlayer and interturn capacitance. The primary winding has $N_P = 7$ turns of 18 awg magnet wire placed at one end of the bobbin. The secondary winding is $N_S = 77$ turns of 24 awg magnet wire in four layers, separated from the primary winding by 6 mm. The first layer has 40 turns, the second 20 turns, the third 10 turns and the top layer is the remaining 7 turns. The layers are insulated by Teflon tape. The transformer primary inductance swings between 5.1 µH at the beginning of the current ramp to 3.4 µH at the peak of the current. The effective permeability of the core at 100 A peak current is $\mu = 18$. Due to this swing in inductance, the ramp time using $V_{DC} = 48$ V power supply is approximately $\tau_R \sim 10$ µs. Estimated temperature rise of the transformer at full power is 32 °C above ambient.

Pseudospark-Based High Voltage System

The pseudospark is a gas phase switch that has some features of thyratrons, but conducts higher current (up to 10's of kA), hold's off higher voltage (typically about 30 kV or more), and switches faster (less than or equal to about 20 nanoseconds). Such a

5   generator will be useful for these applications because of the useful combination of specifications, including variable repetition rate. In one embodiment, the pulse generator delivered pulses of 70 kV peak amplitude and 50 nanoseconds duration. Bursts of 100 pulses with pulse repetition rate of 1 to about 100 Hz were provided within the first phase of the research. The final pulse amplitude was achieved by using a pulse transformer.

10   *Micropulser*

The responses of cell populations (1×10^6 cells in an electroporation cuvette) and of single cells (in groups of 10 or 20) in nanoliter-sized microchambers are used to determine the heterogeneity of the responses of members of a cell population to pulsed electric fields.

Optics and biophotonic methods are used (**FIG. 15**). To support the pulsed power,

15   microscope-slide-size cuvettes are fabricated with electrode structures, and fields are introduced using "micropulser" technology. These microscope-slide-based structures, fabricated with microelectromechanical systems (MEMS) technology, permit direct optical observation of individual cells during and after pulse delivery, in relatively real time (nanosecond time resolution).

20   A miniature solid state pulse generator (about 400 V) designed for the electroperturbation of biological cells in solution is used (**FIG. 16**). Typically, cell electroperturbation with nanosecond pulses is performed on a batch of cells in a cuvette with a volume of less than 1 mL. A "micropulser" designed to produce pulses with several hundred volts to a narrow channel of cells on a microscope slide is based on one or more

25   fast power MOSFETs and form relatively square pulses of variable width. The pulse generator unit and slide holder are compact and designed for optical access and monitoring.

A micropulser (**FIG. 24**) designed to produce relatively intense pulsed electric fields on a microscope slide for cell electroperturbation is described herein. Pulse parameters for electroperturbation include fast rise time, amplitude, and width. The

30   micropulser is designed to provide flexibility in these parameters along with maximum 25 MHz repetition rate. The micropulser provides both miniaturization and flexibility for any pulse width as a single-MOSFET output stage pulse generator.

Biological Load

The load for the micropulser is a glass slide having deposited platinum electrodes that form channels 25μm wide, 25μm deep, and 20 mm in length. Cells suspended in liquid growth medium are pipetted into the channels. The growth medium within one such channel presents an electrical load of 37 ohms in parallel with 14 pF. The microscope slide in process of fabrication has two channels 25μm wide and two channels 50 μm, giving a total parallel load of 12 ohms in parallel with 42 pF.

Physical Requirements

In one embodiment, the microscope slide and micropulser unit fit on the stage of an optical microscope. Having the objective lenses beneath the stage allow for a more spacious working area. In one embodiment, the pulse generator has all RF power devices on stage, leaving the DC power source and trigger signal source as external equipment. Additionally, the fast rise time requirements lead to short current paths for low inductance. In one embodiment, components are surface mounted and coplanar over the ground plane. A MOSFET switched capacitor is well matched to the physical dimensions of the working environment.

Electrical Requirements

In one embodiment, the MOSFET used with the micropulser is the DEI275-501N16A, chosen for its fast 2 nanoseconds rise time and power handling capabilities appropriate for the intended biological load. Derating to 80% provides a maximum voltage of 400 V into 10 ohm load with 40 A current. Its pulsed current rating is 100 A. In one embodiment, only one MOSFET is used to drive the load directly. Integrity of the sharp pulse edge is maintained by mounting the slide coplanar and adjacent to the MOSFET and energy storage capacitor. Conduction paths are copper strips over an insulated ground plane. In one embodiment, the EVIC420 evaluation board serves as the base for the micropulser system.

In one embodiment, the gate driver is the matching DEIC420 chip incorporating the same low inductance design as the MOSFET. The fast switching speed of the MOSFET gate causes large oscillations in the drive circuit. Switching noise is sufficiently large to cause false triggering of the MOSFET after short pulses <60 nanoseconds. The gate pin noise with no filtering is 18.6 Vpeak having an oscillation frequency of 36 MHz. The gate drive IC propagates the noise through even to its logic level input pin. The DEIC420 driver

VCC power pin is 15 V and shows 500 mV peak noise spike with or without gate filtering. Thus, power supply noise is not responsible for the large swings on the gate drive signal. The gate noise is also independent of MOSFET load and drain voltage.

Saturable reactor filtering is placed in series with the gate driver and gate to reduce switching spikes at the gate. Drain fall time is slowed from 3.1 nanoseconds to 3.8 nanoseconds by the addition of gate filtering for 16.2 Vpeak noise and partial false triggering of the MOSEFET after turn-off from a 20 nanoseconds pulse. Sufficient inductance reducing the drain fall time to 4.2 nanoseconds results in 13.2 V peak noise on the gate and no false triggering of the MOSFET. The chosen filter inductor includes a copper wire and two saturable reactors in parallel. Both of the saturable reactors are Toshiba Spike Killer SA7x6x4.5 magnetic cores with one turn each. **FIG. 10** shows the cost in drain fall time to achieve noise suppression using varying combinations of paralleled conductors and saturable reactors. At 13.2 V and below, the MOSFET experiences no false triggering after a 20 nanosecond pulse.

From the oscillation observed on the MOSFET gate pin, the equivalent series resistance and inductance of the gate driver and filter is calculated. The MOSFET has a known gate capacitance of 1.8 nF. The oscillation frequency gives the inductance from Eq. (1) and the known gate capacitance.

$$L = 1/(4\delta^2 F^2 C) \quad (1)$$

Series resistance was determined from the decay constant of the oscillation according to Eq. (2).

$$V_1 = V_0 \exp(-2tL/R) \quad (2)$$

The circuit characteristics are determined for each filter configuration that produced measurable gate oscillation. Specifications for the MOSFET give a gate resistance of 0.3 ohms, leaving 0.28 ohms for the gate driver IC. To achieve 25 MHz pulse repetition rates, a charging network is used to maintain the charge on the primary energy storage capacitor. The duration of 25 MHz burst is limited by tertiary energy storage capacitor C3 in **FIG. 25**. The RF circuit is shown in **FIG. 26**.

In one embodiment, the charging network is designed to maintain the primary energy storage capacitor at >95% of full charge using a 400 W power source. Capacitor C1 is chosen at 20 nF for its appropriate physical size. The maximum allowable burst length

dictates the minimum value of C3. For a 15 nanosecond wide pulse used during 25 MHz operation, the energy per pulse is 0.24 mJ given by Eq. (3).

$$E = tV^2/R \quad (3)$$

The value of C2 is as large as possible while minimizing low stray series inductance to the primary capacitor C1. Additionally, C2 maintains a charge of 380 V. Inductors L1 and L2 represent the equivalent series inductance of the capacitors and conduction paths. Energy efficiency is 96%.

Catheter-Based Micropulser

In several embodiments of the current invention, micropulsers can be designed for incorporation into handheld catheters. This includes, but is not limited to, both small cabled systems with a catheter head and systems with the pulse generation in the catheter, fed by a small pulse charging system. Pulse transmission preserving field is used in these systems for fast rising pulses. Such a system, *i.e.* a pulse generator for high field, fast pulses that can provide 10 to 100 kV/cm fields at the tissue in times of the order nanoseconds, can provide the desired parameters.

A typical catheter available from commercial sources is representative of an impedance-matched device. In one embodiment, the catheter is coupled to a cable matched to the pulse generator, in a manner very similar to UHF (UltraHigh Frequency) coupled cable used for microwave measurements.

D.   Sub-Cellular Responses to Ultrashort Electric Fields

Real-Time Optical Imaging of Sub-Cellular Responses to Ultrashort Electric Fields

The *in-situ* the behavior of the cell over time and capturing events on the order of sub-seconds range are monitored to determine the mechanisms and processes that underlie the therapeutic effects of ultrashort electric fields. Non-invasive, real-time investigations of sub-cellular events resulting from the application of ultrashort electric fields using optical spectroscopy/imaging techniques are performed. These techniques include wide-field, confocal, multiphoton, and lifetime imaging microscopy. Taking advantage of both autofluorescence from native fluorophores in cells and the availability of sensitive and selective fluorescent/molecular probes for living cells, these approaches allow direct investigations of sub-cellular events at cell membranes, organelles and DNA levels. Using these techniques, the electrical response of cells (normal vs. tumorgenic, or terminally differentiated vs. rapidly dividing) to distinct regimes of pulsed electric fields, and the intra-

cellular mechanism triggered by these fields, which may lead to apoptosis, are observed in real time.

An optical spectroscopy/imaging microscopy instrumental apparatus is used for repetitive 3-D functional and structural imaging of live cells treated with ultrashort electric fields. Methodologies for real-time imaging of cellular and sub-cellular events upon exposure to UPSET are used to observe, *inter alia*: (a) membrane dynamics (cytoplasmic and mitochondrial membranes) exposed to various pulsed field regimes (pulse width, intensity, frequency), (b) morphological and functional changes in cells and cell membranes induced at the ultrastructure level (at the cell surface, within the cell, at the organelles levels), (c) changes in intracellular ions homeostasis and Ca2+ channels, and (d) changes of NADH fluorescence emission.

Instrumental Apparatus Design

A microscopy system that would allow, not only for the functional/structural imaging of living cells, but also for direct shocking and incubation of cells (or cell cultures) on the stage of microscope, and temporal monitoring of sub-cellular changes, was used. In one embodiment, this system was achieved by integrating a microscopy system with a micropulser/microchannel system.

This microscopy system extends on current fluorescence microscopy and time-resolved fluorescence spectroscopy systems, including: (i) a motorized fluorescence inverted microscope (Carl Zeiss: Axiovert 200, Nomarski DIC, AxioCam digital camera, 5 photo-ports with confocal/multi-photon accessibility, AxioVision software control, imaging functions including time-lapse, multichannel, Z-stack, mark and find, distance measurements, angle calculations, statistics); (ii) an ultra-high repetition rate gated intensified CCD camera system (LaVision: PicoStar HR-12, gate widths down to 80 picoseconds); (iii) imaging spectrograph (Acton: Spectra Pro 308, dual output; triple-turret 2 gratings one mirror), various detectors (fast photomultiplers tubes, photodiodes), and supporting electronics (fast digitizers, gate delay generators, preamplifiers). Several laser sources (YAG-pumped OPO-doubler pulsed tunable 200 nm-2 micrometers; Argon; He-Ne) can also be used in accordance with several embodiments of the current invention.

Whole-Field Fluorescence Lifetime Imaging Microscopy (FLIM) With Optical Sectioning

In one embodiment, a motorized Axiovert 200 upright microscope, the ultrafast gated ICCD camera system (Image Intensifier, CCD camera, advanced picosecond delay

5   unit, software package including control, image acquisition, processing and analysis), a Ti-Sapphire laser and the supporting opto-electronic components are used in accordance with several embodiments of the current invention. A detailed description of an FLIM system with optical sectioning and its performance has been reported in the imaging art (S.E.D. Webb, *et al.*; A wide-field time-domain fluorescence lifetime imaging microscope with

10   optical sectioning; Review of Scientific Instruments; Volume 73, Number 4; April 2002; M.J. Cole, *et al.*; Time-domain whole-field fluorescence lifetime imaging with optical sectioning; Journal of Microscopy, Vol. 203, Pt. 3, September 2001, pp. 246-257, all herein incorporated by reference. Due to photobleaching or dynamic changes in the fluorescence probes, the use of whole-fields approach based on structural illumination is used to acquire

15   3-D fluorescence information with a minimum excitation intensity and in minimum time. Using a multispectral imager, this technique also provides multiple spectrally resolved images (on a single detector) of a single spatial region. This approach is advantageous for monitoring fast sub-cellular events occurring at short time periods after cells exposure to electric field. The sensitivity of lifetime (time-resolved fluorescence measurements) is

20   exploited for i) monitoring changes in the chemical environment of the fluorophores (ion concentration and binding, Ca, K); ii) monitoring the redox state of pyridine nucleotides NADH and NADPH; iii) contrasting the emission of specific fluorophores against the autofluorescence background arising from the same detected microscopic volume element; and iv) discriminating (in multi-labeling experiments) of molecules with overlapping

25   fluorescence emission bands (different fluorescence decays). (R. Cubeddu, *et al.*; Time-resolved fluorescence imaging in biology and medicine; Topical Review; Institute of Physics Publishing, J. Phys.D; Appl.Phys, 35 (2002) R61-R76); M. Wakita, *et al.*; Some Characteristics of the Fluorescence Lifetime of Reduced Pyridine Nucleotides in Isolated Mitochondria, Isolated Hepatocytes, and Perfused Rat Liver In Situ; J.Biochem. 118, 1151-

30   1160 (1995); B.W. Pogue, *et al.*; *In vivo* NADH Fluorescence Monitoring as an Assay for Cellular Damage in Photodynamic Therapy; Photochemistry and Photobiology, 2001, 74(6); 817-824, all herein incorporated by reference). One skilled in the art will understand

that FLIM can also be used as a technique for DNA chip reading, thus providing direct evaluation of gene expression.

Confocal and Multiphoton Scanning Microscopy

5   The microscopic system described above can be customized for laser scanning microscopy measurements by adding a scanning module and the corresponding electronics and software control modules. Confocal and multiphoton imaging microscopy provide protocols for imaging sub-cellular structure and dynamic processes with high spatial resolution, both *in vitro* and *in vivo*. Applications include, but are not limited to, subcellular imaging of NADH autofluorescence, monitoring of cell division, protein

10   localization and gene expression, Ca^{2+} uncaging and dynamics, and cell developing neuritic outgrowths. Moreover, these techniques provide for imaging thick biological specimens, thus allowing imaging of UPSET effects on cell culture or 3-D geometry.

Fluorescence Spectroscopy

      Although 2- or 3-dimensional display of data provided by fluorescence imaging is

15   useful whenever the localization of any marker is desired, point spectroscopy is particularly advantageous in providing a detailed knowledge of the parameters that characterize the fluorescence emission, such as spectral features, decay time and polarization. These parameters provide a relatively accurate and quantitative interpretation of fluorescence information. These features are provided by integrating a motorized Axiovert 200 upright

20   microscope with an imaging spectrograph (Spectra Pro 308) and a photomultiplier (gated microchannel plate). The dual output of the imaging spectrograph system allows imaging and spectroscopy within the same system. This system facilitates the study of the membrane dynamics and provided quantitative membrane potential data.

NADH Autofluorescence

25   When excited with wavelengths at about a 350-360 nm range, NADH in cells exhibits strong fluorescence with peak emission at about 450-460 nm. Both steady-state and time-resolved (lifetime) fluorescence spectroscopy/imaging methods are used to study fluorescence in living cells. The changes in the cellular NADH fluorescence emission upon UPSET exposure are monitored. Autofluorescence imaging of mitochondrial and nuclear

30   NADH complement the real-time tracking of the mitochondrial membrane potential, providing an additional, time-resolved indicator of the metabolic status of pulsed cells, and revealing information about the role of early PARP activation in stress-induced apoptosis.

Real-Time Life-Cell Imaging of Sub-Cellular Events

In one embodiment of the present invention, subcellular transformations resulting from UPSET exposure are provided in several cell lines, including Jurkat T lymphoblasts, WERI-Rb-1, C6/LacZ7, and DI TNC1. One skilled in the art will understand that other cell types can also be used in accordance with several embodiments of the current invention. In one embodiment, a plurality of cells are shocked using a micropulser/microchamber, as described above. A perfusion microchamber with controlled temperature and atmosphere and with UPSET electrodes for long-term, continuous, microscopic observation of individual cells after pulsed field exposure are used. Data is acquired in real-time for a single cell or a few cells (up to about 10) and cell culture. Wide-field fluorescence microscopy systems are used for imaging.

<u>Membrane dynamics (cytoplasmic and mitochondrial membranes)</u>

The dynamic process occurring at the cell membrane level exposed to various pulsed field regimes , such as pulse width, intensity, frequency, are studied. The fluorescence emission of fast-response voltage-sensitive membrane potential fluorescent probes is measured. Typically, the fluorescence intensity for these dyes changed linearly with the membrane potential. Examples include: (1) RH dyes (*e.g.* RH 421, RH 414) which show (fast decrease of fluorescence upon membrane depolarization. For instance RH 421 has exhibited >20% change in fluorescence per 100 mV applied to neuroblastoma cells; (2) Charge-shift styryl dye di-4-ANEPPS or di-8-ANEPPS, which are sensitive probes for detection of sub-millisecond membrane changes. Di-8-ANEPPS has a fairly uniform 10% per 100 mV changes in fluorescence intensity in a variety of tissue, cell and model membrane systems, for example. These two dyes have been successfully used to investigate the membrane potentials in cell neurobiology studies (mapping of membrane potential along neurons and muscle fibers, imaging of membrane potentials evoked by visual and olfactory stimuli, detection of synaptic and ion channel activity, Ca^{2+} measurements) as well as to study the membrane potential induced by external electric fields during classic electroporation (square-wave electric pulses); (3) JC-1, fluorescence ratio detection, which allow comparative measurements of membrane potential and the determination of the percentage of mitochondria within a population that respond to an electric stimulus, so that subtle heterogeneity in cellular responses are discerned.

Membrane dynamics studies provide valuable information regarding: (i) membrane potential changes under variations in electric field conditions (intensity, duration, number and frequency) and under different environmental conditions (pH, and ionic strength); (ii) time constants for processes ongoing at the membrane; (iii) pore formation kinetics and

5   resealing, (iv) dielectric membrane breakdown, (v) correlations of experimental observations with analytical models; and (iv) differences in membrane dynamics between normal and tumor cells.

Morphological and physiological transformations

The morphological and physiological changes in cells and cell membranes induced

10   at the ultrastructure level, such as at the cell surface, within the cell, and at the organelles, by different regimes of electric fields are monitored in real time. Dynamic sub-cellular changes that take place during shocking, at short time intervals (minutes) and within several hours, are observed. Organelle-specific, DNA-specific and apoptosis-specific fluorescent probes are used, including JC-1, annexin V-FITC, propidium, FITC-VAD-FMK. One

15   skilled in the art will appreciate that other similar probes can also be used in accordance with several embodiments of the current invention.

In several embodiments of the present invention, Green Fluorescence Protein (GFP) and Hoechst 33342 are used as fluorescent probes. GFP is a useful tool for monitoring complex phenomena such as gene expression, protein localization, and organelle structure

20   in prokaryotic, eukaryotic and mammalian living cells. GFP permits direct and indirect biomolecular analysis at the genomic, proteomics or signal transduction level (Zhu, X., Craft C.M., 2000. The carboxyl terminal domain of phosducin finctions as a transcriptional activator. Biochemical and Biophysical Res. Comm. 270:504-509; Zhu, X., Ma, B., Babu, S., Murage, J., Knox, B. E., Craft, C.M., 2002. Mouse cone arrestin gene

25   characterization: promoter targets expression to cone photoreceptors. FEBS Letts 524 (1-3):116-122, all herein incorporated by reference). By co-transfecting GFP mutants, the nucleus and mitochondria are visualized simultaneously in living cell, thus allowing direct study of protein redistribution and protein-protein interaction. By fusing GFP to specific proteins (*eg.,* vesicle docking and fusion, receptors or channels), GFP provides a tool for *in*

30   *vivo* monitoring of the sorting and intracellular fate of these proteins. Hoechst 33342, a DNA stain with blue fluorescence upon binding to DNA, is largely used in many cellular applications, including cell-cycle and apoptosis studies. Rapid, real-time visualization of

changes in cell and organelle shape, size, and function (with phase contrast or with appropriate fluorescent-tagged reporters) can reveal field-induced rearrangement or disruption of vacuoles and intracellular compartments, the time course of membrane phospholipid translocation, and alterations in cytoskeletal integrity and organization.

5   Intracellular Ca^{2+} and Ca^{2+} channels

In several embodiments, ion-sensitive fluorescent probes are used. These probes include, but are not limited to, Fura, Indo, Calcium-Green, Calcium-Crimson; voltage-gated calcium channel blocker Verapamil and stretch-activated calcium channel blockers gadolinium chloride and cobalt chloride. Using well-established protocols, localized or
10   cell-wide changes in intracellular Ca^{2+} concentration following pulse exposure are identified (Fluorescence and luminescent probes for biological activity. A practical guide to technology for quantitative real-time analysis. Biological techniques series, WT Mason Ed., Academic Press, 1999, herein incorporated by reference). Not wishing to be bound by the following theory, it is believed that electric field-induced apoptosis is caused by the
15   perturbation of normal interactions between calcium compartments in the endoplasmic reticulum and the Ca^{2+}-sensitive mitochondria.

D.   Computational Science and Simulations

Computational Modeling

20   Computational modeling has been developed for solving a variety of electromagnetic problems. The primary tools for this type of work are particle-in-cell codes (PIC) that solve self-consistently Maxwell's equations for electromagnetic fields and the motion of particles in those fields (R. G. Hemker, F. S. Tsung, V. K. Decyk, W. B. Mori, S. Lee, and T. Katsouleas, "Development of a parallel code for modeling plasma based
25   accelerators," IEEE Particle Accelerator Conference 5, 3672-3674 (1999), herein incorporated by reference). These codes solve for electric and magnetic fields by solving finite difference equations in the time domain. Typically, these codes use the Finite Difference Time Domain ("FDTD") method to solve wave equations in a medium. The electro-manipulation and diagnosis of cells performed in accordance with several
30   embodiments of the present invention were complemented with a computational modeling program that provided electromagnetic simulation for the study of the electrical response of living cells to tailored electrical pulses.

In order to calculate the electrical response of a cell to a fast-rising, or short electrical pulse, phenomenological data for cell dielectric properties were incorporated as parameters in an electrical circuit model for a cell. The analysis, shown schematically in **FIG. 16**, shows that high frequency, or more precisely, fast-rising pulsed electrical fields,

5   will introduce electric fields into the intracellular media of mammalian cells. The concept can be illustrated using simple lumped circuit elements (**FIG. 17**). Circuit parameters for the distribution of current flow for cells, membranes, etc. were estimated based upon published values (Kotnik, T., and D. Miklavcic. 2000. "Theoretical evaluation of the distributed power dissipation in biological cells exposed to electric fields",

10   Bioelectromagnetics 21:385-394; DeBruin, K. A., and W. Krassowska. 1999, "Modeling electroporation in a single cell. I. Effects of field strength and rest potential", Biophysical Journal 77:1213-1224; Joshi, R. P., and K. H. Schoenbach. 2000, "Electroporation dynamics in biological cells subjected to ultrafast electrical pulses: a numerical simulation study", Physical Review E 62:1025-1033; Marszalek, P., D.-S. Liu, and T. Y. Tsong. 1990,

15   "Schwan equation and transmembrane potential induced by alternating electric field", Biophysical Journal 58:1053-1058; and Freeman, S. A., M. A. Wang, and J. C. Weaver. 1994, "Theory of electroporation of planar bilayer membranes: predictions of the aqueous area, change in capacitance, and pore-pore separation", Biophysical Journal 67:42-56, all herein incorporated by reference).

20   Simulations performed in accordance with several embodiments of the current invention showed penetration of the intense, but low energy, electric fields to the interior of the cell. For these studies, an intracellular organelle was modeled as a small sphere (compared to cell radius) surrounded by a dielectric membrane, typically having a relative dielectric constant of 4 and a thickness of 5 nm. The models provided a clear indication of

25   conditions (pulse width, amplitude) under which field will perturb organelles within the cell. In order to develop an electromagnetic model with more detail than a lumped circuit element model, a finite difference time domain method was used. This method is particularly advantageous because it has the advantage of flexibility and a well-documented code, and is suitable for defining material properties. MAGIC software for electromagnetic

30   calculations in the presence of conductive media, available from Mission Research Corp., was used in several embodiments of the present invention. However, one skilled in the art will understand that other similar software programs can also be used. Initially, the effects

of the larger intracellular structures on the field distribution were determined using simulations with different sizes of mitochondrion membrane to compare differences between MAGIC and the circuit model. **FIG. 19** and **FIG. 20** show the results of MAGIC simulations. The voltage across the nucleus membrane from MAGIC simulations and the

5   circuit simulation for a step pulse with 1 picosecond rise time and 160 V peak voltage applied to the cell are also shown. These results showed that including the geometric effects not present in the circuit model increased the electric field predictions in the interior membrane.

The shape, time duration and amplitude of the applied voltage were factors in cell

10   electro-manipulation. The electrical and hence biological response of a cell differs based on its environment, the state of the cell in its life-cycle, the density of surrounding cells, and the geometry and type of cell (*e.g.*, normal vs. tumorigenic; terminally differentiated vs. rapidly dividing). Thus, a realistic electrical model of the cell and its surroundings was useful in guiding experimental design and in interpreting the results.

15   In several embodiments of the current invention, various computational codes were used to determine cell modeling. The codes described herein are particularly were well-suited to the modeling of biological cells under the influence of pulsed voltages.

In one embodiment, the FDTD approach was used to determine the time-dependent response of the cell. Typically, short pulses have a broad frequency content, making

20   harmonic methods less attractive. In addition, the framework of these codes provided an opportunity to use the resulting fields to "push" particles with appropriately modified force laws in electrically-gated channels. Moreover, the collision and ionization packages were straightforward to modify to model, for example, the electrically-catalyzed formation of key proteins in the mitochondrion. The codes were in 3-D, enabling the modeling of off-

25   axis organelles and mitochondria that lack spherical symmetry. Another advantage of the codes used in several embodiments of the current invention include the ability of the codes to run on parallel platforms. This is particularly useful because the separation of spatial scales between the nanometer-scale cell membranes and the micron-scale cytoplasm and inter-cell spacings forces a small computational mesh or grid to resolve the smallest

30   features and consequently an extremely large number of grids to cover the entire system.

In one embodiment, MAGIC was used. MAGIC is particularly useful because of its ability to handle materials with generalized dielectric constant and conductivity.

However, one skilled in the art will understand that other software codes can also be used. The effect of cell geometry on the circuit properties of the system were modeled. A simple one-dimensional model having 4 layers corresponding to a cell membrane, cytoplasm, mitochondrion and mitochondrion membrane were used as an initial model. The MAGIC

5   simulator was used to analyze the voltage drops across the different layers. The layers were assumed to have constant conductivity and permitivity. The 2-D model provided insight into the effect of cell geometry on the fields reaching into the nuclear membrane. (**FIG. 19** and **FIG. 20**). There are a number of differences introduced by the more realistic geometry. First, as shown in **FIG. 20**, the 2-D MAGIC model yielded higher fields in the nuclear

10   membrane by a factor of two. The deviation is due to the modification of the field in the cytoplasm by the non-negligible size of the nucleus. Second, the distributed model provided information about the amplitude and localization of fields in the cell not readily available from earlier models. An example is shown in **FIG. 27** for a 50 nanosecond pulse at two different times. These data show the propagation of the field from the outer to inner

15   membrane and the localization of the field in the nuclear membrane at t = 50 nanoseconds.

MAGIC was used in 2-D to study in detail the spatial and temporal evolution of the electric fields in spherical cells. This complements laser techniques to spatially resolve the effect of the fields. The 2-D code was used to quantify the effect of size of the interior structure on membrane potentials and other factors. This system also allows investigations

20   into off-axis structures (*e.g.*, mitochondrial membrane potentials) with 3-D codes.

The effects of different cell environments on the electrical response of the cell were also analyzed according to several embodiments of the current invention. The conductivity and other properties of the surrounding fluid and tissue altered the circuit properties of the pulser-fluid-cell system and changed the optimization of pulser characteristics needed to

25   achieve a given field in the cell interior. Once a biological response was optimized empirically using *in vitro* experiments, the simulations were then to used to predict the desired pulser characteristics needed to achieve the same intra-cellular fields under different environmental conditions (*e.g.*, in different tissue, *in vivo*, etc.)

The effects of surrounding cells were also studied. In one embodiment, when the

30   density of surrounding cells was high, the electric field penetration into an individual cell was modified by the surrounding cells. A 2-D periodic model was used to estimate the effect of these surrounding cells. This allowed the pulser design from the *in vitro*

environment with widely spaced cells to be applied more readily to the *in vivo* environment of closely packed cells.

        There are a number of physical situations that benefit from 3- D modeling. These include irregularly shaped cells, as well as off-axis organelles. The importance of the position of the mitochondria on the peak membrane potential it experiences was studied, for example, using 3D modeling. The state of the cell in its life cycle and changes in its electrical response were modeled. For example, during mitosis, microtubules become stretched and more fragile. Models of these aspherical shapes can be created with 3-D electromagnetic models.

        Selectivity modeling was also used to differentiate normal vs. tumorigenic tissue, or terminally differentiated vs. rapidly dividing cells. One difference between the two cell types is the large number of mitochondria present in tumor cells. Thus, pulsed biases that act through modifying the mitochondrial membrane potential typically had a greater effect on tumor cells. However, the high density of mitochondria can alter the electric field structure in the cell.

        In one embodiment, the electric field distribution of the applied fields was used to cause electroporation. Electrode designs, such as the electrode array geometry used in *in vivo* catheter experiments to simulate the effect of non-planar fields (gradients, etc.), were used to provide a desired field distribution (Gilbert, M. Jaroszeski, R. Heller, Biochimica et Biophys. Acta 1334, 9 (1997), herein incorporated by reference).

        In one embodiment, MAGIC in 3-D scaled simulations were used. In one embodiment, cell size was decreased while adjusting the conductivity and permittivity of the cytoplasm and membranes to preserve the time constant for charging the system. The computational time needed to model a single cell for 100 nanoseconds at full-scale in 3-D can be on the order of 10^4 CPU hours and the required memory can be on the order of 10 GBytes. To reduce computational requirements, the biological cell models were implemented on parallelized-PIC and reduced approximation (quasi-static) codes. The quasi-static codes take advantage of parallelized Poisson solver's to find the electrostatic field. The resulting currents were solved either by introducing a local conductivity or by pushing particles with appropriate mobility. The timestep was then advanced either by solving the continuity equation for the charge density or by using standard current deposition routines from the PIC algorithm. The models were solved on a Cartesian grid

(of variable size in the case of MAGIC). In another embodiment, finite element approaches (*e.g.*, tetrahedral mesh generators), such as FEMLAB, can also be used for reducing computation time.

Chemistry modules and non-linear physics modules were incorporated into the electromagnetic models. Electromagnetic models were interfaced with chemistry models developed for the electrically-gated production and transport of key ions and proteins. A force model was implemented in the "pusher" module of the particle-in-cell codes. Electrically gated chemical reactions were directly modified to the case of field-induced chemical production in biological cells by appropriately modifying the cross-sections and types of particles created.

The following Examples illustrate various embodiments of the present invention and are not intended in any way to limit the invention.

<u>**EXAMPLES**</u>

In one embodiment, dose-response and time course apoptosis-induction of UPSET on normal and tumor cell lines *in vitro* were provided. Repetitive 20 nanoseconds, 20 kv/cm pulsed electrical shock of Jurkat T cells at 20 hz led to a shock number-dependent apoptotic effect. Responses of the following terminally differentiated and rapidly dividing cell lines to the UPSET treatment were determined:

1. Jurkat T (ATCC#: TIB-152): In one embodiment, methods using these cells for ultrashort, pulsed electric shock induction of apoptosis are provided .

2. WERI-Rb-1 retinoblastoma cells (ATCC#: HTB-169): In one embodiment, this cell line is used to compare the response of the rapidly proliferating tumor cells with the retinoic acid (RA)-treated, terminally differentiated cells from the same cell lines. RA induces terminal cell differentiation in WERI-Rb-1 cells. This cell line and its global gene expression changes in response to RA during the cell differentiation process has been characterized.

3. C6/LacZ7 glioma cells (brain glial cells) (ATCC#: CRL-2303): This cell line is a subclone of the C6/LacZ cell line (ATCC#: CRL-2199), which was developed from the C6 rat glioma cell line (ATCC#: CCL-107). The C6/LacZ7 cells stably express the *E. coli* LacZ reporter gene, which can facilitate single tumor cell identification on tissue sections by histochemical stain. In one embodiment, these cells aree used to study the therapeutic effect of UPSET on brain tumors in the rat glioma model.

4. DI TNC1 rat brain type 1 astrocytes (ATCC#: CRL-2005): This is one of very few normal brain cell lines available. The response of normal brain cells to the UPSET treatment are characterized and their responses compared with those of the brain tumor cell line C6/lacZ7 to define the appropriate shock parameters for *in vivo* use for brain tumor in the rat glioma animal model.

Cell culture protocol

In one embodiment, both the suspension cell lines Jurkat and WERI-Rb-1 and the adherent cell lines C6/LacZ7 and DI TNC1 are cultured following standard cell culture procedures and ATCC's instruction. All the tumor cell lines (Jurkat, WERI-Rb-1 and C6/LacZ7) are also be treated with appropriate concentrations of RA using an established protocol to induce each cell type to terminally differentiate (Li, A., Zhu, X., Craft, C.M., 2002. Retinoic acid upregulates cone arrestin expression in retinoblastoma cells through a Cis element in the distal promoter region. Invest Ophthalmol Vis Sci 43:1375-1383; Li, A., Zhu, X., Craft, C.M., 2003 (in press). Gene expression networks underlying retinoic acid-induced differentiation of human retinoblastoma *Cells Invest Ophthalmol Vis Sci*, in press, all herein incorporated by reference). Terminal differentiation of the cell phenotype is confirmed by morphological and cell cycle analysis through fluorescence-activated cell sorting (FACS) and global DNA microarray , as described above.

UPSET protocol

A protocol for UPSET treatment of the Jurkat cells is described above. The same protocol may be used for WERI-Rb-1 cells, because it is also a suspension cell line. For the adherent cell lines, the cells were detached with trypsin-EDTA, washed and resuspended in the appropriate growth medium before applying the shock treatment. The dose-response and the time course of the apoptotic effect and gene expression changes after the UPSET treatment were determined. The shock parameters that have the strongest apoptotic effect on the Jurkat cells may be characterized, and then the response of the normal brain cell line DI TNC1 and the RA-treated, terminally differentiated cells with the rapidly dividing tumor cells will be compared using these shock parameters.

Methods and Materials for Apoptosis Analysis:

Cell culture: Jurkat human T-lymphoblast (Weiss A, Wiskocil, RL, Stobo JD. 1984. J. Immunol. 133:123-128.) and Weri-Rb-1 retinoblastoma cells (American Type Tissue Culture, Rockville, MD) were maintained in suspension culture in RPMI 1640

-49-

medium supplemented with 10% fetal bovine serum (FBS), 2 mM L-glutamine, 100 U/ml penicillin and 100 µg/ml streptomycin (growth medium) at 37°C in an atmosphere containing 5% CO_2.

5   *UPSET treatment of the cells*: Cells were seeded at 5 x 10^5 cells/ml in fresh RPMI growth medium the day before the experiment. Cells were harvested by centrifuging at 1,000 rpm for 3 minutes and resuspended in fresh RPMI growth medium to a final concentration of 2 x 10^7 cells/ml. Aliquots of 100 µl of cell suspensions were transferred into standard 1-mm gap electroporation cuvettes and subjected to repetitive ultra-short, pulsed electric shock treatment with a field strength of 40 kV/cm and a pulse duration of 20

10   nanoseconds using 0 (control), 2, 8, 20, and 50 monophasic pulses at room temperature. After shocking, the cells were transferred into 6-well tissue culture plates, diluted with RPMI growth medium to a final concentration of 1 x 10^6 cells/ml and incubated at 37°C. Aliquots of cell suspensions were taken at 0, 1, 2, 5, 8 and 24 hrs after shock for trypan blue exclusion/cell counting, annexin V binding-propidine iodide (PI) penetration assay, JC-1

15   staining and PARP cleavage assays. As a positive control for apoptosis, cells were treated with 0.0075% Triton X-100, which has been shown to induce apoptosis in a variety of cell lines (Borner MW, Schneider E, Pirnia F, Sartor O, Trepel JP, Myers CE. 1994. FEBS Lett. 353:129-132, herein incorporated by reference).

        Annexin V apoptosis assays: The annexin V-FITC apoptosis detection kit I (BD

20   PharMingen) was used to identify apoptotic cells. The assays were performed according to the manufacturer's instructions. Briefly, for each assay, about 4 x 10^5 cells (400 µl of cell suspension) were transferred from the above 6-well plates containing the treated cells into microcentrifuge tubes, washed once with cold PBS (200 g, 3 minutes) and resuspended in 300 µl of 1 × binding buffer. One hundred microliters of resuspended cells was transferred

25   into a culture tube and 10 µl combined annexin-V-PI solution was added. Samples were incubated in the dark for 15 minutes at room temperature, and 400 µl of 1 × binding buffer was added to each tube. Samples were then analyzed by flow cytometry using a FacStar analyzer (Becton-Dickinson, San Jose, CA) within one hour. Results were processed using CellQuest software (Becton-Dickinson).

30   *Analysis of Poly-ADP-ribose)-polymerase (PARP) cleavage*: Poly-ADP-ribose-polymerase (PARP), a 113-kDa DNA binding protein, was cleaved into 89- and 24-kDa fragments during apoptosis, which could serve as an early specific marker of apoptosis. An

anti-PARP polyclonal antibody (Roche Molecular Pharmaceuticals) was used to detect the cleavage of the 113-kDa PARP protein.

Protein immobilization: Cells (5 x 10^5) were collected from the above 6-well plates 5 and 24 hrs after the shock treatments, washed with PBS, and sonicated 1 second x 10 on ice in 100 μl of PBS. Equal amounts (50 μg) of proteins from whole cell homogenates were electrophoresed on 11.5% sodium dodecyl sulfate-polyacrylamide gel electrophoresis (SDS-PAGE) and were electrophoretically transferred to Immobilon-P membranes (Millipore, Bedford, MA) as previously described (Craft CM, Xu J, Slepak VZ, Zhan-Poe X, Zhu X, Brown B, and Lolley RN, 1998. PhLPs and PhLOPs in the phosducin family of G beta gamma binding proteins, Biochemistry 37:15758-15772, herein incorporated by reference). The immobilized immunoreactive proteins were detected on the membrane with anti-PARP (1:1,000) followed with anti-rabbit secondary antibody, using an Enhanced Chemiluminescence Kit (Amersham).

Trypan blue exclusion and cell counting: During observation, cells were stained and inspected under an inverted microscope using trypan blue (Sigma-Aldrich). Normal cells are defined as those that are not stained. Stained cells reflect the uptake of dye due to a permeable outer membrane while normal live cells appear highly illuminated with clearly defined edges.

Preparation of biotinylated probes and hybridization on microarray: Affymetrix huGene FL™ arrays (Santa Clara, CA) containing 6800 genes were used for mRNA expression profiling. Total RNA was isolated from Jurkat T cells treated with 0, 8 or 50 ultra-short electric shocks with a field strength of 40 kV/cm and a pulse duration of 20 nanoseconds as described above. The cells were incubated in RPMI growth medium at a concentration of 1 x 10^6 cells/ml at 37°C for 6 hrs before harvested for total RNA isolation. Double-stranded cDNA was prepared using the Life Technologies superscript choice system and an oligo(dT)$_{24}$-anchored T7 primer. Biotinylated RNA was synthesized using the BioArray™ HighYield™ RNA Transcript Labeling Kit (Enzo Diagnostics, Inc. New York) following the manufacturer's instructions. *In vitro* transcription products were purified using the RNeasy Mini kit (Qiagen).

Affymetrix huGene FL™ array were hybridized with biotinylated *in vitro* transcription products (10 μg/chip) for 16 hrs at 45 °C using the manufacturer's hybridization buffer in a hybridization oven with constant rotation. The array then went

through an automated staining/washing process using the Affymetrix fluidics station and was then scanned using the Affymetrix confocal laser scanner. The digitized image data were processed using the GeneChip software developed by Affymetrix.

Dose-response and time course of Jurkat cells in response to the UPSET treatment: 20 to 50 repetitive UPSET shocks of 20 kv/cm, 20 nanoseconds with a 3 nanosecond rise time at 20 Hz caused significant apoptosis and gene expression changes in Jurkat cells. To characterize the dose-response of the Jurkat cells to the UPSET shocks, parameters were changed sequentially one parameter at a time. The field strength in the range of 10 kv/cm to 300 kv/cm, the pulse width in the range of 0.1 nanosecond to 100 nanoseconds, and the pulse frequency in the range of 1 hz to 10 khz were tested. The pulse pattern and the rising time of the pulses were also examined.

The Jurkat cells were shocked at 2×10^7 cells/ml concentration in a standard 1-mm gap electroporation cuvette. After the shock, the cells were returned to culture dishes and incubated at 37°C in a CO_2 incubator. Aliquots of cells were taken and measured for apoptotic markers at 1, 3, 5, 8 and 24 hrs after shock. Apoptosis was detected with the annexinV/PI flow cytometer method to monitor PS translocation and integrity of the cell membrane, immunoblot analysis of the PARP cleavage, FITC-VAD-FMK stain to detect caspase activation, and genomic DNA isolated and analyzed by gel electrophoresis to determine the rate of DNA fragmentation. Also, real-time optical imaging of subcellular responses to the UPSET treatment were conducted. For example, the time course of changes in mitochondrial membrane potential (depolarization) following exposure to apoptosis-triggering electric pulses were monitored by JC-1 staining, and cytochrome c release by mitochondria were analyzed using immunocytochemical, fluorescence-tagged, and microspectrophotometric analysis of cytochrome c distribution in cells exposed to ultrashort, high-field electric pulses. Release of cytochrome c from the mitochondrial intermembrane space was a recognized early event in apoptosis.

The responses not only of cell populations (2×10^6 cells in an electroporation cuvette), but also of single cells (in groups of 10 or 20 cells) in nanoliter-sized microchambers are examined in order to determine the heterogeneity of the responses of members of a cell population to pulsed electric fields. The microchamber containing 10-20 cells in a single row is electric shocked on the objective stage of a microscope, and the real-time response of the cells to the shock is recorded by real-time optical imaging.

Gene expression regulation by UPSET treatment:

In one embodiment of the resent invention, global DNA microarray analysis of pulse-treated Jurkat cells revealed up-regulation and down-regulation of specific genes by the UPSET treatment. The time course of gene expression changes were analyzed

5   following the apoptosis-inducing shock treatment. Also, the up-regulated and down-regulated genes in the above cell lines were compared to determine whether or not the shock treatment specifically activates or inactivates certain genetically programmed pathways. The Affymetrix oligo array technology and the human gene full-length array containing about 6,800 human genes was used for these analyses. However, one skilled in

10   the art will appreciate that other array technologies can also be used. Although not wishing to be bound by the following theory, it is believed that specific pathways of early gene activation are involved in later downstream activation/inactivation of signal transduction pathways leading to apoptosis. Proteomic analysis with mass spectroscopy (MALDI) was also performed, where the role of the newly identified proteins and their posttranslational

15   modifications from pathways of the identified transcribed genes were characterized by the Affymetrix Genechip technology.

The apoptotic response of the four different cell lines above are compared. First, the normal brain cell line DI TNC1 and the tumor cell lines Jurkat, WERI-Rb-1 and C6/LacZ7 are shocked with the most effective apoptosis-inducing parameters defined for

20   Jurkat cells and are tested for the appearance of apoptotic markers at various time points after shock. Jurkat, WERI-Rb-1 and C6/LacZ7 tumor cell lines are then treated with RA to induce cell differentiation. The suspension cell lines are treated in suspension and the adherent cells in attachment cultures. Terminal differentiation of each cell line is confirmed by morphological and cell cycle analysis using the FACS method. The treated, terminally

25   differentiated and untreated cells were shocked and apoptosis induction is examined.

In one embodiment, the therapeutic effects of UPSET are analyzed in an *in vivo* animal model of brain cancer. In one embodiment, the rat glioma animal model is used (DeAngelis, M. 2001. Brain Tumors New England Journal of Medicine 344:114-123. See also Watanabe, K., Sakamoto, M., Somiya, M., Amin, MR, Kamitani, H, Watanabe, T.

30   Feasibility and limitations of the rat glioma model by C6 gliomas implanted -at the subcutaneous region. Neurol Res 2002. 24(5):485-90; and Barth, RF. Rat brain tumor models in experimental neuro-oncology: the 9L, C6, T9, F98, RG2 (D47), RT-2 and CNS-1

gliomas. J Neurooncol. 1998. 36(1):91-102, all herein incorporated by reference). Using the *in vitro* data (*i.e.* for rat glioma cells and normal astrocytes) as a foundation, the effects of UPSET in C6 glioma cells are studied *in situ* by placing a microcatheter directly within the tumor to deliver the pulses. A time course study is conducted to assay the tumors for

5   induction of apoptosis using a variety of histochemical measures, including the FITC-VAD-FMK stain to detect caspase activation and the TUNEL method to detect DNA fragmentation. Both caspase activation and DNA fragmentation are demonstrated in *in vitro* experiments during UPSET induction of apoptosis in C6/LacZ7 cells and other cell lines. In one embodiment, the animal model allows evaluation of the UPSET technology in

10   the normal brain and provided a method for investigating neurotoxicity of UPSET. This novel technology has important therapeutic relevance as an adjunct to surgical therapy, where delivery of UPSET pulses to the surgical resection cavity following tumor removal can lead to improved local disease control. In one embodiment, the stereotactic placement of a microcatheter to deliver an electric pulse directly to a surgically inaccessible tumor in

15   the brain will complement stereotactic radiosurgery or be used instead of stereotactic radiosurgery .

        The biological effects of ultrashort, high-field electric pulses *in vitro* using a well-established glioma cell line C6/LacZ7, as well as a normal brain astrocyte cell line D1 TNC1, are studied. The parameters derived from these *in vitro* investigations form the

20   basis for further *in vivo* study using C6/LacZ7 cells. Here, the therapeutic effects of UPSET are evaluated in both an intracranial and a flank model of rat glioma using C6/LacZ7 cells. The flank model provides ready access to the C6/LacZ7 tumors, which grow as a solid mass in the subcutaneous tissue. The flank model provides an advantage over the intracranial model in that animals with intracranial masses typically die within 3

25   weeks. The flank model is used to investigate the response of C6 tumors to UPSET pulses, define the optimal working parameters and assess the apoptotic response and then transition to the intracranial model to evaluate UPSET in the setting of a brain tumor. The LacZ marker of the tumor cells provides single tumor cell identification on tissue sections.

        In one embodiment, Wistar rats are injected with 100,000 C6/LacZ7 cells

30   subcutaneously in the flank. The tumors are allowed to grow to approximately 1 cm^3. The tumors are exposed and the microcatheter device are directly placed into the tumors for both the control and the experimental groups of the rats. Tumors of the experimental group

are treated with the ultrashort high electric field pulses delivered through the microcatheter device, while the control group is not treated. Tumor tissues are harvested for histological and immunohistochemical analysis for apoptotic markers (FITC-VAD-FMK stain to detect caspase activation and TUNEL stain to detect DNA fragmentation), as well as tumor cell

5   markers (LacZ) at various time points (hours to days). The sizes of the tumors are also measured. The cells that are positive for apoptotic markers are significantly increased in the treated animal group as compared to the untreated group. In contrast, the sizes of the tumors in the treated group are significantly decreased compared to the control group. Through repeated application of the UPSET treatment, removal of the tumors is provided

10   according to several embodiments of the current invention.

In one embodiment, for intracranial studies, animals are stereotactically injected with 100,000 C6/LACZ7 cells into the right parietal lobe of the brain. After 10 days, the animals are re-anesthetized, and using the original bony openings, the microcatheter device is placed directly into the tumor for delivery of ultrashort high field electric pulses. Half of

15   the animals are treated with the UPSET as the experimental group, and the other half is not be treated and thus serves as a control group. At various time points (hours to days) after the pulse treatment, the animals are sacrificed and the brains are harvested for histology and immunohistochemical analysis, as described above for the flank studies. There are fewer LacZ-positive cells and more apoptotic cells in the experimental group than in the control

20   group. Although not wishing to be bound by the following theory, it is believed that the LacZ-positive tumor cells are killed through apoptosis induction without extensive injury of the normal brain tissues by repeated pulse treatment or by controlling the pulse dosage (repetitive pulses for each treatment).

II.   COMBINATION THERAPY

25   In one embodiment, a method of sensitizing a eukaryotic cell to a therapeutic agent is provided. In one embodiment, at least one electric field pulse is applied to a cell to produce a sensitized cell. Each electric field pulse has a pulse duration of less than about 100 nanoseconds. In one embodiment, at least one electric field pulse has a pulse duration of less than about 10 nanoseconds. In another embodiment, the pulse duration is less than

30   about 1 nanosecond. One or more therapeutic agents is applied to the sensitized cell and the effect of the therapeutic agent is enhanced in the sensitized cells. Therapeutic agents include, but are not limited to, nucleic acids, polypeptides, viruses, enzymes, vitamins,

minerals, antibodies, vaccines and pharmaceutical agents. In one embodiment, the pharmaceutical agent is a chemotherapeutic compound. One skilled in the art will understand that one or more therapeutic agents can be applied to the cell and that these agents can be applied before, after or during sensitization of the cell. In one embodiment,

5   the pulse duration is less than about 1 nanosecond and the electric field is greater than about 10 kV/cm.

In another embodiment, a method of sensitizing a eukaryotic cell to a therapeutic method is provided. In one embodiment, at least one electric field pulse is applied to a cell, wherein each electric field pulse has a pulse duration of less than about 100 nanoseconds, to

10   produce a sensitized cell. One or more therapeutic methods is then applied to the cell. The effect of the therapeutic method is enhanced in the sensitized cells. Therapeutic methods include, but are not limited to, photodynamic therapy, radiation therapy and vaccine therapy. One skilled in the art will understand that one or more therapeutic methods can be applied to the cell and that these methods can be applied before, after or during

15   sensitization of the cell. In one embodiment, at least one electric field pulse has a pulse duration of less than about 10 nanoseconds. In one embodiment, the pulse duration is less than about 1 nanosecond and the electric field is greater than about 10 kV/cm.

III.   CELLULAR MARKING

In several embodiments of the current invention, a method is provided in which one

20   or more electric field pulses are applied to a cell to mark or target the cell for diagnostic or therapeutic procedures. In one embodiment, at least one electric field pulse is applied to one or more cells. At least one electric field pulse has a pulse sufficient to induce a cellular response in said cell, wherein the cellular response marks the cell for diagnostic or therapeutic procedures. In a further embodiment, the duration of each pulse is less than

25   about 100 nanoseconds. In one embodiment, at least one electric field pulse has a pulse duration of less than about 10 nanoseconds. In another embodiment, the pulse duration is less than about 1 nanosecond. In one embodiment, the cell is "marked" by affecting one or more characteristics of the cell, including but not limited to, gene transcription, gene translation, protein synthesis, post-translational modifications, protein processing, cellular

30   biosynthesis, degradative metabolism, cellular physiology, cellular biophysical properties, cellular biochemistry and cellular morphology. In one embodiment, the cellular response induced by the electric field pulse includes the inversion of the phosphatidylserine

component of the cytoplasmic membrane of the cell. In another embodiment, intracellular membranes including, but not limited to, the cytoplasmic membrane, nuclear membrane, mitochondrial membrane and segments of the endoplasmic reticulum are affected. In one embodiment, the diagnostic or therapeutic procedure includes lysing the cell.

5   In another embodiment of the present invention, a method of disrupting an intracellular membrane of a eukaryotic cell is provided, including, but not limited to, the cytoplasmic membrane, nuclear membrane, mitochondrial membrane and segments of the endoplasmic reticulum. In a further embodiment, at least one electric field pulse is applied to a cell at a voltage and duration sufficient to induce disruption of the intracellular

10   membrane. In a further embodiment, each electric field pulse has a pulse duration of less than about 100 nanoseconds. In another embodiment, the duration is less than about 1 nanosecond. In a further embodiment, the electric field is greater than about 10 kV/cm. Disruption of the intracellular membrane includes, but is not limited to, translocating membrane components. These components include, but are not limited to, phospholipids,

15   including phosphatidylserine, proteins or other components. One skilled in the art will understand that translocating membrane components includes inverting or rearranging one or more membrane proteins, phospholipids, etc.

In another embodiment of the present invention, a method of marking a eukaryotic cell for phagocytosis is provided. In a further embodiment, at least one electric field pulse

20   is applied to a cell at a voltage and duration sufficient to induce a cellular response in the cell, wherein the cellular response marks the cell for phagocytosis. The cellular response includes, but is not limited to, translocating membrane components. These components include, but are not limited to, phospholipids, including phosphatidylserine, proteins or other components. In a further embodiment, each electric field pulse has a pulse duration

25   of less than about 100 nanoseconds. In one embodiment, the duration is less than about 1 nanosecond. In another embodiment, the electric field is greater than about 10 kV/cm.

In one embodiment, cells are exposed to one or more pulsed electric fields, as described above. These pulses cause translocation of the membrane phospholipid phosphatidylserine to the outer leaflet of the cytoplasmic membrane, which is assayed as

30   described above. Rearrangement of other components of the cytoplasmic membrane are detected by the fluorescent microscopic or flow cytometric observation of migration of

fluorescent-tagged membrane lipids and proteins, or by changes in binding of fluorescent-tagged antibodies to membrane constituents.

IV.   CELL TOLERANCE

It is yet another object to provide a method in which one or more electric pulses are applied to a cell to determine cellular tolerance to electric pulses. In one embodiment, a first electric field pulse is applied to one or more cells, and electroperturbed cell are identified, isolated and assayed for one or more indicators of cellular response. Then, a second electric field pulse that is not equal to the first electric field is applied to the cells. After this second treatment, the electroperturbed cell are again identified, isolated and assayed for one or more indicators of cellular response. The indicators of cellular response after application of the first electric field are compared with the indicators of cellular response after application of the second electric field. The indicators of cellular response include, but are not limited to, changes in gene transcription, gene translation, protein synthesis, post-translational modifications, protein processing, cellular biosynthesis, degradative metabolism, cellular physiology, cellular biophysical properties, cellular biochemistry and cellular morphology. Methods of applying electric pulses to cells and methods of determining cellular responses to these pulses are performed in a manner similar to that described above. Clinical applications in accordance with several embodiments of the current invention include the assessment of cellular tolerance to radiation emissions from cellular phones and to microwave radiation.

V.   SELECTIVE ELECTROPERTURBATION

In several embodiments of the current invention, a method is provided to selectively electroperturb a population of cells based upon the cell's dielectric constant. In one embodiment, the dielectric constant is exploited to selectively reduce proliferation of rapidly dividing cells in a patient. In one embodiment, dielectric properties of one or more cells in two populations of cells is determined. An electric field pulse based on these dielectric properties is then determined, wherein the electric field pulse selectively electroperturbs the first sub-population of cells without substantially affecting the second population of cells. This electric field pulse is then applied to the cells. The first sub-population of cells includes, but is not limited to an abnormal or unhealthy cells, such as rapidly dividing cells. The second population of cells includes cell that are to remain unaffected by the electric pulse, such as terminally differentiated cells. In another

embodiment the first sub-population of cells includes one type of rapidly dividing cell and the second population of cells includes a second type of rapidly dividing cell. In a further embodiment, the electroperturbation induces changes in a cellular response, including, but not limited to, changes in gene transcription, gene translation, protein synthesis, post-translational modifications, protein processing, cellular biosynthesis, degradative metabolism, cellular physiology, cellular biophysical properties, cellular biochemistry and cellular morphology. Methods of applying electric pulses to cells and methods of determining cellular responses to these pulses are performed in a manner similar to that described above.

In another embodiment, a method of selectively regulating gene transcription in rapidly dividing cells is provided. In this embodiment, a group of cells, containing both rapidly dividing cells and terminally differentiated cells, is obtained and at least one electric field pulse is applied to the cells. Each electric field pulse has a pulse duration and intensity sufficient to induce gene transcription primarily only in the rapidly dividing cells.

In one embodiment, dielectric properties of a given cell type include critical voltage and charging time constants for external and internal membranes. Because of the complexity of the extracellular and intracellular environments, these are determined empirically for each cell type. The critical voltage, or the voltage at which a large increase in membrane conductance is observed, is determined by loading the medium (extracellular or intracellular, depending on the membrane being characterized) with a membrane-impermeant fluorochrome, and observing at which point in a stepped-voltage sequence the membrane becomes permeable. In some cases, it is desirable or necessary to use a patch-clamp measurement of the pulse current across the membrane.

In another embodiment, one or more dielectric permittivities and conductivities of membranes and extracellular and intracellular fluids, from which the charging time constant are derived, is determined by time domain dielectric spectroscopy as described in Poleyva, Y., I. Ermolina, M. Schlesinger, B.-Z. Ginzburg, and Y. Feldman, Time domain dielectric spectroscopy study of human cells II. Normal and malignant white blood cells, Biochim. Biophys. Acta 1419:257-271, 1999, herein incorporated by reference. Once the dielectric properties of a given cell population are known, pulse amplitude, duration, and sequence may be tailored to the critical voltage and charging time constant of the target structures. In one embodiment, structures with shorter time constants and lower critical voltages are

selectively affected by pulses which are too short and-or too low in amplitude to disturb other structures.

VI.   TREATING TARGET TISSUES

In several embodiments of the present invention, a therapeutic method is provided in which a patient's tissue is removed and subsequently treated with one or more electric field pulses. In one embodiment, a method of reducing proliferation of rapidly dividing cells in a patient is provided, in which a portion of a patient's tissue that contains rapidly dividing cells and terminally differentiated cells is removed. At least one electric field pulse is applied to one or more cells in the tissue, wherein each electric field pulse has a pulse duration of less than about 100 nanoseconds. The tissue is then reintroduced to the patient. The tissue includes, but is not limited to, blood, cerebrospinal fluid, lymphatic fluid and bone marrow. In one embodiment, at least one electric field pulse has a pulse duration of less than about 10 nanoseconds. In another embodiment, the pulse duration is less than about 1 nanosecond. In one embodiment, electric field pulses greater than about 100 nanoseconds in length are combined with pulse durations of less than 100 nanoseconds.

In another embodiment, a method of reducing proliferation of rapidly dividing cells in a patient is provided. In one embodiment, a target cell population in the patient is identified, where the cell population includes rapidly dividing cells and terminally differentiated cells. At least one electric field pulse is applied to a portion of the target cell population, thereby reducing proliferation of the rapidly dividing cells in the target population. Each electric field pulse has a pulse duration of less than about 100 nanoseconds. In one embodiment, at least one electric field pulse has a pulse duration of less than about 10 nanoseconds. In another embodiment, the pulse duration is less than about 1 nanosecond. Electric field pulses greater than about 100 nanoseconds in length can also be combined with pulse durations of less than about 100 nanoseconds. In one embodiment, the rapidly dividing cells are tumorigenic cells. In another embodiment, the terminally differentiated cells are non-tumorigenic cells.

In a further embodiment, a method of treating a tumor in a patient is provided. In one embodiment, one or more tumor in a patient is identified. A catheterized electrode is then applied proximate to the tumor. The catheterized electrode is capable of providing at least one electric field pulse. One or more one electric field pulses is then applied to a portion of the tumor, thereby treating said tumor. Each electric field pulse has a pulse

duration of less than about 100 nanoseconds. In one embodiment, at least one electric field pulse has a pulse duration of less than about 10 nanoseconds. In another embodiment, the pulse duration is less than about 1 nanosecond. Electric field pulses greater than about 100 nanoseconds in length can also be combined with pulse durations of less than about 100

5   nanoseconds. In one embodiment, treating the tumor includes reducing the proliferation of rapidly dividing cells in the tumor. In one embodiment, the catheterized electrode is coupled to an endoscope. In another embodiment, the catheterized electrode is applied to the patient in conjunction with an endoscopic procedure.

VII.   COMBINED LONG AND SHORT PULSE TECHNOLOGY

10   It is another object of several embodiments of the current invention to provide a method in which at least two electric field pulses are applied to a cell to facilitate entry of a diagnostic or therapeutic agent into a cell's organelles. In one embodiment, a "long" electric field pulse is applied to cell followed by a "short" electric field pulse. In one embodiment, the method includes applying at least one first electric field pulse to the cell

15   sufficient to cause electroporation, incubating the cell with the therapeutic agent, and applying one or more second electric field pulses to one or more cells in the tissue, wherein each second electric field pulse has a pulse duration of less than about 100 nanoseconds. The therapeutic agent includes, but is not limited to, nucleic acids, polypeptides, viruses, enzymes, vitamins, minerals, antibodies, vaccines and pharmaceutical agents. In a further

20   embodiment, the pulse duration of the "short" pulse is less than about 1 nanosecond and the electric field is greater than about 10 kV/cm. In another embodiment, the pulse duration of the "long" pulse is greater than about 100 nanoseconds. The application of electric pulses to cells and the evaluation of cellular responses to these pulses are performed in a manner similar to that described above.

25   In one embodiment, the long pulse, or series of pulses, permeabilizes the external membrane, and serves as a conventional electroporating pulse. Amplitude, duration, and sequence for this pulse, or series of pulses, are determined by the cell type and medium as described above. The short pulse, or series of pulses, facilitates entry of the therapeutic agent into an intracellular structure, which may or may not require permeabilizing the

30   internal membrane. Pulse parameters are determined by the methods described above and optimized empirically for each agent and cell type.

VIII. IDENTIFICATION OF THERAPEUTIC AGENTS

In one embodiment of the present invention, a method of identifying an effective therapeutic agent is provided. In one embodiment, at least one putative therapeutic agent is applied to a cell. The regulation of at least one cell-cycle control gene, stress-response gene or immune response gene is then determined. If at least one of these genes is up-regulated, the putative therapeutic agent is identified as an effective therapeutic agent. Such an agent can be an effective therapeutic agent in reducing cell proliferation. Agents that induce apoptosis can also be identified in accordance with several embodiments of the current invention. In one embodiment, the cell-cycle control genes, stress-response genes or immune response genes include, but are not limited to ASNS, CHOP (GADD153), CLIC4, CD45, CD53, p36, CD58, AICL FOS, FOSB, DUSP1, JUN, TOB2, GADD34, CLK1, HSPA1B, JUND, EGR1, CACNA1E, CD69, ETR01, ITPKA, AHNAK, EMP3, ADORA2B, POU2AF1, AIM1, ATP1G1, ASNS, ETS2, CD45, VIM, TGIF, LAT, CLIC4, SLC7A5, ZFP36L2, RUNX1, SLC3A2, IFRD1 and PrP.

In one embodiment, the putative therapeutic agent includes, but is not limited to, nucleic acids, polypeptides, viruses, enzymes, vitamins, minerals, antibodies, vaccines and pharmaceutical agents.

While a number of preferred embodiments of the invention and variations thereof have been described in detail, other modifications and methods of use will be readily apparent to those of skill in the art. Accordingly, it should be understood that various applications, modifications and substitutions may be made of equivalents without departing from the spirit of the invention or the scope of the claims.

WHAT IS CLAIMED IS:

1. A method of sensitizing a eukaryotic cell to a therapeutic agent, comprising:

applying at least one electric field pulse to a plurality of cells, wherein each electric field pulse has a pulse duration of less than about 100 nanoseconds, to produce one or more sensitized cells; and

applying one or more therapeutic agents to said one or more sensitized cells, wherein the effect of said one or more therapeutic agents is enhanced in said one or more sensitized cells.

2. The method of Claim 1, wherein said pulse duration is less than about 1 nanosecond.

3. The method of Claim 1, wherein the at least one electric field pulse is greater than 10 kV/cm.

4. The method of Claim 1, wherein said one or more therapeutic agents consists of at least one of the following: nucleic acids, polypeptides, viruses, enzymes, vitamins, minerals, antibodies, vaccines and pharmaceutical agents.

5. The method of Claim 4, wherein said pharmaceutical agent is a chemotherapeutic compound.

6. A method of sensitizing a eukaryotic cell to a therapeutic method, comprising:

applying at least one electric field pulse to a plurality of cells, wherein each electric field pulse has a pulse duration of less than about 100 nanoseconds, to produce one or more sensitized cells; and

applying one or more therapeutic methods to said one or more sensitized cells, wherein the effect of said one or more therapeutic methods is enhanced in said one or more sensitized cells.

7. The method of Claim 6, wherein said pulse duration is less than about 1 nanosecond.

8. The method of Claim 6, wherein the at least one electric field pulse is greater than 10 kV/cm.

9. The method of Claim 6, wherein said one or more therapeutic methods consists of the group consisting of: photodynamic therapy, radiation therapy and vaccine therapy.

10. A method of regulating transcription of a gene in a eukaryotic cell, comprising:

selecting at least one gene selected from the group consisting of ASNS, CHOP, CLIC4, CD45, CD53, p36, CD58, AICL FOS, FOSB, DUSP1, JUN, TOB2, GADD34, CLK1, HSPA1B, JUND, EGR1, CACNA1E, CD69 and ETR01; and

applying at least one electric field pulse to the cell, wherein each electric field pulse has a pulse duration of less than about 100 nanoseconds.

11. The method of Claim 10, wherein said pulse duration is less than about 1 nanosecond.

12. The method of Claim 10, wherein the at least one electric field pulse is greater than 10 kV/cm.

13. A method of regulating transcription of a gene in a eukaryotic cell, comprising:

selecting at least one gene selected from the group consisting of ITPKA, AHNAK, EMP3, ADORA2B, POU2AF1, AIM1, ATP1G1, ASNS, ETS2, CD45, VIM, TGIF, LAT, CLIC4, SLC7A5, ZFP36L2, RUNX1, SLC3A2, IFRD1, and PrP; and

applying at least one electric field pulse to the cell, wherein each electric field pulse has a pulse duration of less than about 100 nanoseconds.

14. The method of Claim 13, wherein said pulse duration is less than about 1 nanosecond.

15. The method of Claim 13, wherein the at least one electric field pulse is greater than 10 kV/cm.

16. A method of regulating transcription of a gene in a eukaryotic cell, comprising:

selecting at least one gene selected from the group consisting of cell-cycle control genes, stress-response genes and immune response genes; and

applying at least one electric field pulse to the cell, wherein each electric field pulse has a pulse duration of less than about 100 nanoseconds.

5

17. The method of Claim 16, wherein said pulse duration is less than about 1 nanosecond.

18. The method of Claim 16, wherein the at least one electric field pulse is greater than 10 kV/cm.

10

19. A method of regulating transcription of a gene in a eukaryotic cell, comprising:

selecting at least one gene to be regulated; and

applying at least one electric field pulse to the cell, wherein each electric field pulse has a pulse duration of less than about 100 nanoseconds, thereby regulating said at least one gene.

15

20. The method of Claim 19, wherein said pulse duration is less than about 1 nanosecond.

20

21. The method of Claim 19, wherein the at least one electric field pulse is greater than 10 kV/cm.

22. The method of Claim 19, wherein said at least one gene is selected from the group consisting of: ASNS, CHOP, CLIC4, CD45, CD53, p36, CD58, AICL FOS, FOSB, DUSP1, JUN, TOB2, GADD34, CLK1, HSPA1B, JUND, EGR1, CACNA1E, CD69 and ETR01.

25

23. The method of Claim 19, wherein said at least one gene is selected from the group consisting of: ITPKA, AHNAK, EMP3, ADORA2B, POU2AF1, AIM1, ATP1G1, ASNS, ETS2, CD45, VIM, TGIF, LAT, CLIC4, SLC7A5, ZFP36L2, RUNX1, SLC3A2, IFRD1, and PrP.

30

24. The method of Claim 19, wherein the at least one electric field pulse is greater than 10 kV/cm.

25. A method of determining induction of gene transcription in response to electropertubation, comprising:

suspending a plurality of cells in a medium;

applying at least one electric field pulse to said plurality of cells, wherein each electric field pulse has a pulse duration of less than about 100 nanoseconds;

identifying at least one cell which is electroperturbed;

isolating said electroperturbed cell; and

determining cellular gene transcription in said electroperturbed cell.

26. The method of Claim 25, wherein the electroperturbed cell is identified based upon cellular morphology or cellular biochemistry.

27. The method of Claim 25, wherein the electroperturbed cell is identified using fluorescent staining.

28. A method of marking a eukaryotic cell for diagnostic or therapeutic procedures, comprising:

suspending a plurality of cells in a medium;

electroperturbing said plurality of cells, thereby inducing a cellular response in at least a portion of the cells, wherein said cellular response marks said at least a portion of the cells for a diagnostic or therapeutic procedure; and

identifying said at least a portion of the cells that were electroperturbed by the presence of said cellular response.

29. The method of Claim 28, wherein said electroperturbing comprises applying at least one electric field pulse to said plurality of cells, wherein each electric field pulse has a pulse duration of less than about 100 nanoseconds.

30. The method of Claim 28, wherein said marking comprises affecting one or more characteristics of the cell, said characteristic selected from the group consisting of: gene

transcription, gene translation, protein synthesis, post-translational modifications, protein processing, cellular biosynthesis, degradative metabolism, cellular physiology, cellular biophysical properties, cellular biochemistry and cellular morphology.

5   31. The method of Claim 28, wherein said diagnostic or therapeutic procedure comprises lysing the cell.

32. The method of Claim 28, wherein said cellular response comprises the translocation of at least one membrane component of an intracellular membrane of said

10   cell.

33. The method of Claim 32, wherein said one membrane component is a phospholipid or a protein.

15   34. The method of Claim 33, wherein said phospholipid is phosphatidylserine.

35. The method of Claim 28, wherein said cellular response comprises the disruption of least one intracellular structure without substantially affecting the external membrane of the cell.

20

36. The method of Claim 35, wherein said at least one intracellular structure is selected from the group consisting of: nucleus, mitochondria, storage vacuoles, endoplasmic reticulum compartments, cytoplasmic stores and cytoskeletal-membrane attachments.

25

37. A method of disrupting an intracellular membrane of a eukaryotic cell, comprising:

applying at least one electric field pulse to the cell, wherein each electric field pulse has a pulse duration of less than about 100 nanoseconds, thereby

30   inducing disruption of the intracellular membrane.

38. The method of Claim 37, wherein said intracellular membrane is selected from the group consisting of: cytoplasmic membrane, nuclear membrane, mitochondrial membrane and segments of the endoplasmic reticulum.

39. The method of Claim 37, wherein said pulse duration is less than about 1 nanosecond.

5   40. The method of Claim 37, wherein said disruption of the intracellular membrane comprises translocating at least one membrane component.

41. The method of Claim 40, wherein said membrane compon_ent is a phospholipid or protein.

10

42. The method of Claim 41, wherein said phospholipid is phosphatidylserine.

43. The method of Claim 37, wherein the at least one electric field is greater than 10

15   kV/cm.

44. A method of marking a eukaryotic cell for phagocytosis, comprising:

suspending a plurality of cells in a medium;

applying at least one electric field pulse to said plurality of cells, wherein

20   each electric field pulse has a pulse duration of less than about 100 nanoseconds, thereby inducing a cellular response in at least a portion of said cells, wherein said cellular response marks said cells for phagocytosis.

45. The method of Claim 44, wherein said cellular response comprises translocating

25   at least one membrane component.

46. The method of Claim 45, wherein said membrane component is a phospholipid or protein.

30   47. The method of Claim 46, wherein said phospholipid is phosphatidylserine.

48. A method of disrupting one or more intracellular structures of a eukaryotic cell, comprising:

applying at least one electric field pulse to the cell, wherein each electric field pulse has a pulse duration of less than about 100 nanoseconds, thereby inducing disruption of at least one intracellular structure, without substantially affecting the external cell membrane.

5

49. The method of Claim 48, wherein said at least one intracellular structure is selected from the group consisting of: nucleus, mitochondria, storage vacuoles, endoplasmic reticulum compartments, cytoplasmic stores and cytoskeletal-membrane attachments

10

50. A method of determining cellular tolerance to electropertubation, comprising:

(a) suspending one or more cells in a medium;

(b) applying a first electric field pulse to one or more cells,

(c) identifying electroperturbed cells;

15

(d) isolating said electroperturbed cells;

(e) identifying one or more indicators of cellular response in said electroperturbed cells;

(f) applying a second electric field pulse to one or more cells;

(g) repeating steps (c) - (e)

20

(h) comparing said one or more indicators of cellular response after application of the first electric field with said one or more indicators of cellular response after application of the second electric field.

51. The method of Claim 50, wherein said second electric field is not equal to said

25   first electric field.

52. The method of Claim 50, wherein said one or more indicators of cellular response is selected from the group consisting of changes in: gene transcription, gene translation, protein synthesis, post-translational modifications, protein processing, cellular

30   biosynthesis, degradative metabolism, cellular physiology, cellular biophysical properties, cellular biochemistry and cellular morphology.

53. A method of selectively electroperturbing a population of cells, comprising:

determining a dielectric property of one or more cells in a first sub-population of cells;

determining a dielectric property of one or more cells in a second population of cells;

determining an electric field pulse based on said dielectric property of said first sub-population of cells and said dielectric property of said second population of cells, wherein said electric field pulse selectively electroperturbs the first sub-population of cells without substantially affecting the second population of cells.

obtaining a cell suspension, wherein said cell suspension contains said first sub-population of cells and said second population of cells; and

applying said electric field pulse to said cell suspension, thereby electroperturbing said first sub-population of cells without substantially affecting the second population of cells.

54. The method of Claim 53, wherein said first sub-population of cells comprises rapidly dividing cells and wherein said second population of cells comprises terminally differentiated cells.

55. The method of Claim 53, wherein said first sub-population of cells comprises a first type of rapidly dividing cell and wherein said second population of cells comprises a second type of rapidly dividing cell.

56. The method of Claim 53, wherein said electroperturbing induces changes in cellular response, wherein said cellular response is selected from the group consisting of: gene transcription, gene translation, protein synthesis, post-translational modifications, protein processing, cellular biosynthesis, degradative metabolism, cellular physiology, cellular biophysical properties, cellular biochemistry and cellular morphology.

57. The method of Claim 54, wherein said rapidly dividing cells are tumorigenic cells.

58. The method of Claim 54, wherein said terminally differentiated cells are non-tumorigenic cells.

59. A method of selectively regulating gene transcription in rapidly dividing cells, comprising:

    obtaining a cell suspension, wherein said cell suspension contains rapidly dividing cells and terminally differentiated cells; and

    applying at least one electric field pulse to the cell, wherein each electric field pulse has a pulse duration and intensity sufficient to induce gene transcription primarily only in said rapidly dividing cells.

60. The method of Claim 59, wherein said rapidly dividing cells are tumorigenic cells.

61. The method of Claim 59, wherein said terminally differentiated cells are non-tumorigenic cells.

62. A method of reducing proliferation of rapidly dividing cells in a patient, comprising;

    removing a portion of a patient's tissue, wherein said tissue contains rapidly dividing cells and terminally differentiated cells;

    applying at least one electric field pulse to one or more cells in said tissue, wherein each electric field pulse has a pulse duration of less than about 100 nanoseconds; and

    reintroducing said tissue into said patient.

63. The method of Claim 62, wherein said tissue consists of one or more of the following: blood, cerebrospinal fluid, lymphatic fluid and bone marrow.

64. The method of Claim 62, wherein said rapidly dividing cells are tumorigenic cells.

65. The method of Claim 62, wherein said terminally differentiated cells are non-tumorigenic cells.

66. A method of reducing proliferation of rapidly dividing cells in a patient, comprising;

    identifying a target cell population in the patient, wherein said cell population comprises rapidly dividing cells and terminally differentiated cells;

    applying at least one electric field pulse to at least a portion of said target cell population, wherein each electric field pulse has a pulse duration of less than about 100 nanoseconds, thereby reducing proliferation of rapidly dividing cells in said target cell population.

67. The method of Claim 66, wherein said rapidly dividing cells are tumorigenic cells.

68. The method of Claim 66, wherein said terminally differentiated cells are non-tumorigenic cells.

69. The method of Claim 66, further comprising applying at least one electric field pulse to at least a portion of said target cell population, wherein each electric field pulse has a pulse duration of more than about 100 nanoseconds.

70. A method of treating a tumor in a patient, comprising;

    identifying a tumor in the patient;

    applying a catheterized electrode to said patient proximate to said tumor; wherein said catheterized electrode is capable of providing at least one electric field pulse; and

    applying said at least one electric field pulse to at least a portion of said tumor, wherein each electric field pulse has a pulse duration of less than about 100 nanoseconds, thereby treating said tumor.

71. The method of Claim 70, wherein said treating said tumor comprises reducing proliferation of rapidly dividing cells in said tumor.

72. The method of Claim 70, further comprising applying at least one electric field pulse to at least a portion of said tumor wherein each electric field pulse has a pulse duration of more than about 100 nanoseconds.

73. The method of Claim 70, wherein said catheterized electrode is coupled to an endoscope.

5   74. The method of Claim 70, further comprising applying said catheterized electrode to said patient in conjunction with an endoscopic procedure.

75. A method of facilitating entry of a diagnostic or therapeutic agent into a cell's intracellular structures, comprising:

10   applying at least one first electric field pulse to the cell, said first electric pulse sufficient to cause electroporation;

incubating said cell with the therapeutic agent; and

applying one or more second electric field pulses to one or more cells in said tissue, wherein each second electric field pulse has a pulse duration of less than

15   about 100 nanoseconds.

76. The method of Claim 75, wherein said therapeutic agent consists of one or more of the following: nucleic acids, polypeptides, viruses, enzymes, vitamins, minerals, antibodies, vaccines and pharmaceutical agents.

20
77. The method of Claim 75, wherein said pulse duration is less than about 1 nanosecond.

78. The method of Claim 75, wherein said intracellular structure is selected from the

25   group consisting of: nucleus, mitochondria, storage vacuoles, endoplasmic reticulum compartments, cytoplasmic stores and cytoskeletal-membrane attachments

79. A method of identifying an effective therapeutic agent, comprising:

applying at least one putative therapeutic agent to at least one cell; and

30   determining whether at least one gene selected from the group consisting of ASNS, CHOP, CLIC4, CD45, CD53, p36, CD58, AICL FOS, FOSB, DUSP1, JUN, TOB2, GADD34, CLK1, HSPA1B, JUND, EGR1, CACNA1E, CD69, ETR01, ITPKA, AHNAK, EMP3, ADORA2B, POU2AF1, AIM1, ATP1G1, ASNS, ETS2,

CD45, VIM, TGIF, LAT, CLIC4, SLC7A5, ZFP36L2, RUNX1, SLC3A2, IFRD1, and PrP are up-regulated in said cell, wherein if at least one of said genes is up-regulated, the putative therapeutic agent is identified as an effective therapeutic agent.

80. The method of Claim 79, wherein said putative therapeutic agent consists of one or more of the following: nucleic acids, polypeptides, viruses, enzymes, vitamins, minerals, antibodies, vaccines and pharmaceutical agents.

81. The method of Claim 79, wherein said putative therapeutic agent is an anti-proliferation agent.

FIG. 1A

FIG. 1B

FIG. 2A

FIG. 2B

FIG. 2C

FIG. 2D

a) 20 X   b) 60 X
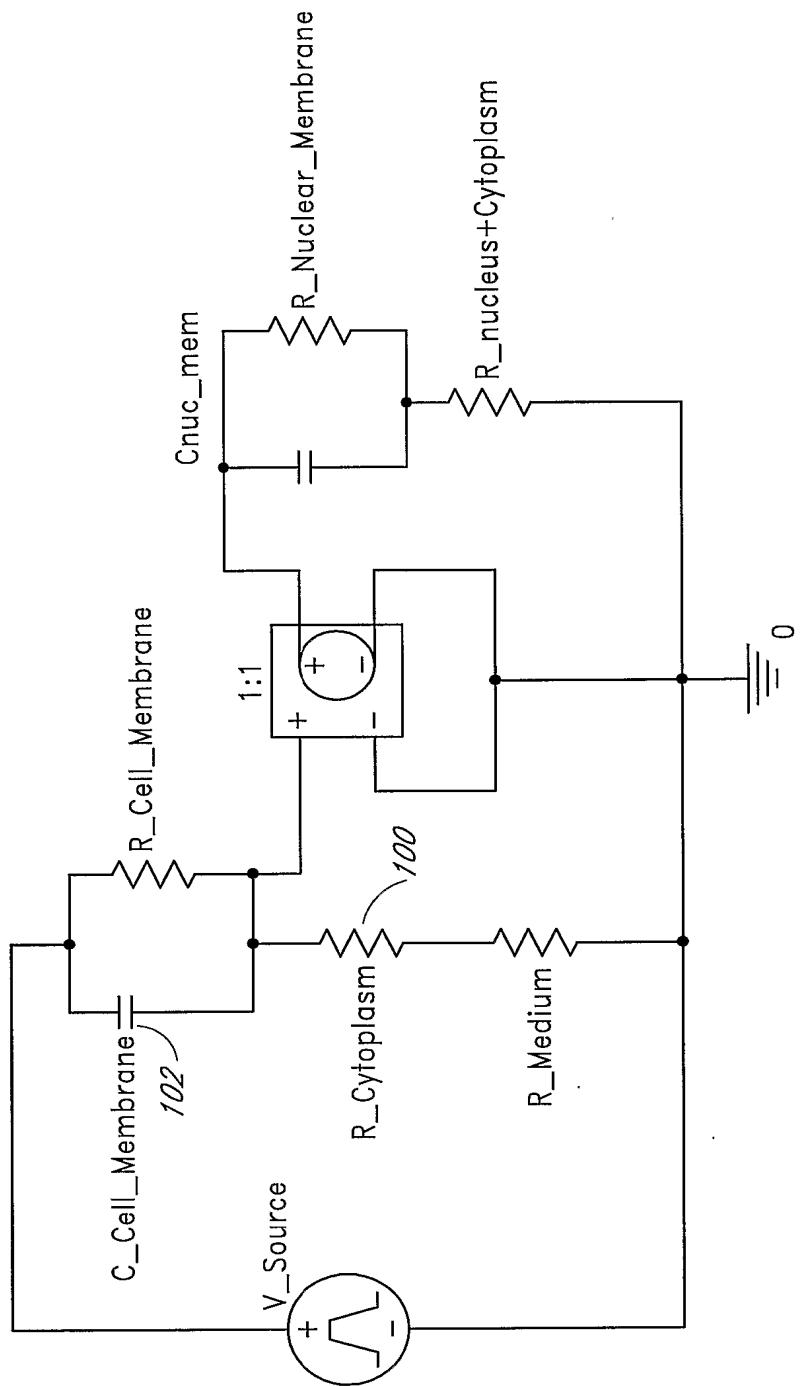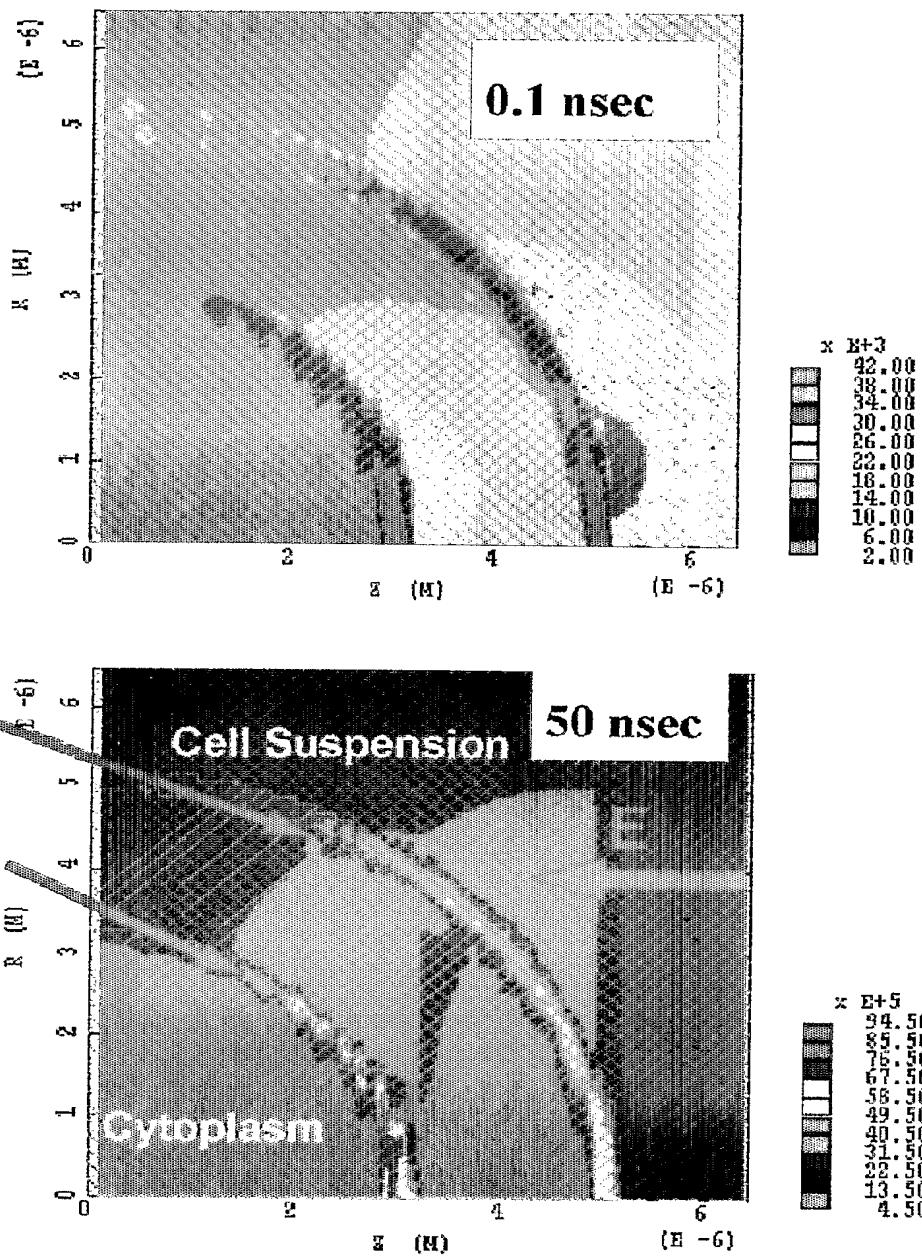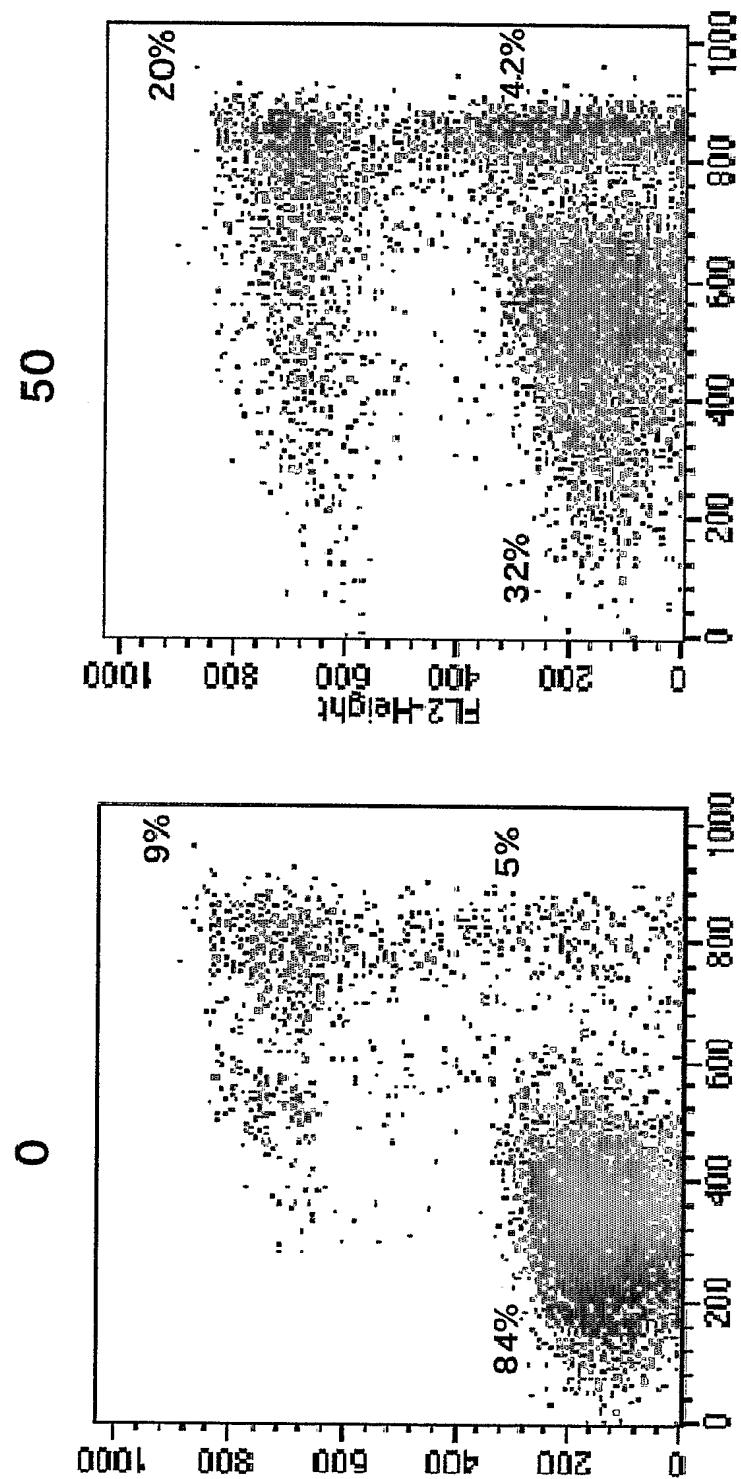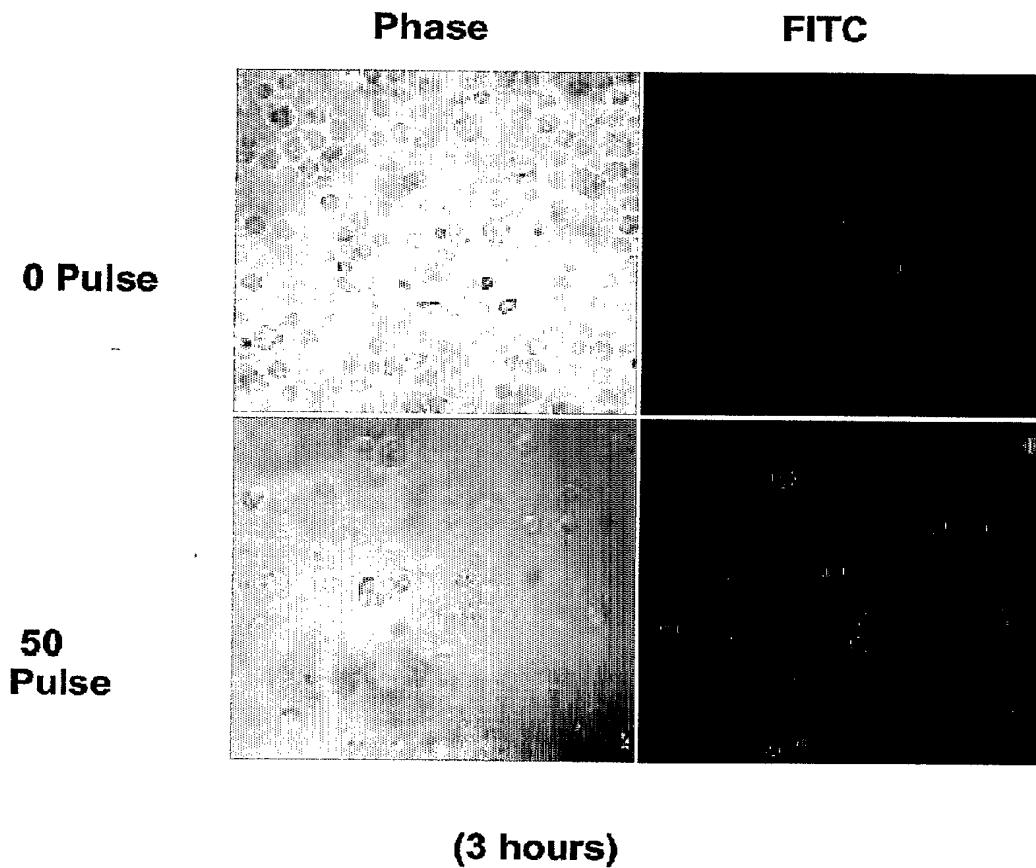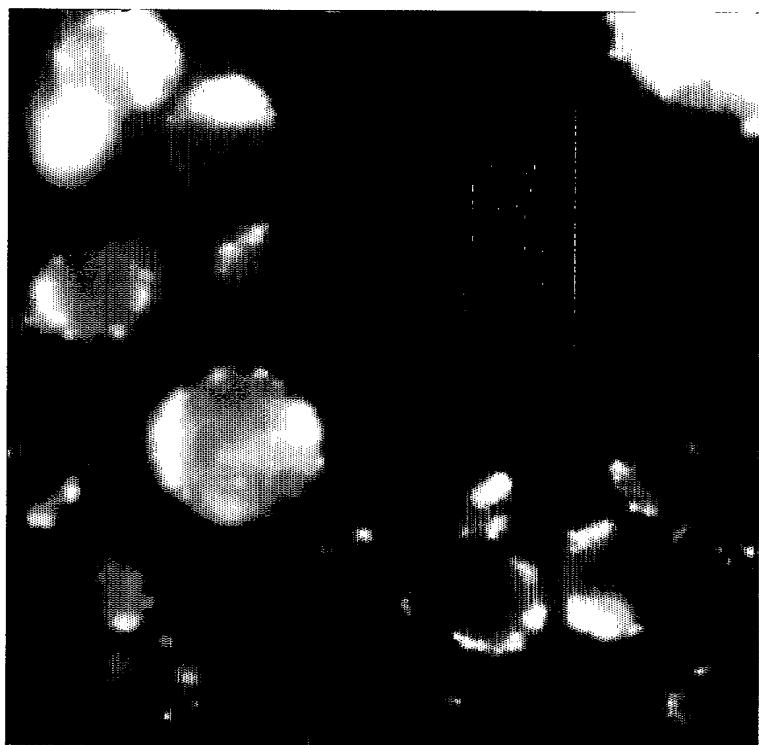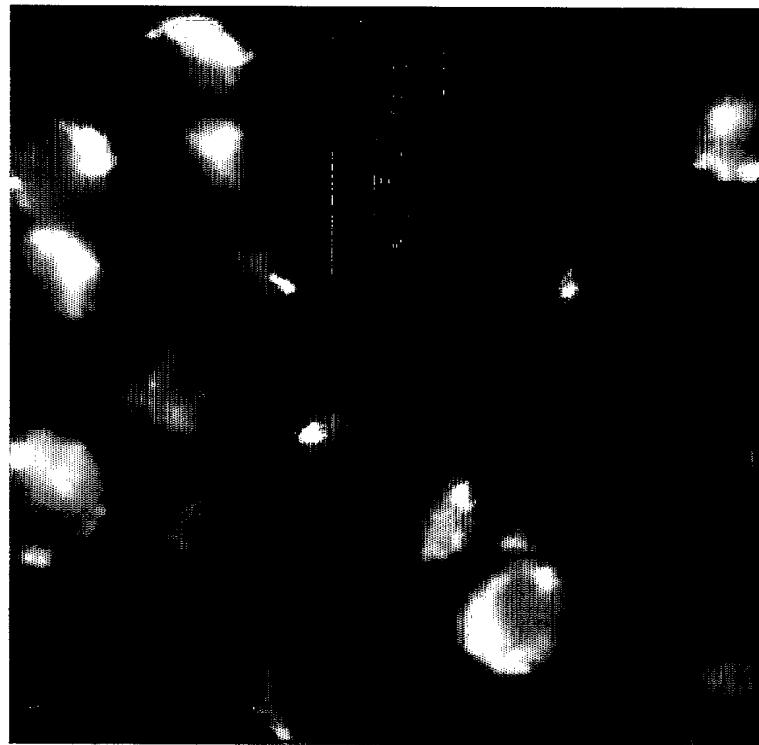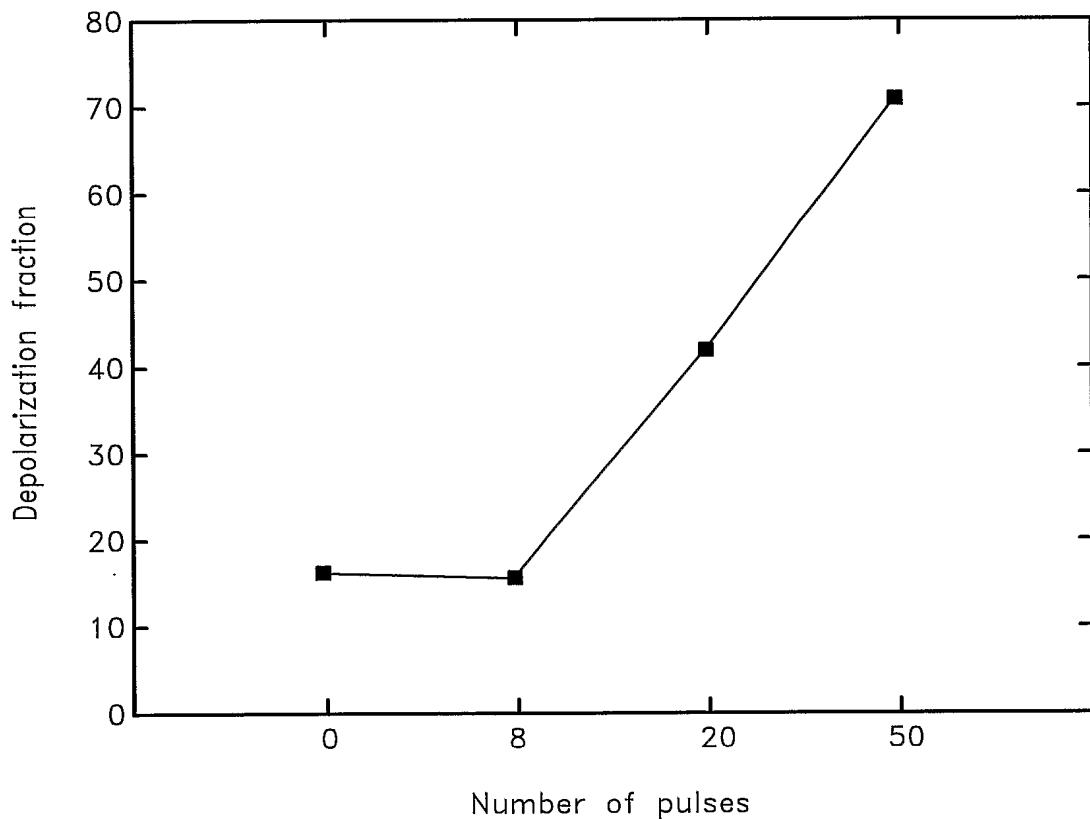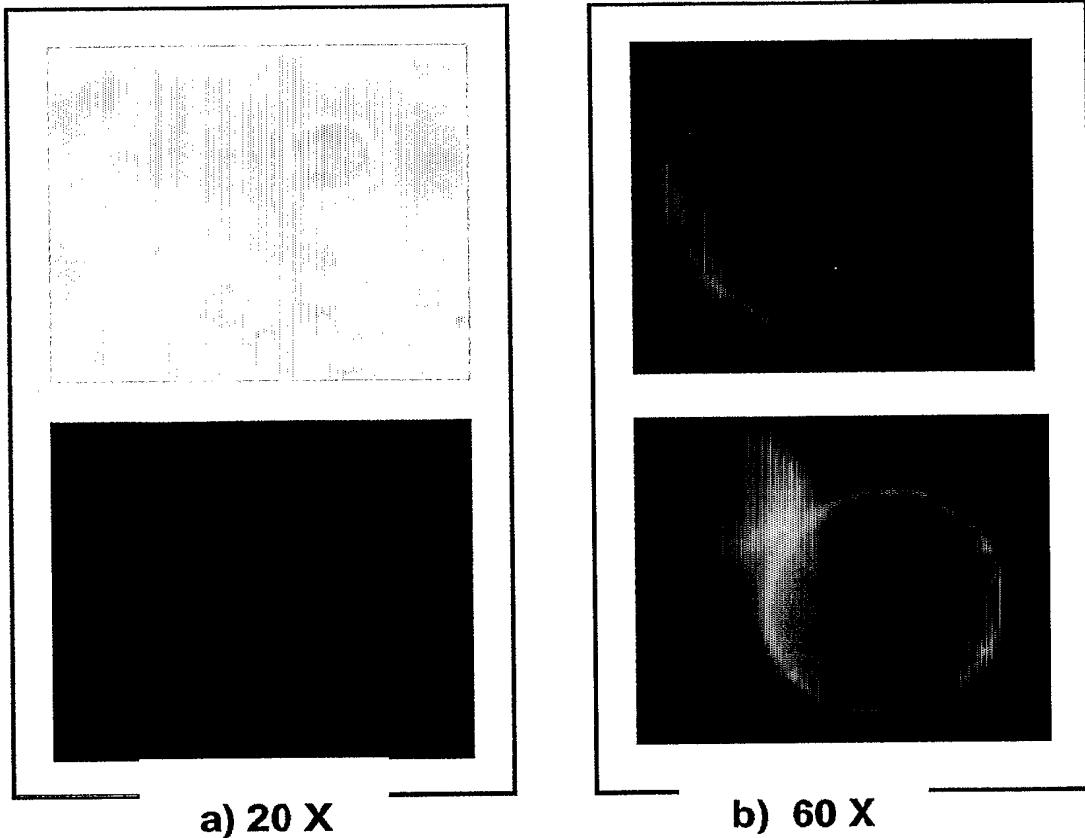
FIG. 2E
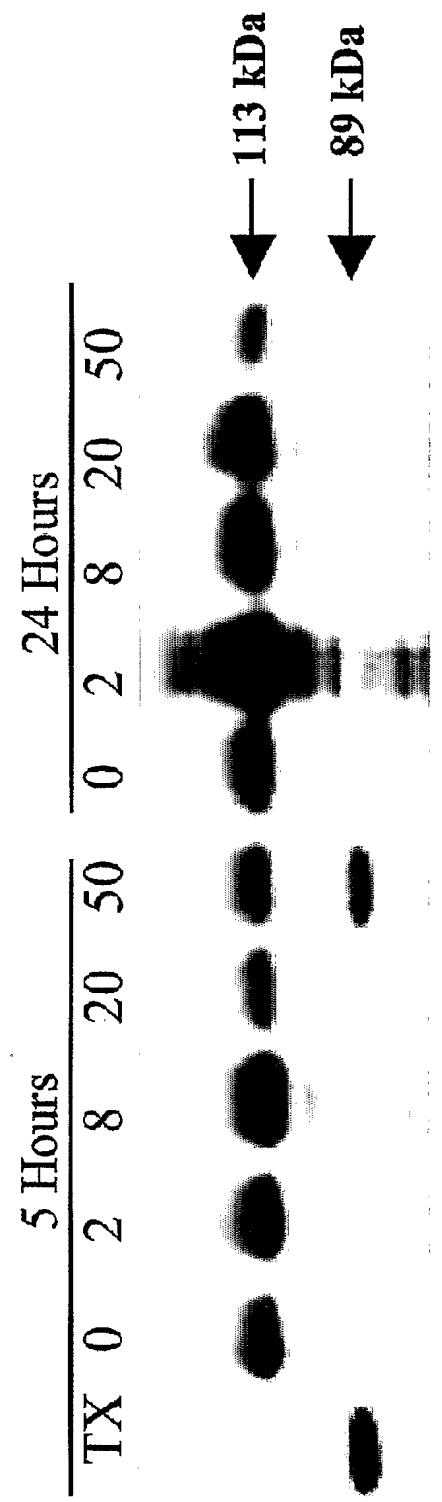
FIG. 3

TABLE 1   50 vs 0   shocks increased genes after 6 hours

Fold increase	GenBank # ID	Gene	Function
6.8	X15376	GABA-A receptor gamma 2 subunit	Inhibit synaptic transmission
6.7	A1535946	EST	Unknown
6.6	X92720	Mitochondrial phosphoenolpyruvate carboxykinase	Essential for gluconeogenesis and for growth
5.4	A1095013	EST	Unknown
4.9	U26648	Syntaxin 5 (transmembrane protien)	Regulating transport vesicle docking
4	U33635	Human colon carcinoma kinase-4(CCK4)	Receptor tyrosine kinase (RTK transmembrane glycoprotein)
3.7	D16532	Very low density lipoprotein receptor	Delivery of VLDL-derived fatty acids into adipose tissue
3.6	X68487	A2b adenosine receptor	Anti-inflammation
3.5	J04027	Plasma membrane Ca2+ pumping ATPase	Ca+Mg2+-ATPase expels Ca2+ from cells
3.4	U83981	Apoptosis associated protein (GADD34)	DNA damage and growth arrest-inducible gene
3.3	AA126515	EST	Unknown
3.2	M80899	Novel protein AHNAK	Activates Phospholipase C-gamma1
3.1	M25756	Secretogranin II gene	Neuropeptide secreted by the ciliary epithelial cells
3	A1806222	EST	Unknown
3	X95632	Arg protien tyrosine kinase-binding protien P55pik (regulatory subunit for phosphatidylinositol 3-kinase)	Regulator and/or effector of Arg function
2.8	D88532	Phosphatidylinositol 3-kinase catalytic subunit	Regulate insulin-like growth factor-1 receptor signaling
2.8	S81752	Diphthamide biosynthesis protein 2-like (DP112L)	Candidate tumor suppressor gene
2.6	D31797	CD40 ligand gene	Stimulates B cell proliferation and IgE secretion
2.6	L27476	Human tight junction protien ZO-2 gene (X104)	Unknown
2.6	M37815	T cell membrane glycoprotein CD28	Modulate T cell activation
2.5	U16307	Glioma pathogenesis-related protein (GliPR)	highly expressed in the brain tumor glioblastoma multiforme
2.5	D87077	KIAA0240	Unknown
2.4	A1961743	EST	Unknown
2.3	Z29090	Phosphatidylinositol 3-kinase catalytic subunit	Regulate tyrosine kinase receptor signaling
2.2	D80010	KIAA0188	Potential serine protease
2.1	U83115	Non-lens beta gamma-cristallin like protein (AIM1)	Putative supressor of malignant melanoma
2.1	U26424	Ste20-like kinase (MST2)	Induce apoptosis
2.1	Y10183	MEMD protein	Cell adhesion molecule
2.1	I194881	S1	Probable tumor suppressor
2.1	D28364	Annexin II	Calcium-regulated exocytosis (absent in prostrate cancer)
2.1	U87947	Hematopoietic neural membrane protein (HNMP-1)	Possible role during active myelination
2	AL080061	cDNA DKFZp564H182	Unknown
2	X66435	HMG-C0A-Synthase	Rate-limiting enzyme in the cholesterol synthetic pathway

FIG. 4A

TABLE 1   50 vs 0   shocks increased genes after 1 hour

Fold increase	GenBank # ID	Gene	Function
27.2	S62138	TLS-CHOP (FUS) or GADD153, CHOP (DDIT3)	Tumor-associated fusion gene
25.0	V01512	Proto-oncogene c-fos (FOS)	Stress response gene
21.3	L49169	GoS3 (FOSB)	Stress response gene
15.9	X68277	CL 100 (DUSP1)	Tumor suppresor
9.8	J04111	C-jun proto oncogene (JUN)	Stress response gene
6.9	D64109	Tob family (TOB2)	Anti-proliferative protein
4.0	S62138	TLS-CHOP (FUS) or GADD153, CHOP (DDIT3)	Tumor-associated fusion gene
3.1	U83981	GADD34 (PP1R15A)	Stress response and growth arrest gene
2.7	M59287	CDC-like kinase (CLK1)	Phosphorylation
2.7	M59830	MHC class III HSP70-2 gene (HSPA1B)	Heat shock protein
2.7	X63575	Plasma membrane calcium ATPase (ATP2B2)	Enzyme
2.6	AJ005694	Short form of beta II spectrin (SPTBN1)	Membrane binding
2.4	X56681	JunD (JUND)	Transcription factor
2.2	X52541	Early growth response protein 1 (RGR1)	Transcriptional regulator
2.2	U66589	Ribosomal protein L5 (RPL5)	5S RNA binding protein
2.1	L27745	Voltage-operated calcium channel, alpha-1 (CACNA1E)	Modulation of calcium
2.1	Z22576	CD69	Signal transmitting receptor
2.1	M62831	ETR101	Transcription factor

FIG. 4B

Fold increase	GenBank # ID	Gene	Function
2.4	D85730	Heat shock protein 70 testis variant	Anti-stress, anti-apoptosis
2.3	L26318	JNK1	Induce apoptosis
2.2	Y18264	SAIL1 gene	Zinc Encrypt transaction factor
2.1	M14758	Multidrug resistance (MDR1) gene	Multidrug-resistance

TABLE 2   50 vs 0   shocks decreased genes after 6 hours

FIG. 5

TABLE 3   8 vs 0   shocks increased genes after 6 hours

Fold increase	GenBank # ID	Gene	Function
18.3	X97198	Receptor protein tyrosine phosphate (PCP-2)	Cell-cell recognition and adhesion
15.6	u49260	Mevalonate pyrophosphate dacarboxylase	Enzyme in the cholestrol synthetic pathway
11.7	AD001530	XAP-5	Unknown
4.6	A1362017	EST	Unknown
3.4	U40992	Heat shock protein 40 (hsp40)	Anti-stress, anti-apoptosis
2.9	S81752	Diphthamide biosynthesis protein 2-like (DPH2L)	Candidate tumor suppressor gene
2.6	Z22534	Activin receptor-like kinase (ALK)-2	Putative transmembrane protein serine/threonine kinase
2.3	AF014837	m6 A methyltransferase (MT-A70)	Posttranscriptional mRNA modification
2.2	AC006276	Unknown	Unknown
2.1	W28235	Human retina cDNA randomly primed sublibrary	Unknown
2.1	X77196	Lysosome-associated membrane protein-2	critical for autophagy

FIG. 6

TABLE 4   8 vs 0   shocks decreased genes after 6 hours

Fold increase	GenBank # ID	Gene	Function
4.4	L16895	Lysyl–oxidase (LOX) gene	Extracellular matrix biosynthesis
3.5	AL050043	Clone DKFZp566M0524	Unknown
3.4	U91963	Tolloid–like protein	Extracellular matrix biosynthesis
3.1	AA903299	EST	Unknown
3.1	M29540	Carcinoembryonic antigen (CEA)	
2.8	A1097085	EST	Unknown
2.6	U32439	Regulator of G protein signaling similarity (RGS7)	Regulate G protein signaling
2.5	U79298	Clone 23803	Unknown
2.4	AB018326	KIAA0783	Unknown
2.1	AB002438	mRNA for chromosome 5q21–22	Unknown
2.1	W28256	Human retina cDNA randomly primed sublibrary	Unknown
2	A1375033	EST	Unknown
2	M63108	Luteinizing hormone–choriogonadrotropin receptor	
2	Y18264	SALL1 gene	Zinc finger transcription factor

FIG. 7

FIG. 8A

FIG. 8B

FIG. 9
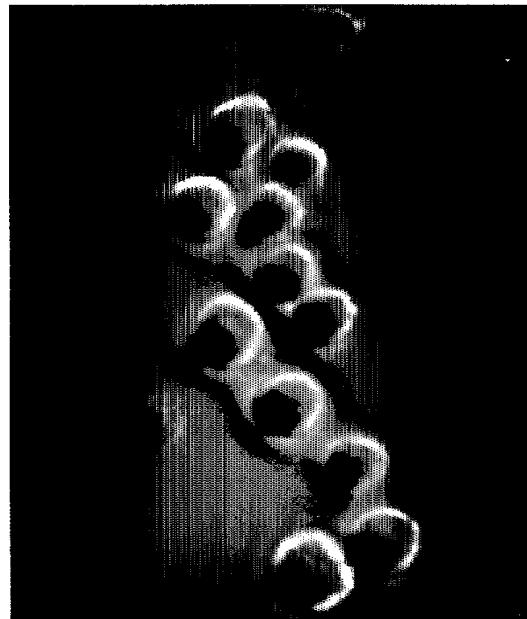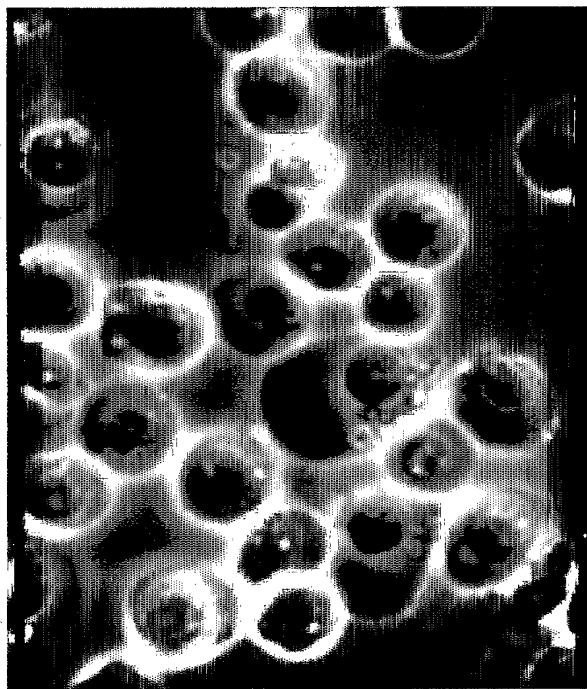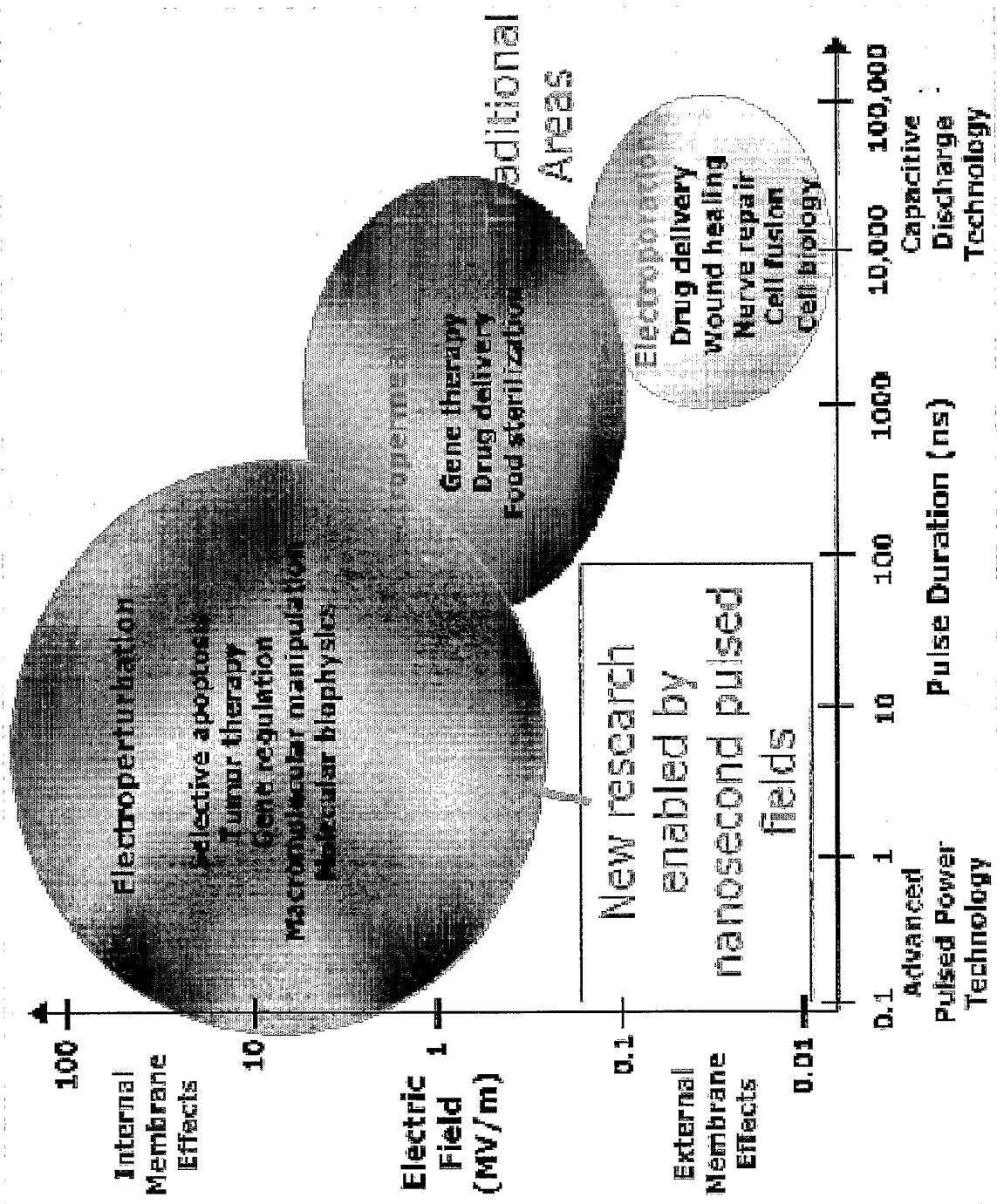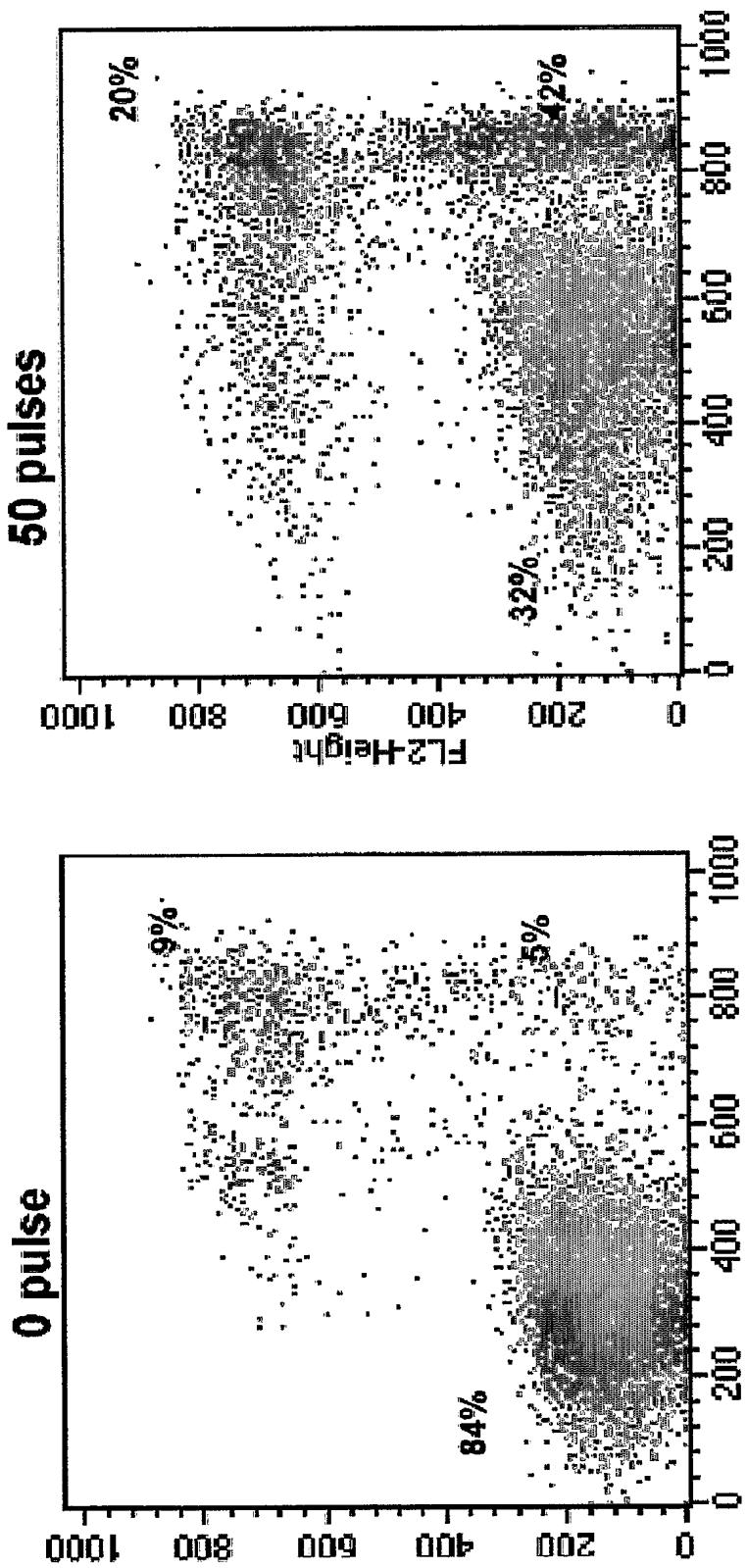
FIG. 10
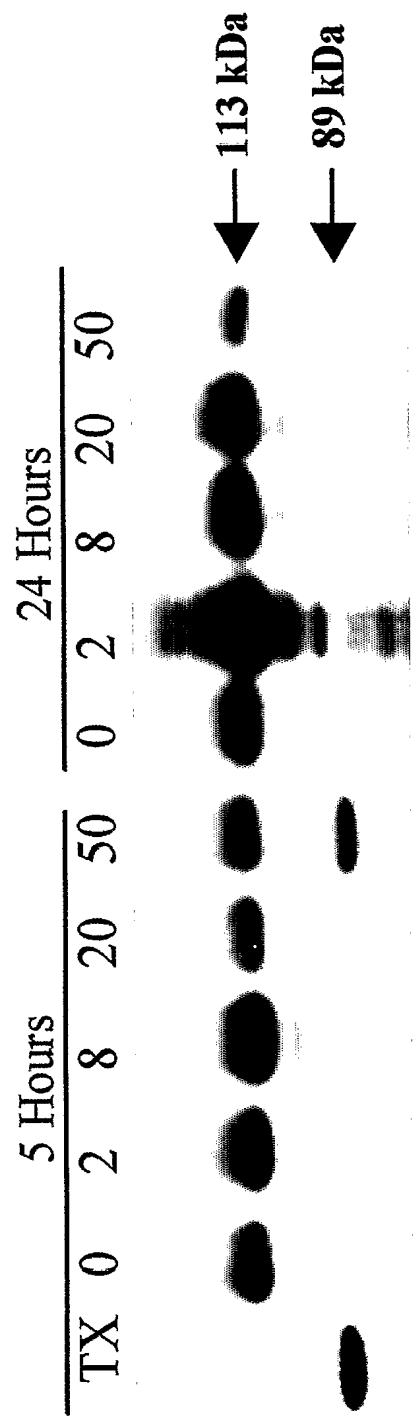
FIG. 11

JC-1 Flow Cytometry Scatter Plots - Green (x-axis):Red (y-axis)

Depolarized fraction

0 pulses

8 pulses

20 pulses

50 pulses
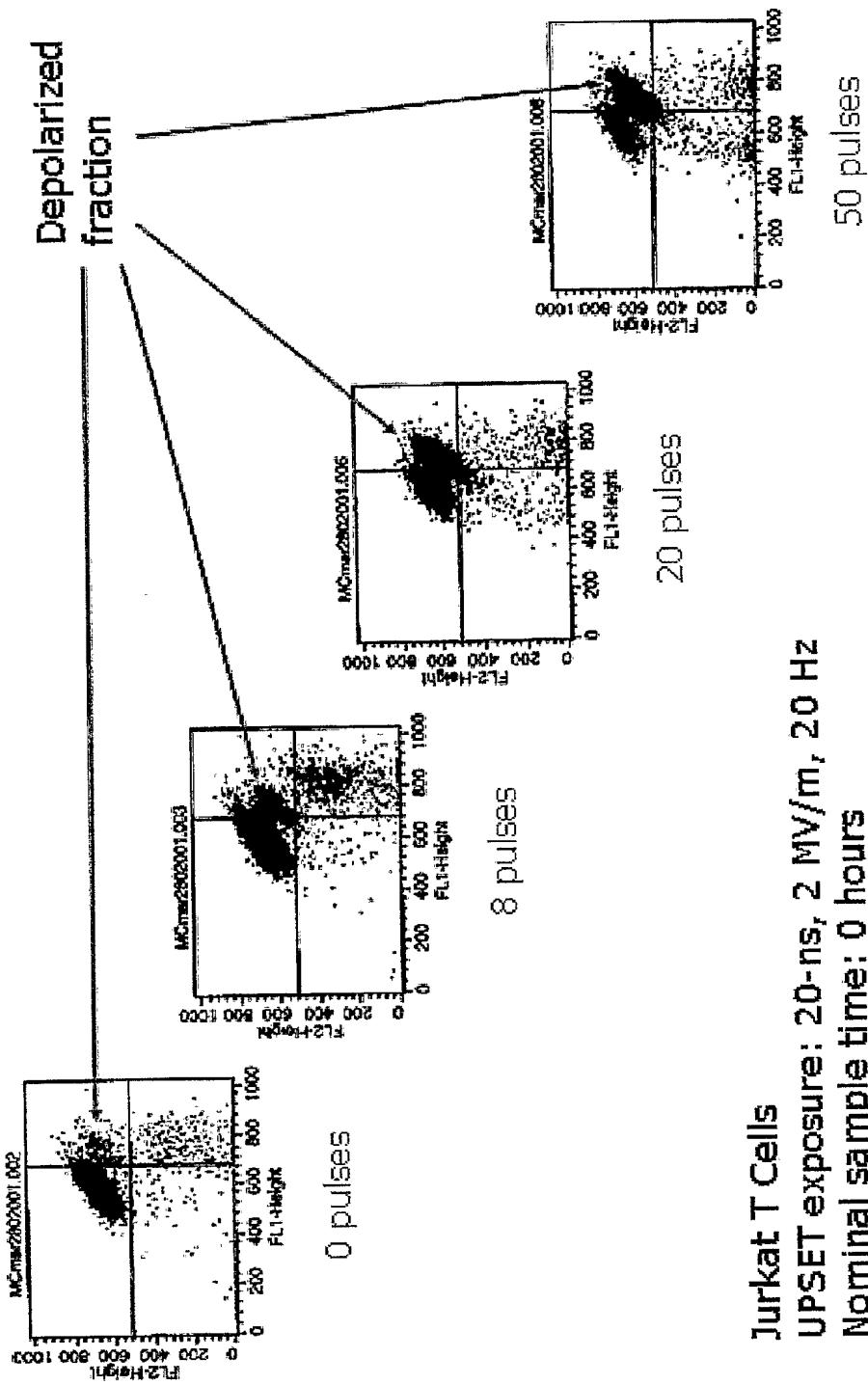
Jurkat T Cells
UPSET exposure: 20-ns, 2 MV/m, 20 Hz
Nominal sample time: 0 hours
Actual assay time after shock: 1 hour

FIG. 12
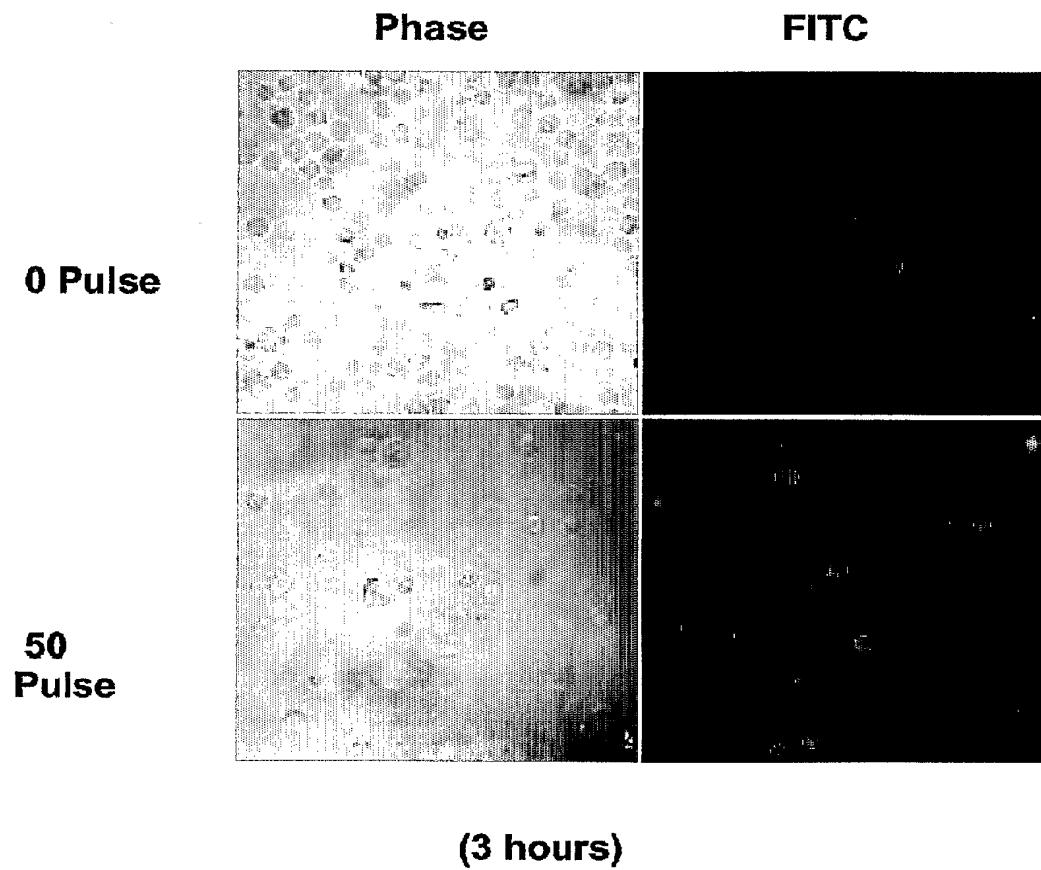
FIG. 13
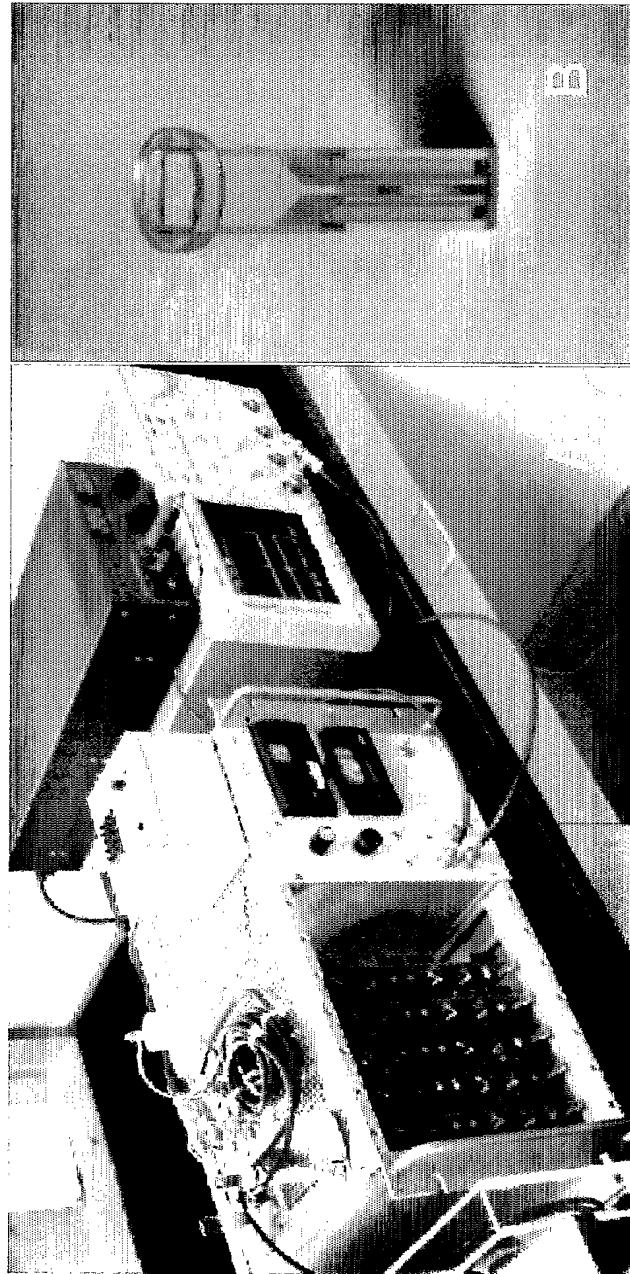
FIG. 14A   FIG. 14B
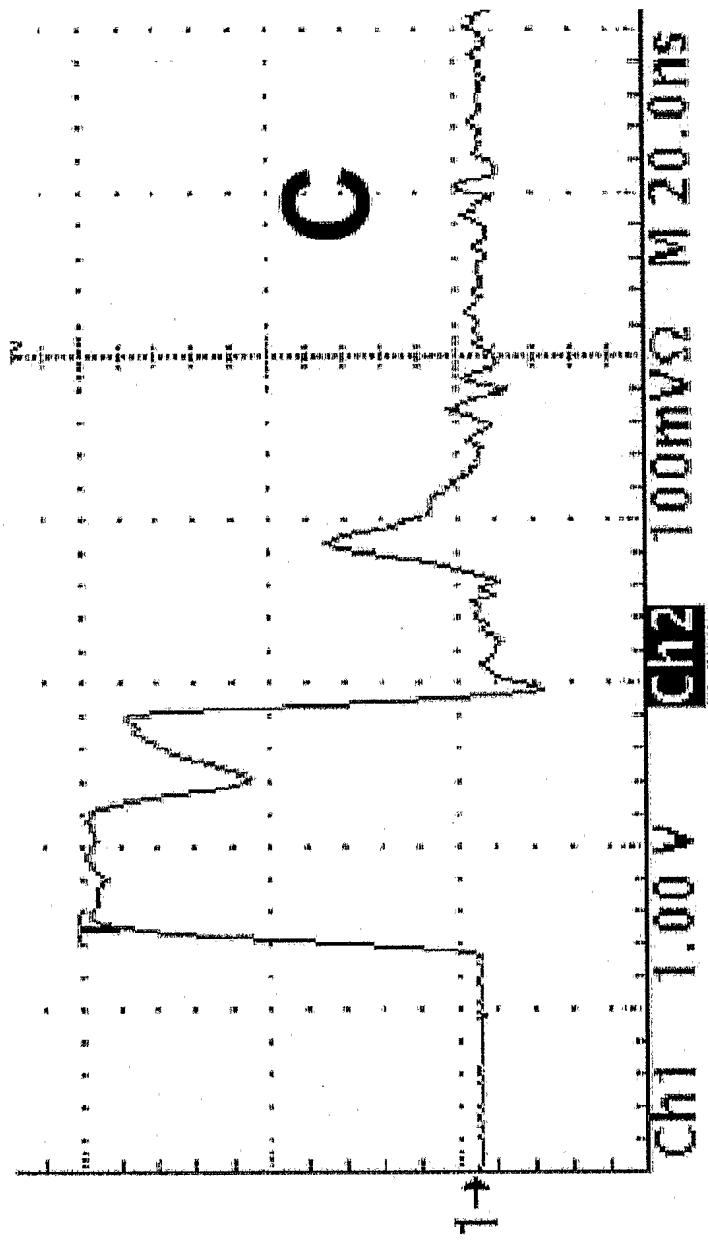
FIG. 14C
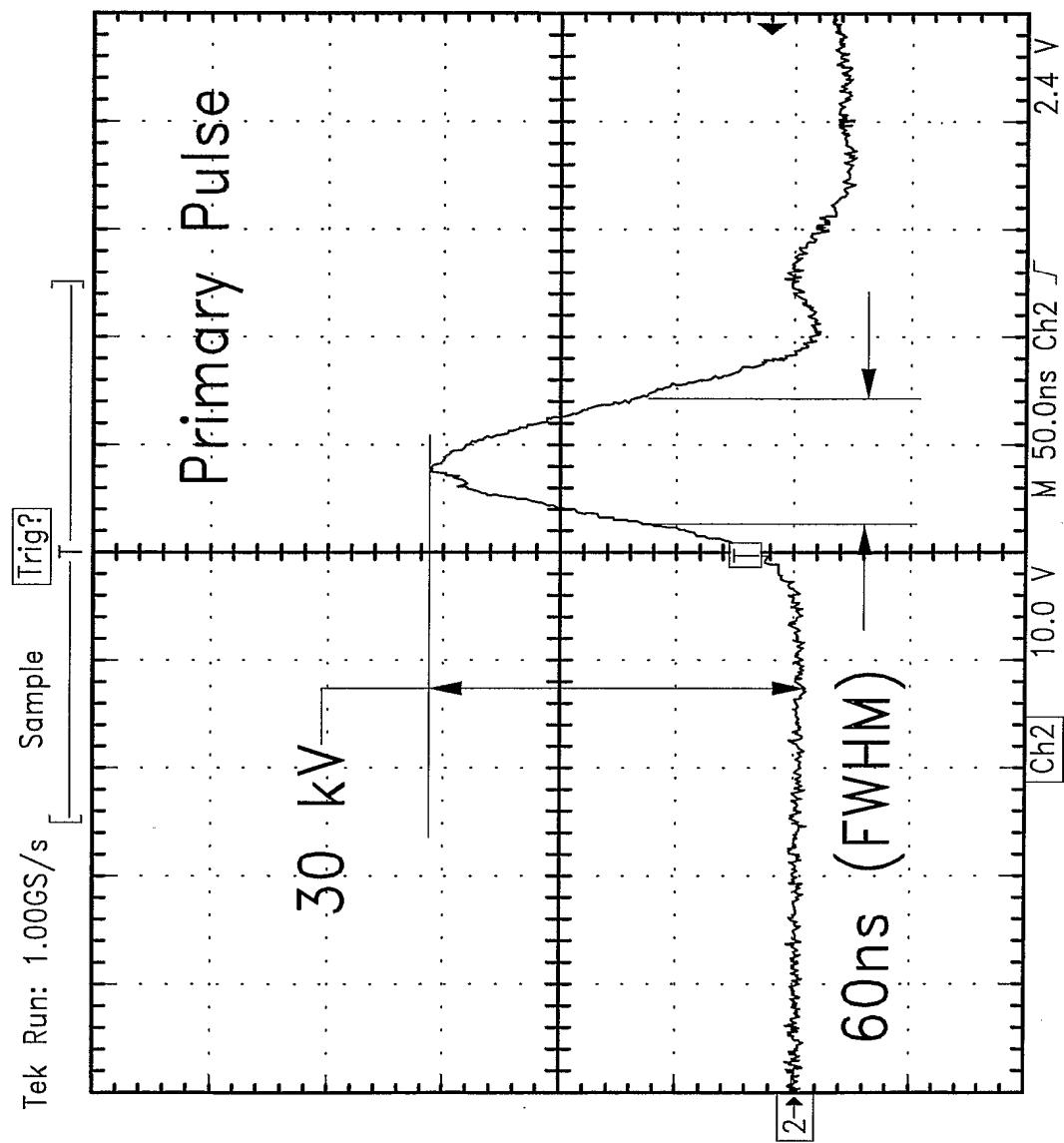
FIG. 15
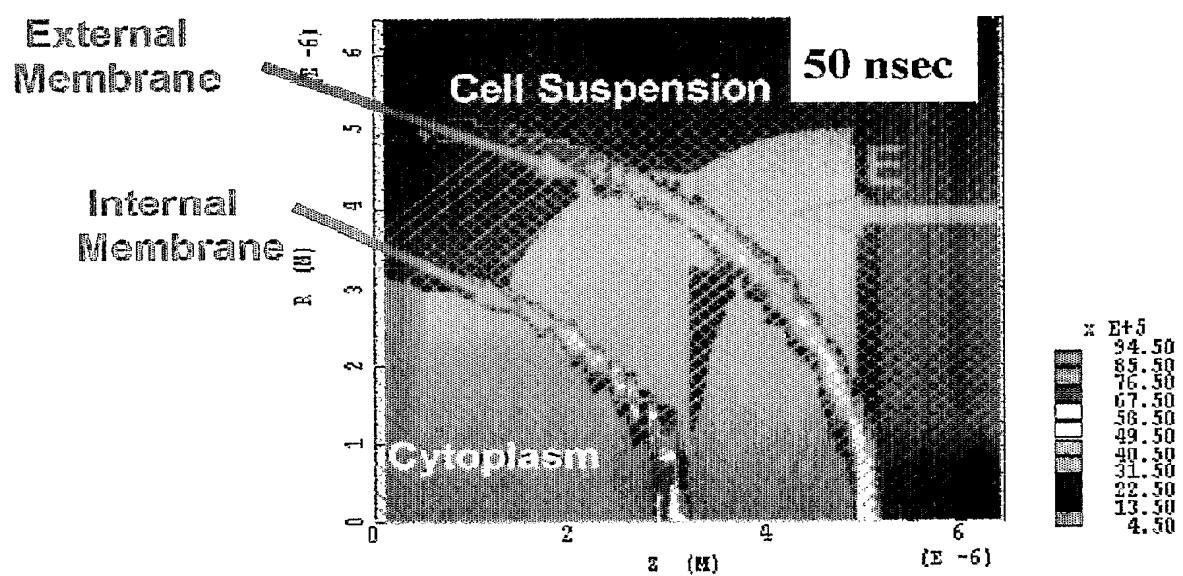
FIG. 16
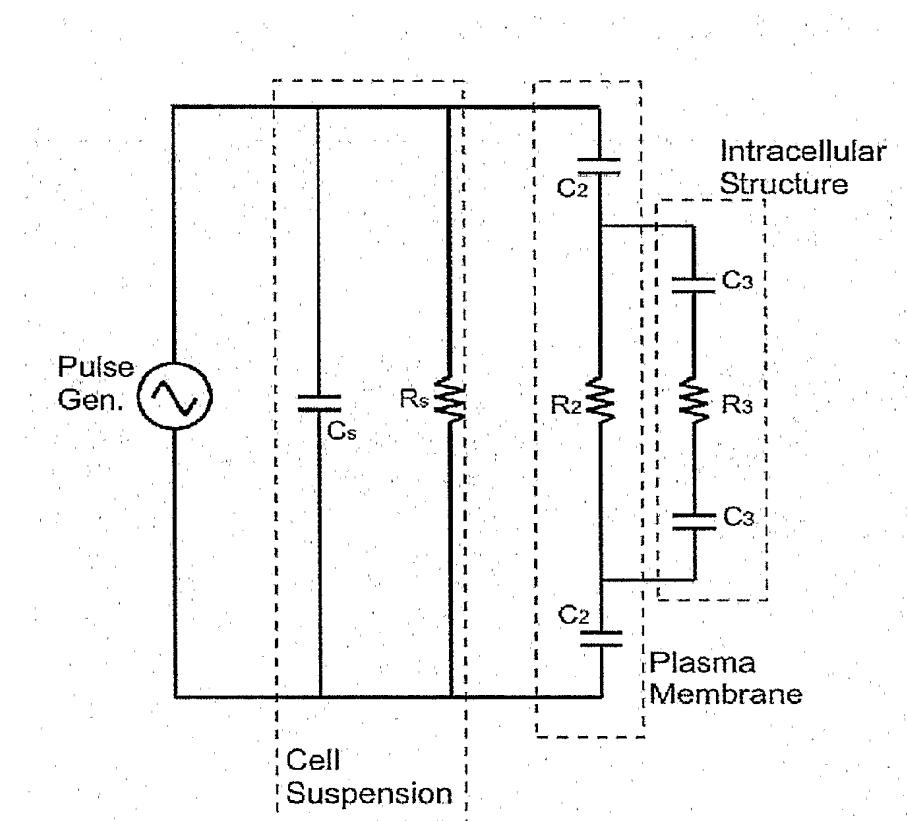
FIG. 17
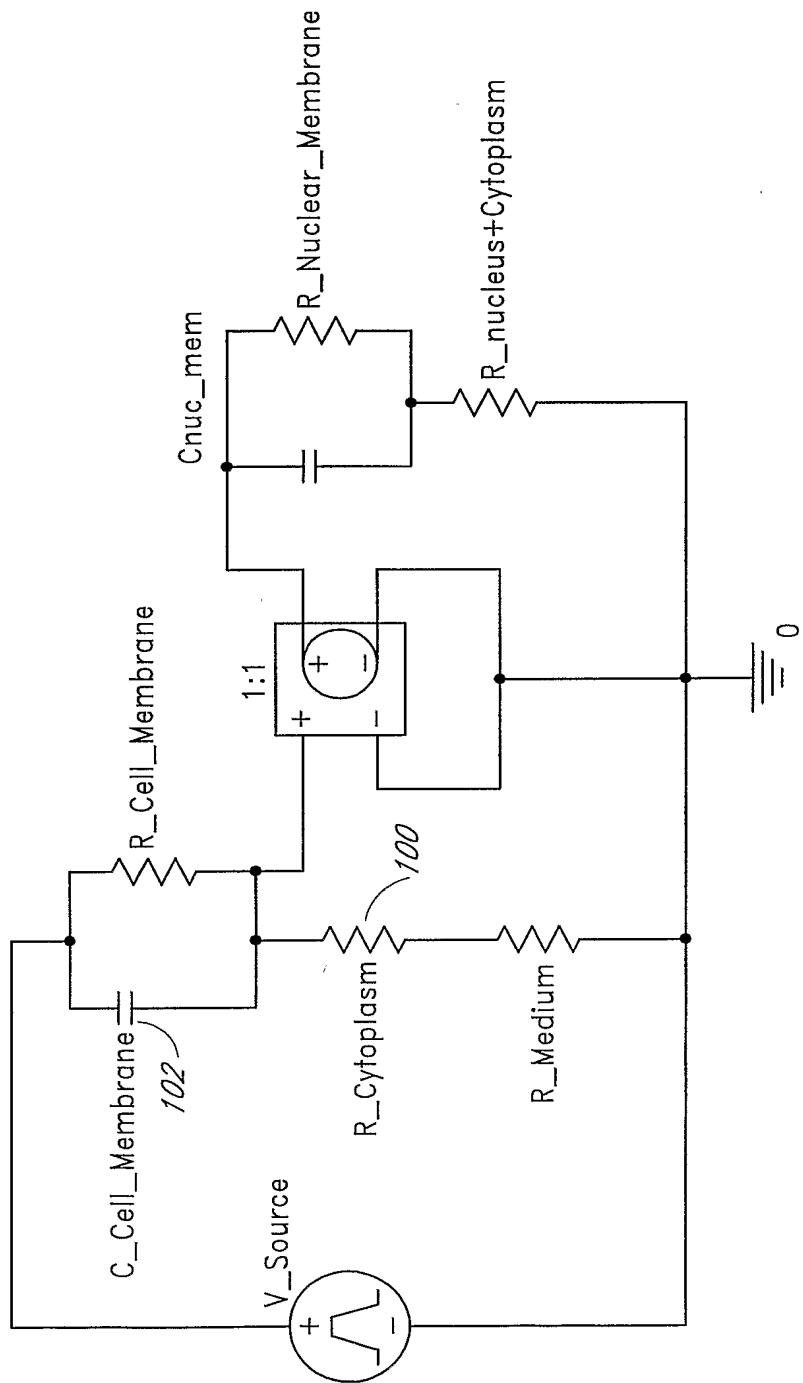
FIG. 18

FIG. 19

FIG. 20

FIG. 21

WATER

TEFLON
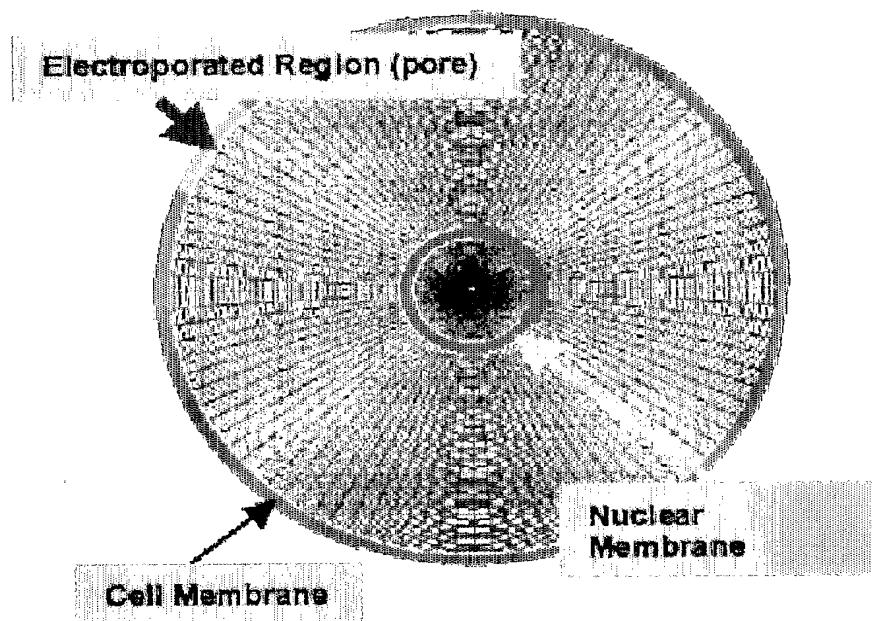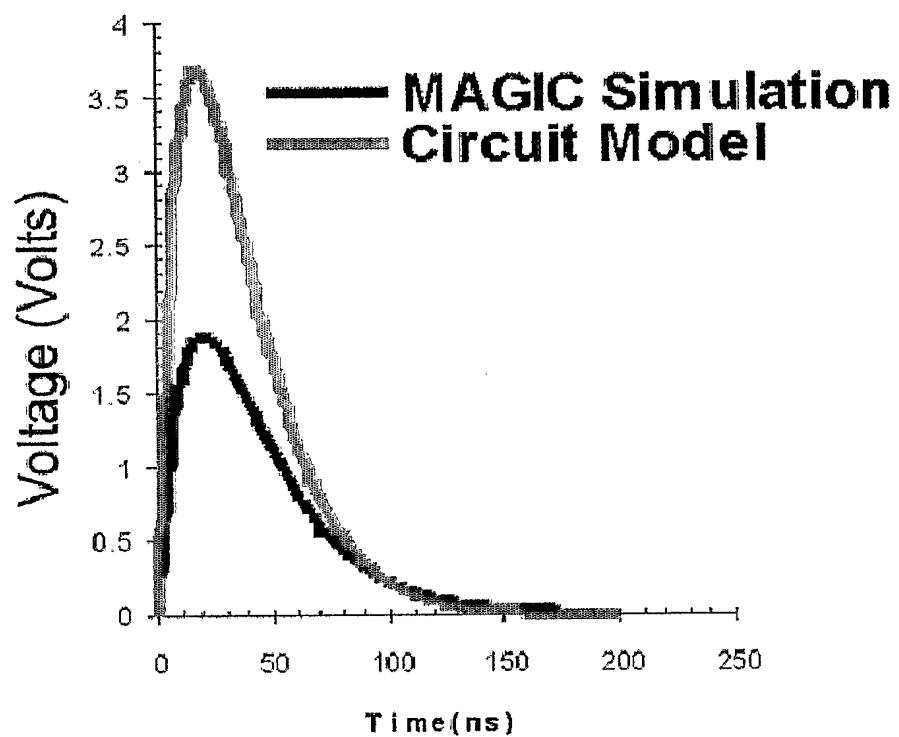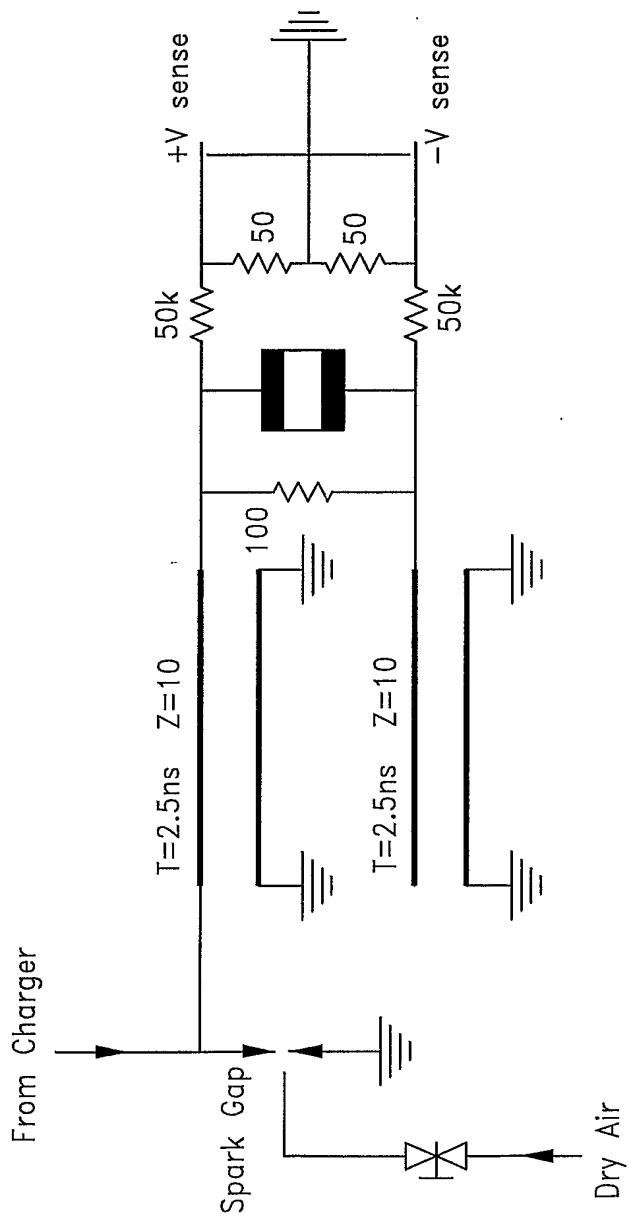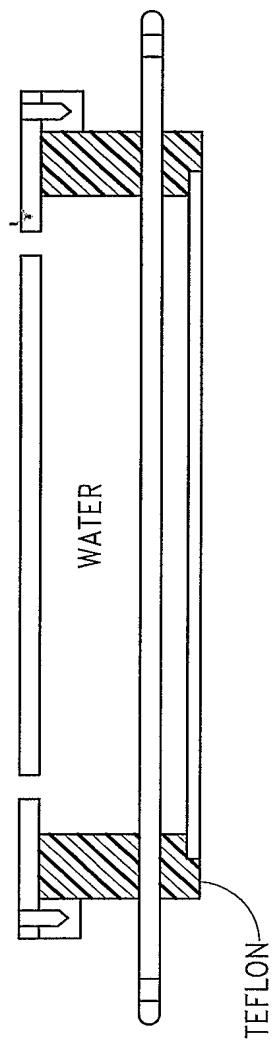
FIG. 22
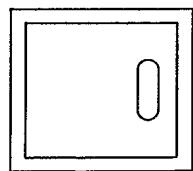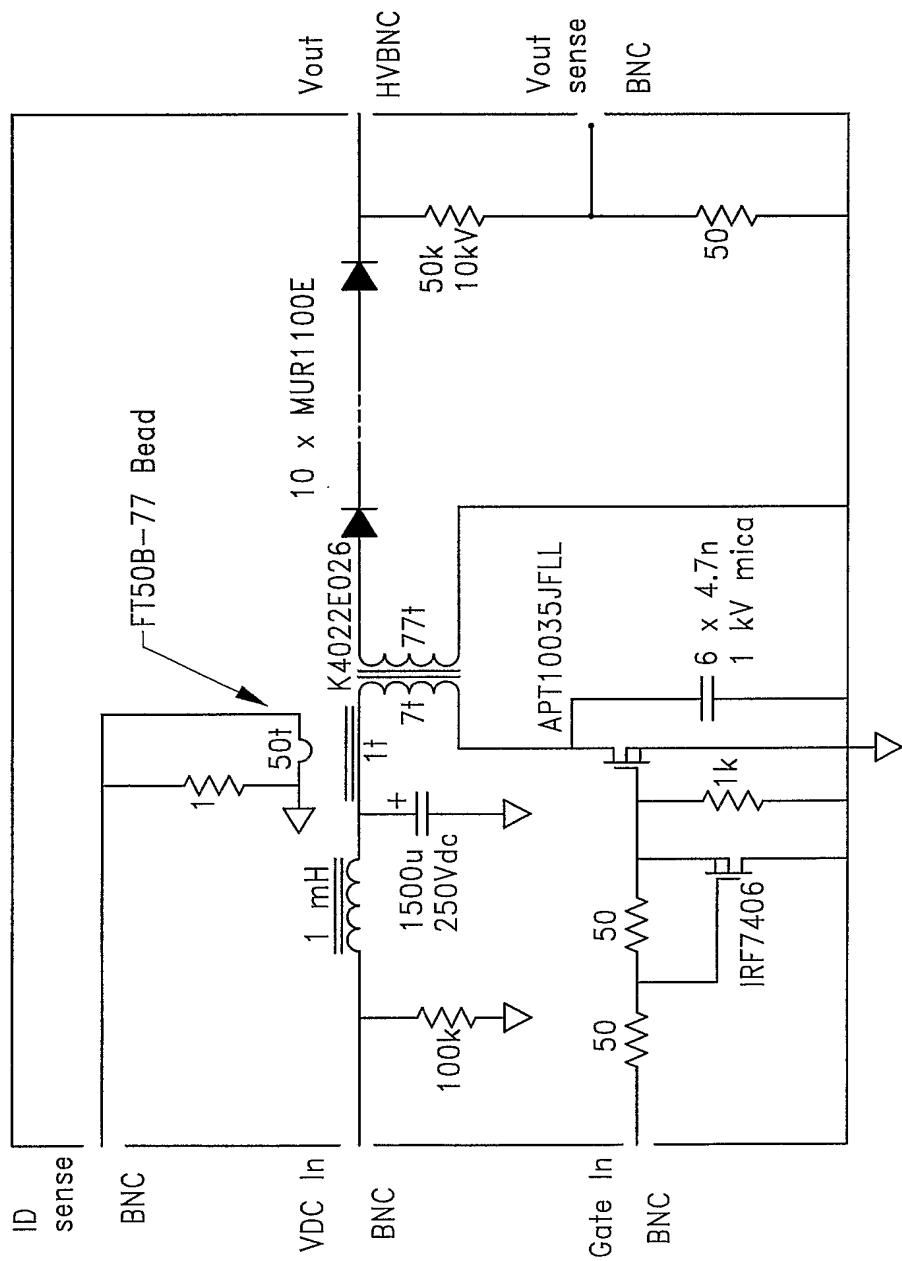
FIG. 23
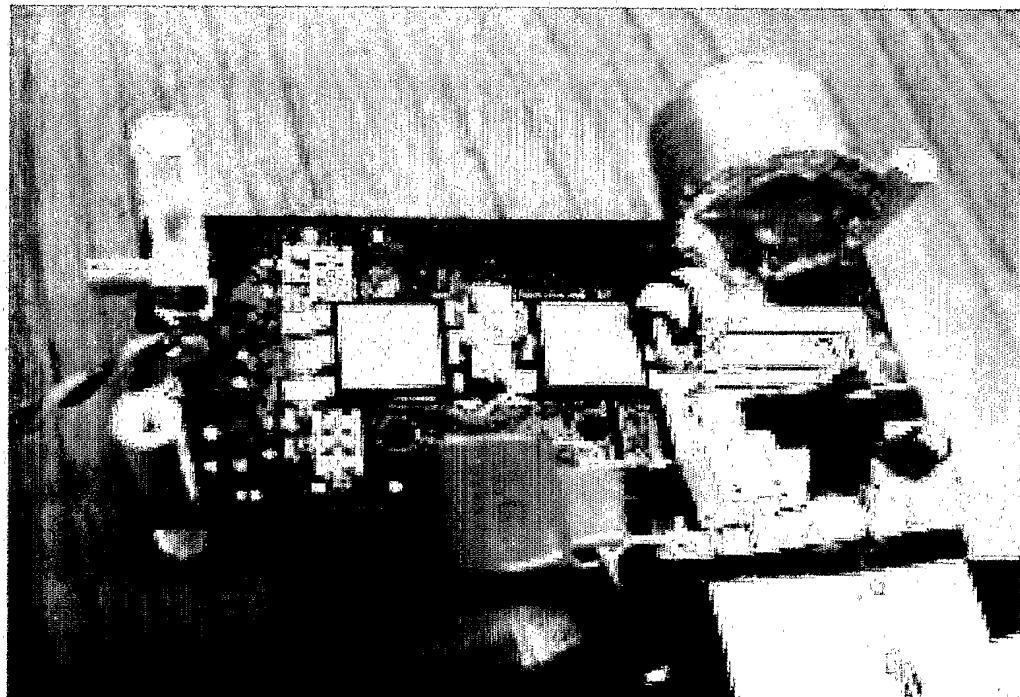
FIG. 24
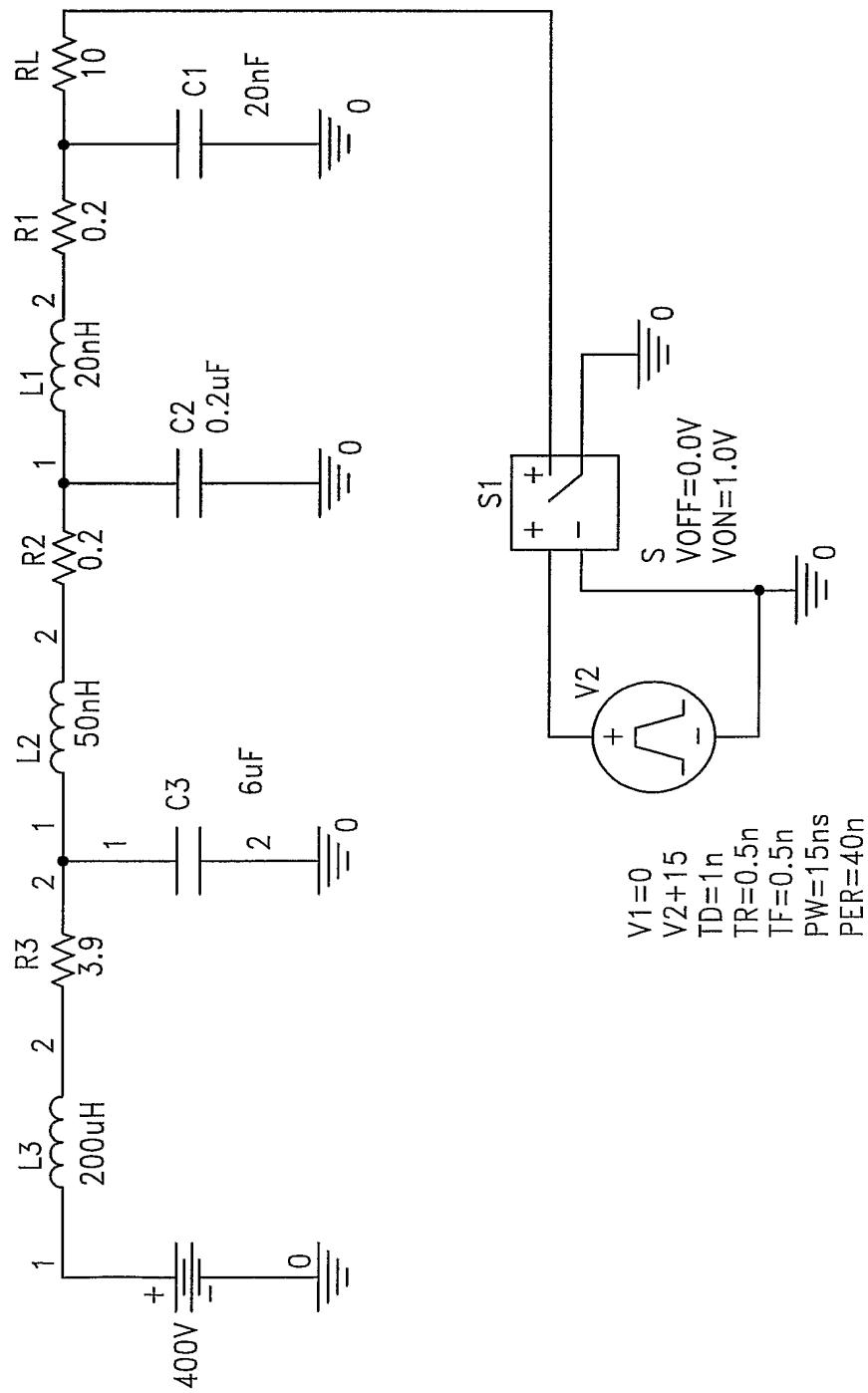
FIG. 25

FIG. 26

FIG. 27A

FIG. 27B

Viable Cells (Trypan Blue–Negative) Versus UPSET Pulses
(20-ns pulses, 40 kV/cm, 20Hz)

Number of Pulses

Viable Cells (cells/mL)
Millions

FIG. 28

FIG. 29

Intermediate

Apoptotic

Proliferative

FIG. 30

FIG. 31

FIG. 32

Intracellular Potentials Versus Time
ideal rectangular step, E=20 kV cm −1
tau_cm=75 ns; tau_mm=11 ns; r_cell=5 um; r_mitochondrion=0.5 um

V_mitochondrion
V_mit_internal
V_mit_membrane
V_mit_mbrn, 10 kV/cm
V_c_membrane

V (Volts)

Time (ns)

FIG. 33